Old Dominion University Research Foundation

DEPARTMENT OF OCEANOGRAPHY
COLLEGE OF SCIENCES
OLD DOMINION UNIVERSITY
NORFOLK, VIRGINIA 23529

NUMERICAL MODELING STUDY OF THE GULF OF MEXICO BASIN: SKILL ASSESSMENT

By

B. L. Lipphardt, Jr.
A.D. Kirwan, Principal Investigator

Final Report
For the period March 25, 1993 through June 30, 1996

Prepared Under Contract for
Don Johnson
Naval Research Laboratory (NRL-SSC)
Code 7322
Stennis Space Center, MS 39529-5004

Under
Research Contract N00014-93-C-6011
Dollar Amount: $64,542.00
Competitively Awarded

August 1996

DISCLAIMER NOTICE

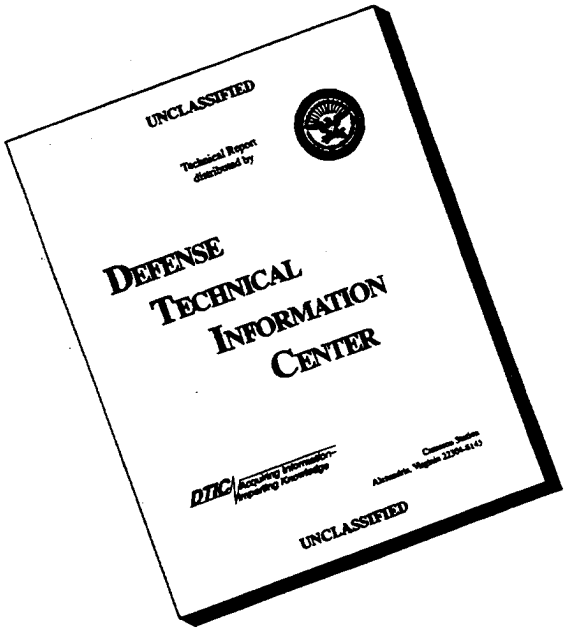

THIS DOCUMENT IS BEST QUALITY AVAILABLE. THE COPY FURNISHED TO DTIC CONTAINED A SIGNIFICANT NUMBER OF PAGES WHICH DO NOT REPRODUCE LEGIBLY.

DEPARTMENT OF OCEANOGRAPHY
COLLEGE OF SCIENCES
OLD DOMINION UNIVERSITY
NORFOLK, VIRGINIA 23529

NUMERICAL MODELING STUDY OF THE GULF OF MEXICO BASIN: SKILL ASSESSMENT

By

B. L. Lipphardt, Jr.
A.D. Kirwan, Principal Investigator

Final Report
For the period March 25, 1993 through June 30, 1996

Prepared Under Contract for
Don Johnson
Naval Research Laboratory (NRL-SSC)
Code 7322
Stennis Space Center, MS 39529-5004

Under
Research Contract N00014-93-C-6011
Dollar Amount: $64,542.00
Competitively Awarded

Submitted by the
Old Dominion University Research Foundation
P.O. Box 6369
Norfolk, VA 23508-0369

August 1996

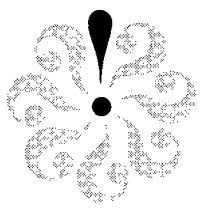

REPORT DOCUMENTATION PAGE

Form Approved
OMB No. 0704-0188

1. AGENCY USE ONLY (Leave blank)	2. REPORT DATE	3. REPORT TYPE AND DATES COVERED
	August 1996	Final - 93 March 25 to 96 June 30

4. TITLE AND SUBTITLE

"Numerical Modeling Study of the Gulf of Mexico Basin: Skill Assessment"

5. FUNDING NUMBERS

C-N00014-93-C-6011

6. AUTHOR(S)

B. L. Lipphardt, Jr.
A. D. Kirwan, Jr.

7. PERFORMING ORGANIZATION NAME(S) AND ADDRESS(ES)

A. D. Kirwan, Jr.
Center Coastal Physical Oceanography
Old Dominion University
Norfolk, VA 23529

8. PERFORMING ORGANIZATION REPORT NUMBER

96-02

9. SPONSORING/MONITORING AGENCY NAME(S) AND ADDRESS(ES)

Naval Research Laboratory
NRL-SSC
Code 3250, Contracts Office
Stennis Space Center, MS 39529-5004

10. SPONSORING/MONITORING AGENCY REPORT NUMBER

CR/7332--96-0003

11. SUPPLEMENTARY NOTES

12a. DISTRIBUTION/AVAILABILITY STATEMENT

Unclassified, Unlimited

12b. DISTRIBUTION CODE

13. ABSTRACT *(Maximum 200 words)*

This report contains the results of an assessment of a three dimensional primitive equation model simulation of the Gulf of Mexico for the year 1993, using surface drifter observations collected as part of the SCULP program. The assessment focuses mainly on the surface circulation of the Louisiana-Texas shelf. The model is fully thermodynamic, and it assimilates both TOPEX and ERS-1 altimetric data. The drifter observations were used to assess the model's ability to accurately describe the surface circulation on the Louisiana-Texas shelf. Twenty-six model drifter trajectories were used to make side-by-side comparisons between the model and observations on this shelf. The statistical properties of these 26 modeled and observed drifters were also compared.

This assessment shows that the model produces many mesoscale flow structures similar to those seen in the observations. Nevertheless, the model generally does not well describe specific observed shelf circulation events. Errors in the wind field used to force the model are suspected to be an important cause of these descrepancies. Apparently, these wind forcing errors masked any underlying problems in the model's ability to describe the dynamics on the shelf.

14. SUBJECT TERMS

15. NUMBER OF PAGES

16. PRICE CODE

17. SECURITY CLASSIFICATION OF REPORT	18. SECURITY CLASSIFICATION OF THIS PAGE	19. SECURITY CLASSIFICATION OF ABSTRACT	20. LIMITATION OF ABSTRACT
Unclassified	Unclassified	Unclassified	Unclassified

Abstract

This report contains the results of an assessment of a three dimensional primitive equation model simulation of the Gulf of Mexico for the year 1993, using surface drifter observations collected as part of the SCULP program. The assessment focuses mainly on the surface circulation of the Louisiana–Texas shelf. The model is fully thermodynamic, and it assimilates both TOPEX and ERS–1 altimetric data. The drifter observations were used to assess the model's ability to accurately describe the surface circulation on the Louisiana–Texas shelf. Twenty six model drifter trajectories were used to make side–by–side comparisons between the model and observations on this shelf. The statistical properties of these 26 modeled and observed drifters were also compared.

This assessment shows that the model produces many mesoscale flow structures similar to those seen in the observations. Nevertheless, the model generally does not well describe specific observed shelf circulation events. Errors in the wind field used to force the model are suspected to be an important cause of these discrepancies. Apparently, these wind forcing errors masked any underlying problems in the model's ability to describe the dynamics on the shelf.

Contents

List of Tables

List of Figures

1 Introduction

This report contains the results of our assessment of the skill of an advanced thermodynamic three–dimensional circulation model in describing the surface currents in the Gulf of Mexico (GOM). The model that we have assessed is a three–dimensional primitive equation model that assimilates altimetric data on a track–by–track basis. The simulation period was one year, representing the year 1993.

Our assessment consists largely of comparisons between the model surface velocity field and satellite tracked drifting buoy observations plus some historical circulation data. We focus primarily on the surface circulation of the Louisiana–Texas (LATEX) shelf, since most of the available drifter observations are from that region. Surface drifter trajectories collected as part of the Surface CUrrent Lagrangian Program (SCULP) were provided by P. P. Niiler at the Scripps Institution of Oceanography.

2 Model Description

The model assessed here is the University of Colorado (CU) model, derived from the Princeton ocean model (Blumberg and Mellor, 1987) and applied to the GOM. It is a fully thermodynamic three–dimensional primitive equation model. The CU model has a new mixed layer formulation developed by L. Kantha, and it assimilates both TOPEX and ERS–1 altimetric data on a track–by–track basis using an optimal interpolation scheme.

The model has 1/5 degree resolution in longitude, while latitudinal resolution starts at 1/5 degree (between 18° and 28° latitude) and becomes finer moving northward, to 1/25 degree resolution above 30° latitude. It uses 21 vertical σ levels.

The model was initialized using climatology, and was forced with 6–hourly FNOC wind data from a 1.25° grid, interpolated onto the model grid. Tidal effects are *not*

included. The model has open boundaries at the Yucatan Straits, where monthly mean transport, temperature, and salinity are used to prescribe the inflow conditions, and at the Florida Straits, with a prescribed outflow derived from recent observations there. Inflow from the Mississippi River is constant and is specified at two locations (Atchafalaya and Mississippi). The model was run for one year, with wind and runoff appropriate for 1993.

3 Summary of Drifter Observations

The SCULP drifter program launched a total of 374 drifters between 2 June 1993 and 21 October 1994. Two hundred of these drifter trajectories were 50 days or more in length, and all drifters were launched near the center of the LATEX shelf. Figure 1 shows the Gulf of Mexico, with the SCULP drifter launch region on the LATEX shelf. The bulk of the SCULP drifter observations occurred between October 1993 and October 1994, as shown in Figure 2. These observations do *not* have an equal seasonal distribution, since most of them occurred either between October 1993 and April 1994 (winter–early spring) or between July 1994 and October 1994 (summer–early fall).

While many of the drifter observations were made during 1994, after the end of the model simulation period, it was useful to look at all of the drifter trajectories collectively at first, to determine what they revealed about the LATEX shelf circulation. To better understand possible mechanisms for transport of water off the LATEX shelf, we focused only on the 200 trajectories that were of at least 50 days duration. These 200 "long–lived" drifters were divided into four categories that described their circulation pattern relative to the deployment region. Table 1 shows the circulation pattern and number of drifters associated with each category. Figure 3 shows a simplified schematic description of the four circulation pathways described by these categories.

Note that the 200 long–lived drifters are distributed approximately equally among

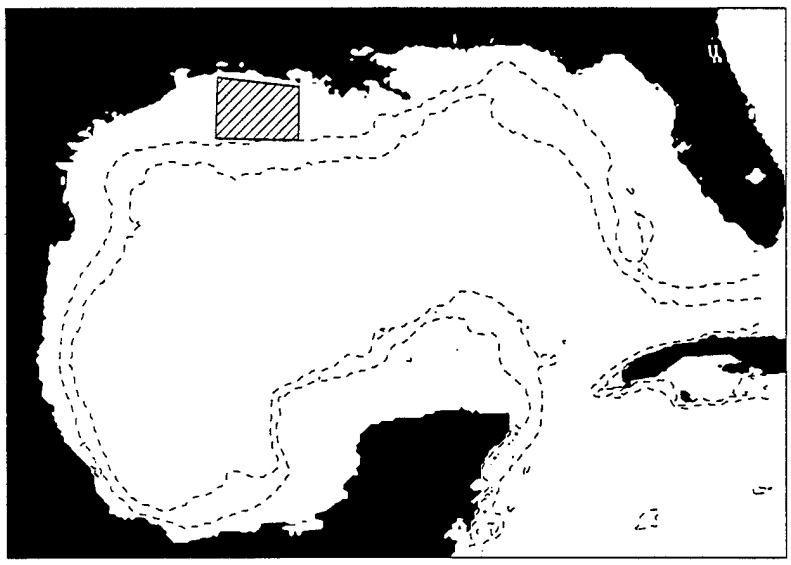

Figure 1: The Gulf of Mexico – the hatched box represents the launch region for the SCULP drifters

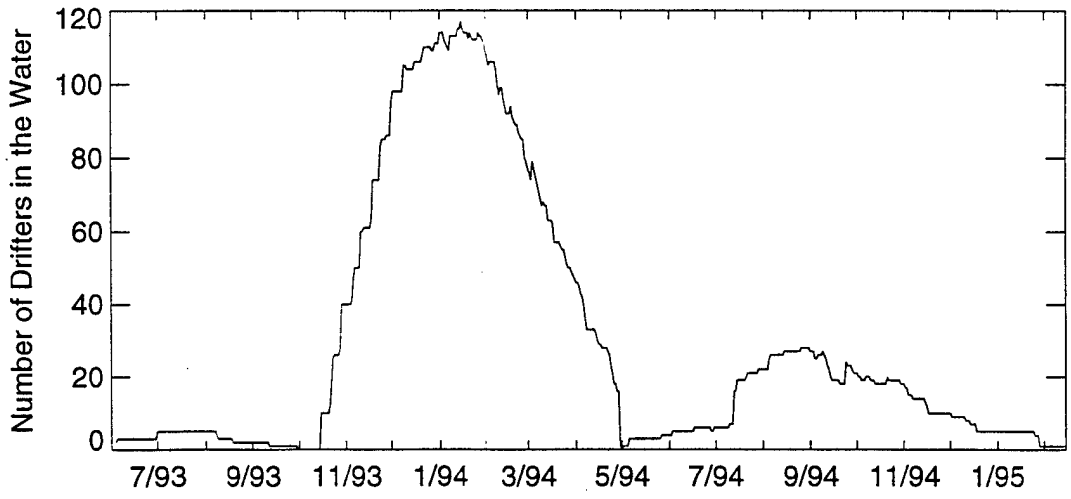

Figure 2: Distribution of SCULP drifter observations for trajectories of at least 50 days duration

Table 1: Categories of SCULP drifters with duration of at least 50 days

Category	General flow path	# Drifters
1	Southwest along inner shelf	39
2	Southwest along inner shelf and out into GOM near 25° latitude	49
3	South or east into open GOM	48
4	Remained on LATEX shelf	64

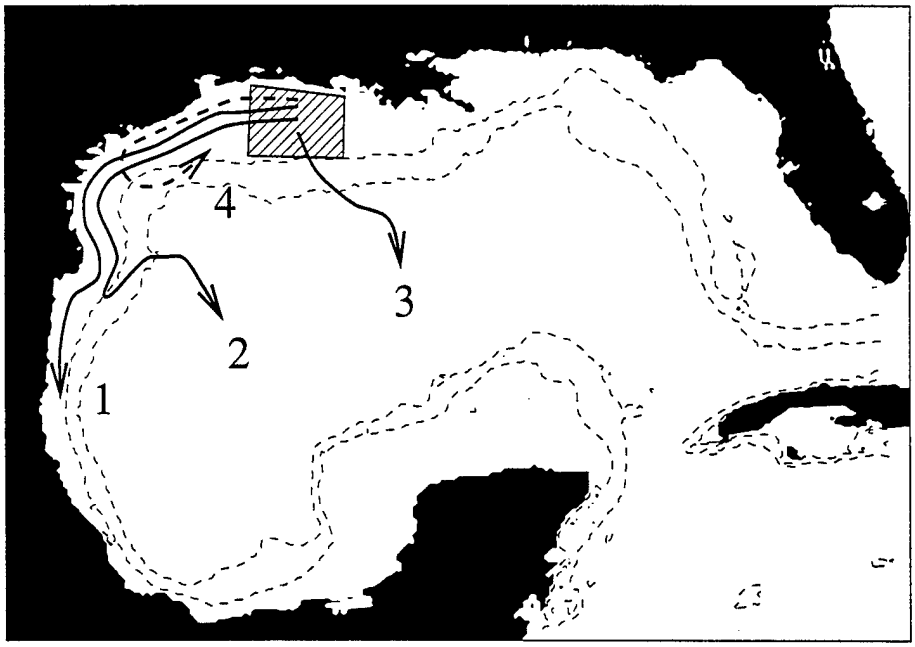

Figure 3: Simplified representations of four flow paths described by long–lived SCULP drifters

the four flow path categories. The largest group of drifters are in category 4, the drifters that remain on the LATEX shelf ("recirculate") for their entire lifetime. Observation of a large number of recirculating drifters supports the concept of a persistent LATEX shelf gyre, as discussed by Cochrane and Kelly (1986), but the significant number of drifters in categories 1–3 clearly shows that transport off the LATEX shelf is common.

The category 1 drifters leave the LATEX shelf by continuing south along the Mexican shelf. Category 2 drifters leave the LATEX shelf near 25° latitude, while category 3 drifters migrate directly into the deep GOM. Many category 2 and 3 trajectories are the result of shelf circulation induced by Loop Current rings in the western GOM.

4 Assessment Plan

4.1 Shelf circulation

The following comparisons will be made to assess the model's ability to accurately describe the surface circulation on the LATEX shelf:

- *Side–by–side drifter comparison* – Twenty six SCULP drifter trajectories will be compared to trajectories from model drifters (initialized at the same time and place), to determine how well the model describes surface flow features apparent in the drifter observations.
- *Off–shelf flow characteristics* – The 26 model generated drifter trajectories will be examined to determine whether they describe the four major flow pathways (categories 1–4) apparent in the SCULP drifter data.
- *Statistical comparisons*
  - Modeled and observed daily drifter positions will be compared, and position errors will be calculated.

- Lag correlations between each of the perturbation velocity components will be calculated and compared for each observed and modeled drifter.
- Observed and modeled Reynolds stress components will be compared for each drifter.
- For individual drifters, the Lagrangian diffusion tensor will be calculated for the first ten days of each drifter record. Diffusion tensors for observed and modeled drifters will be compared.
- Representative Lagrangian diffusion coefficients (for the first ten days of each record) will be compared for each observed and modeled drifter.
- For the last eight weeks of the year, weekly mean model surface velocities on the LATEX shelf will be compared to weekly mean velocities derived from SCULP drifter trajectories.

- *Shelf event study* – Evolving groups of drifter trajectories will be compared with the evolving model surface velocity field to determine whether specific flow events apparent in the drifter data are described by the model.
- *Comparison with historical data* – Mean monthly surface velocities will be analyzed to determine if the model describes the observed reversal of the coastal current during July and August described by Cochrane and Kelly (1986).

4.2 Deep Gulf circulation

In the deep Gulf, model surface velocities will be compared with satellite images of sea surface height, to determine how well the model describes the mesoscale flow features apparent in the imagery. This comparison is simply a check on how well the model assimilates the altimeter data.

5 Results

5.1 Side–by–side drifter comparison

Twenty six model–generated drifter trajectories were available for comparison with observations. These drifters were initialized at times and locations that correspond to the launch of a SCULP drifter, so that a detailed comparison between model and observed drifter trajectories is possible. Although the model simulation ended on 1 January 1994 and many of the observed drifters continued to provide position information well beyond this date, all of the model generated trajectories were at least 44 days in length, with some as long as 72 days.

In general, the model generated trajectories exhibited many qualitative properties of the observed drifters – they tended to move in the same general direction and with comparable velocity scales. Several of the model drifters, however, became widely separated from the observed trajectory over time.

Figure 4 shows four cases of good agreement between the model and observed drifter trajectories. The most recent drifter position (on 25 December 1993) is marked with a diamond, and five day intervals along each trajectory are marked with an 'X'. The drifter number is shown at the upper left in each panel. Note that even in these cases which show comparatively good agreement between the observations and the model, there are several flow details apparent in the observed trajectories that are not apparent in the model.

Figure 5 shows four examples of poor agreement between the model and observed drifters. The trajectories are marked as in Figure 4. Although some of these drifters initially follow the observed path, all of them diverge markedly from the observations over time, indicating that the model surface velocities are in error. The upper left panel in Figure 5 shows a case of particularly poor agreement, since the model trajectory

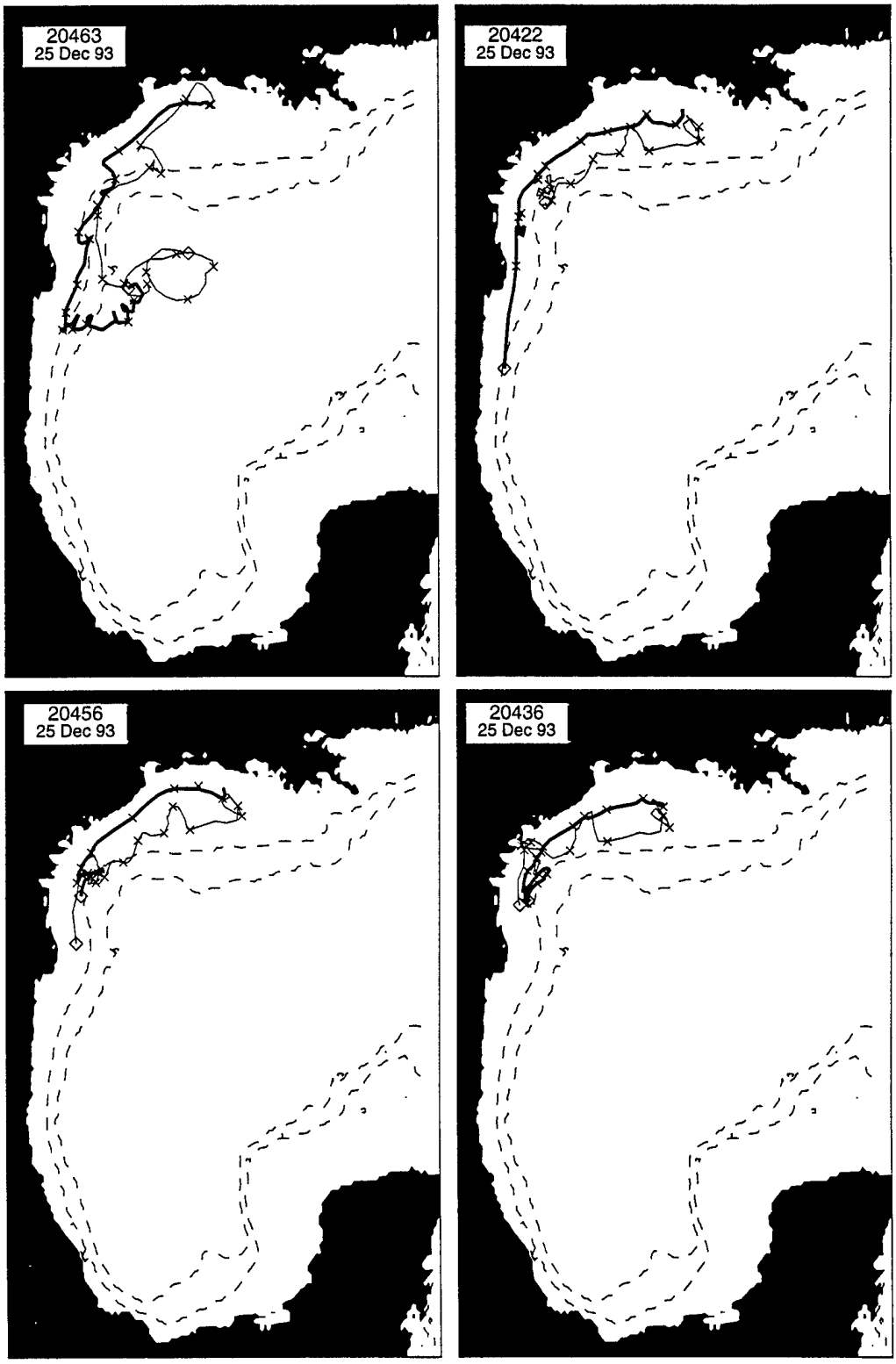

Figure 4: Side–by-side comparison of four SCULP drifters (heavy black line) with model generated drifters (thin black line). These four drifters show rather good agreement between the observations and the model.

Table 2: Categories of model and observed drifters

Category	# Observed drifters	# Model drifters
1	2	6
2	16	4
3	8	7
4	0	9

moves immediately southeastward, while the observed path is seen to be along–shelf, toward the southwest.

5.2 Off–shelf flow characteristics

The 26 drifters simulated with the model were categorized by their flow path relative to their launch location. using the same categories as shown in Table 1. Only six of the 26 model trajectories fell into the same category as the observed drifter (23% agreement). The distribution of model and observed drifters in each category is shown in Table 2. Note that none of the 26 drifters selected to be simulated by the model came from category 4, since the focus of this comparison was on off–shelf transport mechanisms.

Although the agreement between model and observations was poor for this comparison, it should be noted that model drifters existed for each category, indicating that the model is capable of describing all of the flow pathways present in the observations, including the three distinct mechanisms of off–shelf transport. The fact that the model generated 9 drifters in category 4 ("recirculating" drifters) when none were present in the observations suggests that the model is missing some important off–shelf transport events.

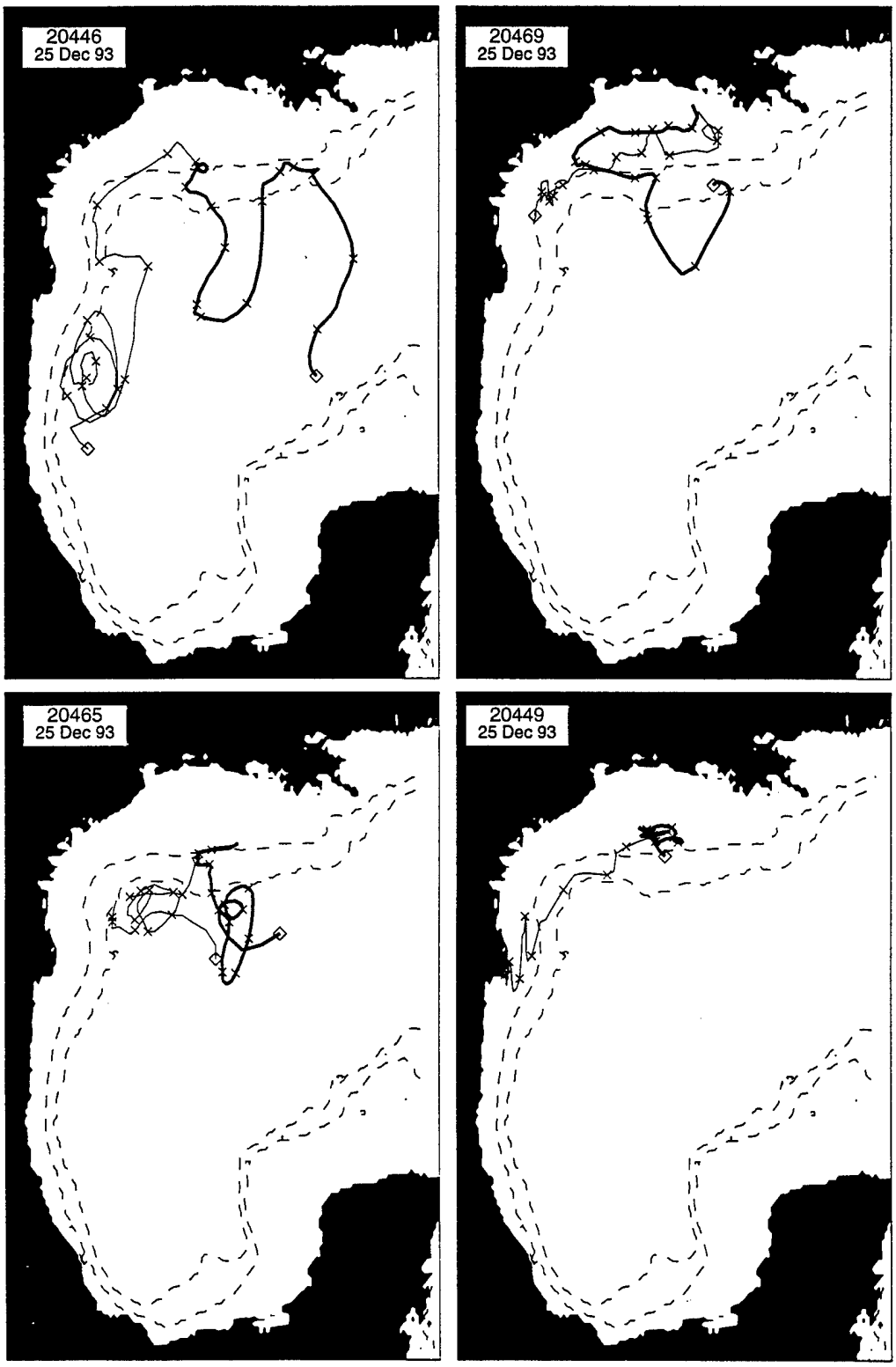

Figure 5: Side–by-side comparison of four SCULP drifters with model generated drifters, similar to Figure 4. These four drifters show poor agreement between the observations and the model.

5.3 Statistical comparisons

The following sections contain a discussion of the results of the six statistical comparisons that were made for 26 observed and modeled drifter trajectories. The details of each statistical comparison, and individual results, are contained in Appendix A.

5.3.1 Drifter position errors

As discussed in section 5.1, the observed and modeled drifter trajectories were often qualitatively similar, but many of the drifter pairs became widely separated over time. The position error plots shown in figures 8–14 show this. Typically, the modeled drifter trajectory remains close to the observed trajectory for 10–20 days. After that period, position errors increase, often to as much as 200–300 km after about 50 days.

5.3.2 Velocity correlations

The velocity lag correlation tensor C_{ij} is defined in Appendix A, section A.2. From the time series plots of C_{ij} shown in figures 15 – 40, it is apparent that the observed and modeled drifters exhibit quite different correlation characteristics over the 30–day interval shown. It is interesting to note, however, that both the C_{11} and C_{22} components often have very similar correlation characteristics over lag intervals of 0–10 days. The C_{12} and C_{21} correlations typically did *not* agree well, even over small lag intervals.

The lag time where C_{ij} first reaches zero, $\hat{\tau}_{ij}$, is also defined in Appendix A, section A.2. The $\hat{\tau}_{11}$ and $\hat{\tau}_{22}$ data in Table 3 show that, while C_{11} and C_{22} often show good agreement over small lag intervals, there are several cases where the lag time of the first zero crossing for these components differs by as much as 8 days or more.

5.3.3 Reynolds stresses

The components of the Reynolds stress, R_{ij}, are defined in Appendix A, section A.3.

The scatter plots in Figure 41 show that, for most of the modeled drifters, the three R_{ij} components differ substantially from the observed values. In addition, since the data points are scattered uniformly about the line of perfect agreement, there is no clear trend in the R_{ij} errors.

5.3.4 Lagrangian diffusion tensors

The Lagrangian diffusion tensor, L^2_{ij}, is defined in Appendix A, section A.4. Figures 42 – 67 show times series of each L^2_{ij} component. Analysis of these time series reveals the following:

- For 17 out of 26 drifters simulated, the modeled L^2_{11} was *greater* than the observed value after 10 days, so that the model typically *overestimates* L^2_{11}.
- For 21 out of 26 drifters simulated, the modeled L^2_{12} was *less* than the observed value after 10 days, so that the model typically *underestimates* L^2_{12}.
- For 22 out of 26 drifters simulated, the modeled L^2_{21} was *greater* than the observed value after 10 days, so that the model typically *overestimates* L^2_{21}.
- For 24 out of 26 drifters simulated, the modeled L^2_{22} was *greater* than the observed value after 10 days, so that the model typically *overestimates* L^2_{22}.

5.3.5 Lagrangian diffusion coefficients

The Lagrangian diffusion coefficients, D_{ij}, are defined in Appendix A, section A.5. The scatter plots in figure 68 show that the modeled D_{ij} did not agree well with the observations. Specifically:

- Though the D_{11} data are quite scattered, the model tends to *overestimate* D_{11}.
- In all but three cases, the model *underestimates* D_{12}.
- In all but four cases, the model *overestimates* D_{21}.

- In all cases but one, the model *overestimates* D_{22}.

5.3.6 Weekly mean surface velocities

The results presented in section A.6 show that, near the LATEX shelf break, the model does not describe the surface flow accurately. Most of the shelf break velocity comparisons shown in Figures 69 – 72 show significant errors in both magnitude and direction.

5.4 Shelf event study

The SCULP drifter observations during October and November 1993 include two dynamical "events" on the LATEX shelf. The first event is a change in surface flow direction ("veering") between 28 October and 30 October. On 28 October, the inner shelf surface flow is directed to the southwest. Prior to 30 October, ten drifters distributed across the shelf show a sharp change in direction, moving to the southeast, probably due to a change in surface winds. The second event is the entrainment of one SCULP drifter by an anticyclone at the shelf break between 1 November and 7 November.

The drifter observations that describe these two shelf events were compared with the model surface velocities to determine whether the model accounts for shelf dynamical events like these.

Figure 6 shows the surface current veering event. The model surface velocity field is shown at 2–day intervals between 24 October and 30 October. Each panel also shows 10–15 SCULP drifter trajectories with the current drifter position marked with a diamond. Each drifter trajectory includes 10 days of position history, with 2 day position intervals marked with an 'X'. The drifter trajectories in the bottom two panels of Figure 6 show the sharp direction change associated with the veering event. The model surface velocities between 24 October and 28 October were directed generally

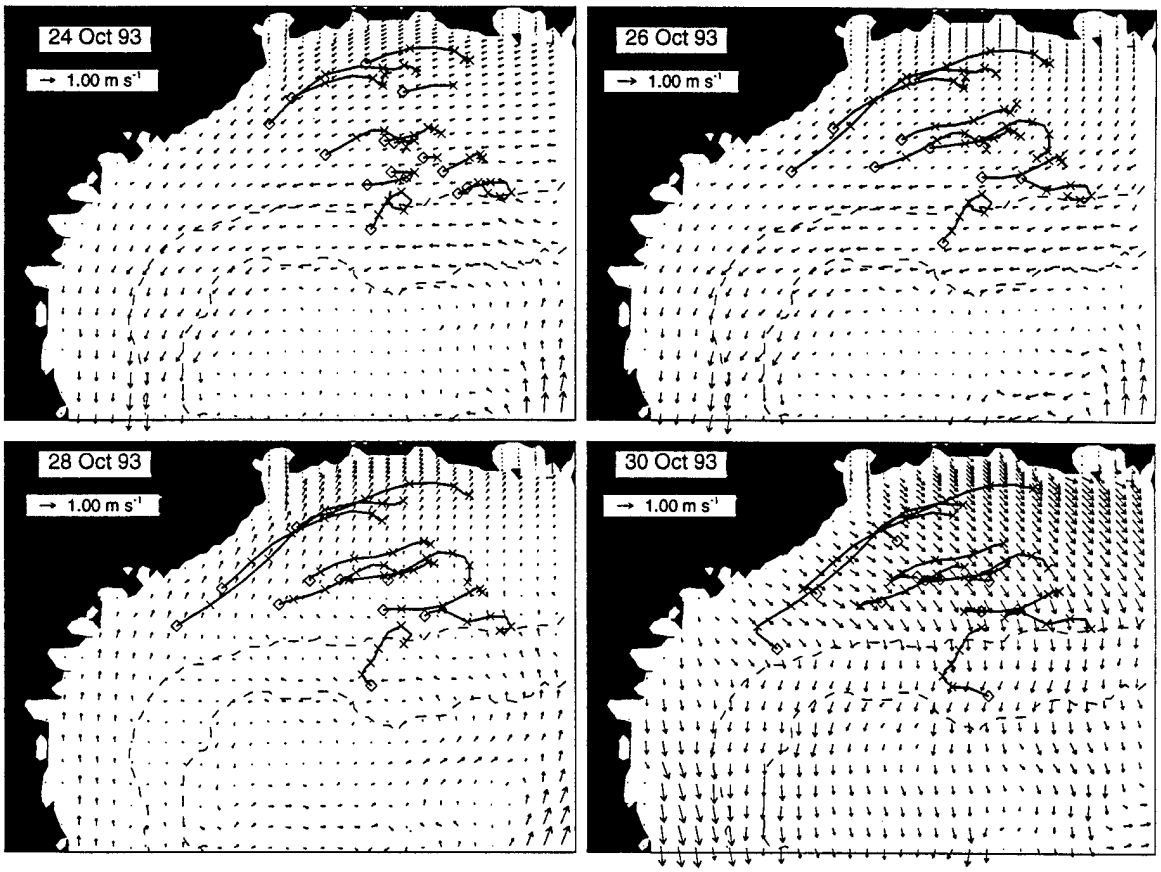

Figure 6: Comparison of model surface velocities with drifter trajectories during an observed surface current veering between 24 October and 30 October.

southwestward (first 3 panels of Figure 6), and show the same veering toward the southeast in on 30 October (fourth panel of Figure 6). For this event, then, the model accurately describes an observed veering in shelf surface currents.

Figure 7 shows the anticyclone entrainment event. Model surface velocities are shown at 2–day intervals between 1 November and 7 November. Again, each panel includes 10–15 SCULP drifter trajectories as in Figure 6. The southernmost drifter in each panel is the drifter that is being entrained in a clockwise sense by an anticyclone located at the shelf break. When the movement of this drifter (generally southeast and south) is compared to the model surface velocity field, it is clear that the model velocities at the shelf break are in error, since the drifter appears to be moving "against

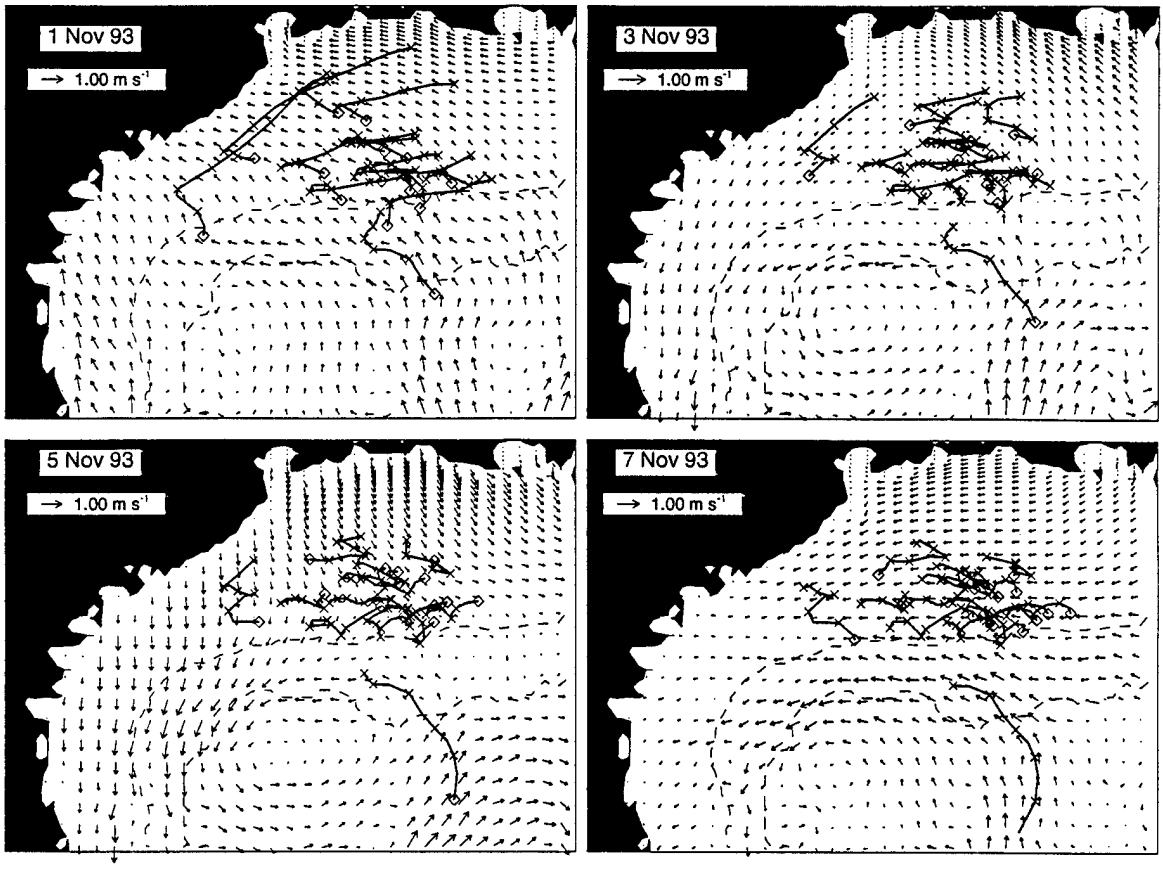

Figure 7: Comparison of model surface velocities with drifter trajectories during an observed entrainment by a shelf break anticyclone between 1 November and 7 November.

the model current". For this event, then, the model does not accurately describe the observed mesoscale flow at the shelf break.

5.5 Comparison with historical data

Cochrane and Kelly (1986) have postulated that the annual surface circulation on the LATEX shelf is dominated by a closed gyre, with nearshore currents generally directed to the southwest, and shelf break currents directed to the northeast. They observed that the nearshore surface currents are directed southwestward for most of the year, but reverse direction to the northeast annually, during July and August. The monthly mean model surface currents on the LATEX shelf for July and August 1993

accurately describe this observed reversal in coastal current. These monthly mean velocities will not be shown here.

5.6 Deep Gulf circulation

To determine whether the model accurately describes the surface mesoscale flow in the deep GOM, model sea surface heights were compared with altimetry and with the trajectory for one drifter that was entrained in a clockwise sense around an anticyclone in the deep GOM. Two model runs were compared; the first run assimilated only TOPEX altimetry data, while the second run assimilated both TOPEX and ERS–1 data. When both TOPEX and ERS–1 data were assimilated, the model accurately described the presence of a strong anticyclone, in good agreement with the drifter trajectory. Additionally, the inclusion of ERS–1 data in the assimilation process greatly improved the accuracy of the anticyclone's position, when compared with the drifter trajectory. This comparison suggests that the assimilation of altimetric data improves the model's ability to describe the surface mesoscale flow field in the deep GOM. Details about this comparison are shown on the World Wide Web at URL http://shaman.colorado.edu/~jkchoi/gom.html.

6 Conclusions

The comparisons discussed above show that the model is capable of describing many of the features of the LATEX shelf surface circulation, but examination of the flow details on the shelf reveals many discrepancies with the model. In the deep GOM, the assimilation of altimetric data is an important model improvement, and results in a more accurate description of the highly variable deep GOM surface mesoscale field. Based on the above comparisons, the following conclusions are made:

- For shelf processes, uncertainties about wind forcing mask any dynamical prob-

lems that *may* exist in model. The comparisons made here illustrate that interpolating wind data from a 1.25° resolution wind array onto the model grid is probably *not* sufficient to permit accurate description of shelf surface flow.

- Model drifters appear to have some of the same qualitative properties as the observed drifters, but some details of the shelf surface flow apparent in the drifter observations are not described by the model. Errors in the model can lead to significant divergence between model and observed drifters over periods less than 50 days.
- Although collectively the model drifters describe the same off–shelf flow paths apparent in the observations, individual drifter comparisons reveal that the model drifters often don't follow the same off–shelf path as the observed drifter.
- The following conclusions can be made regarding the statistics of observed and modeled drifters:
  - Although the modeled drifter positions agreed with observations for 10–20 days, position errors increased to as much as 200–300 km after about 50 days.
  - Although the modeled drifter velocity correlation characteristics were very different from those of the observed drifters, the C_{11} and C_{22} correlations showed generally good agreement over lag intervals of 0–10 days.
  - Modeled drifter Reynolds stresses differed substantially from the observed values, with no trend apparent in the errors.
  - After 10 days, the model overestimated three components of the Lagrangian diffusion tensor (L_{11}^2, L_{21}^2 and L_{22}^2), and it underestimated the remaining component (L_{12}^2).
  - After 10 days, the model overestimated three of the Lagrangian diffusion coefficients (D_{11}, D_{21} and D_{22}), and it underestimated the remaining coefficient

(D_{12}). This is not surprising, in view of the results obtained for L_{ij}^2.

  - Comparisons of weekly mean surface velocities show errors in both direction and magnitude between the model and the drifter observations.

- The model accurately describes a strong surface current veering event that was observed on the shelf. Errors in the model's surface mesoscale field at the shelf break prevent the model from accounting for an observed entrainment of one drifter by a shelf break anticyclone.

- The model accurately describes a July–August coastal flow reversal that is observed in historical data.

- In the deep Gulf, the assimilation of both TOPEX and ERS–1 altimeter data results in a model surface mesoscale flow field that agrees well with one observation of a drifter entrained by an anticyclone. The assimilation of multiple altimeter data sets (TOPEX and ERS–1) results in improved model accuracy in describing deep GOM surface flows.

7 Recommendations

The following recommendations are made, based on this model assessment:

- Before further attempts are made to assess the model's dynamics (particularly on the LATEX shelf), higher resolution wind data should be used to force the model. It is likely that higher resolution wind forcing will reduce the errors observed in the model's surface shelf velocities.

- Since the majority of the SCULP drifter observations occurred during 1994, it would be worthwhile to conduct a model simulation in the GOM for 1994. With model surface velocities from 1994, the comparisons discussed above could be

made with a larger set of drifter observations that span a greater portion of the year, including the spring and early summer.

8 Acknowledgments

We wish to thank L. H. Kantha and J. K. Choi at CCAR, University of Colorado, for their assistance in providing details about their model, as well as making model velocity data available for our analysis. They also were kind enough to calculate 26 model drifter trajectories at our request. We also want to thank P. P. Niiler (Scripps Institution of Oceanography) and W. Johnson (Minerals Management Service) for making the SCULP drifter data available for our use.

A Comparison of Observed and Modeled Drifter Statistics

Six different statistical comparisons were made between observed drifter trajectories and model results. Five of these were direct comparisons between individual observed and modeled drifter trajectories, for the 26 available model drifters. The sixth comparison (for weekly mean surface velocities) was made between weekly mean model surface velocity fields and weekly mean surface velocities derived from groups of SCULP drifter observations.

For the five direct comparisons between observed and modeled drifter trajectories, the trajectory data consisted of one drifter position per day. When the observed and modeled drifter record lengths were unequal, the comparison was based on the shorter of the two record lengths. Drifter velocities were calculated as simple centered differences of the daily drifter positions.

A.1 Drifter position errors

Figures 8 – 14 show time series of drifter position errors (in km) for each of the 26 modeled drifters. Solid lines show east–west errors, and dashed lines show north–south errors. All errors are referenced to the observed drifter position, so that positive errors indicate the modeled drifter is located to the east or north of the observed position.

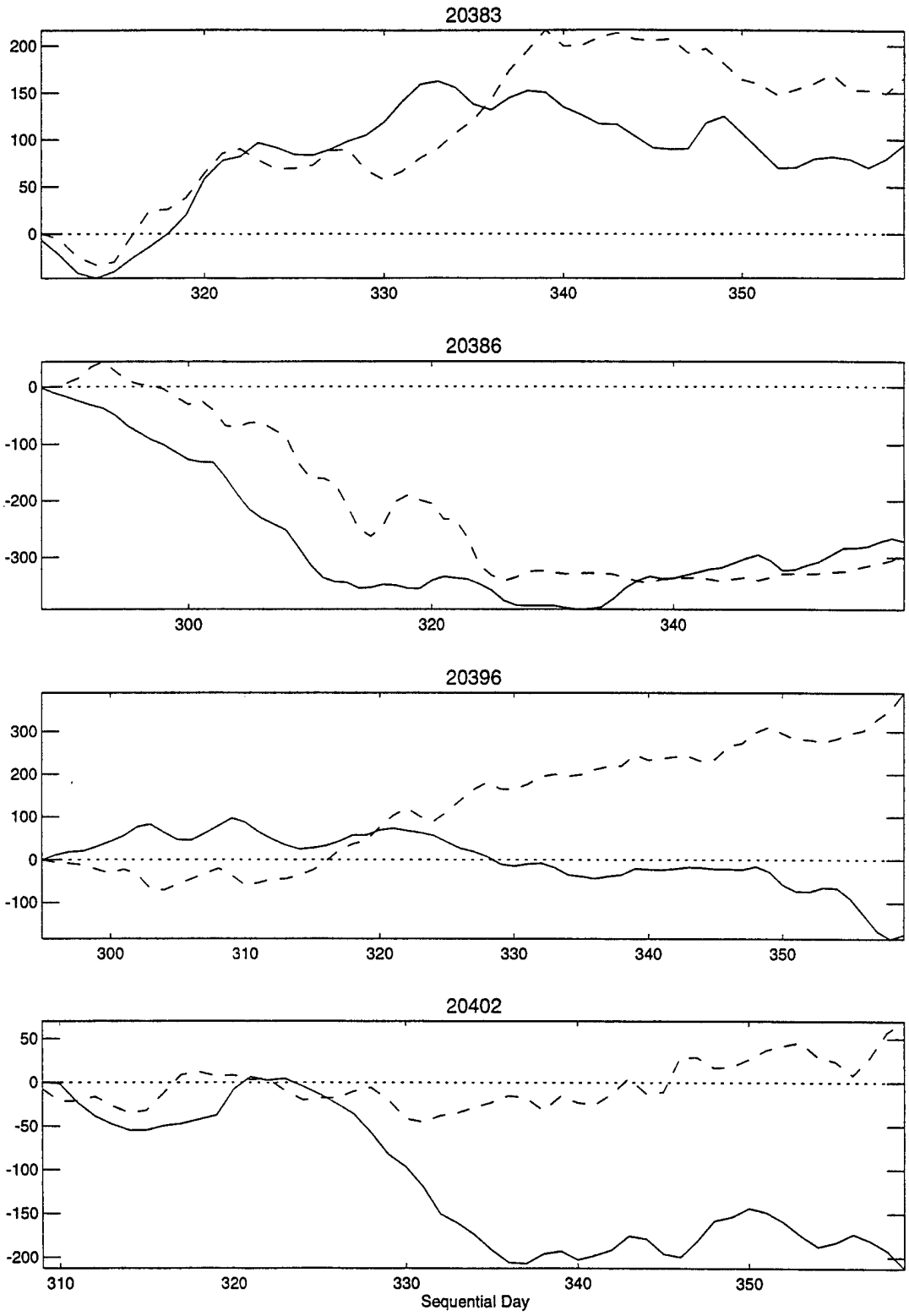

Figure 8: Position errors for drifters 20383 – 20402.

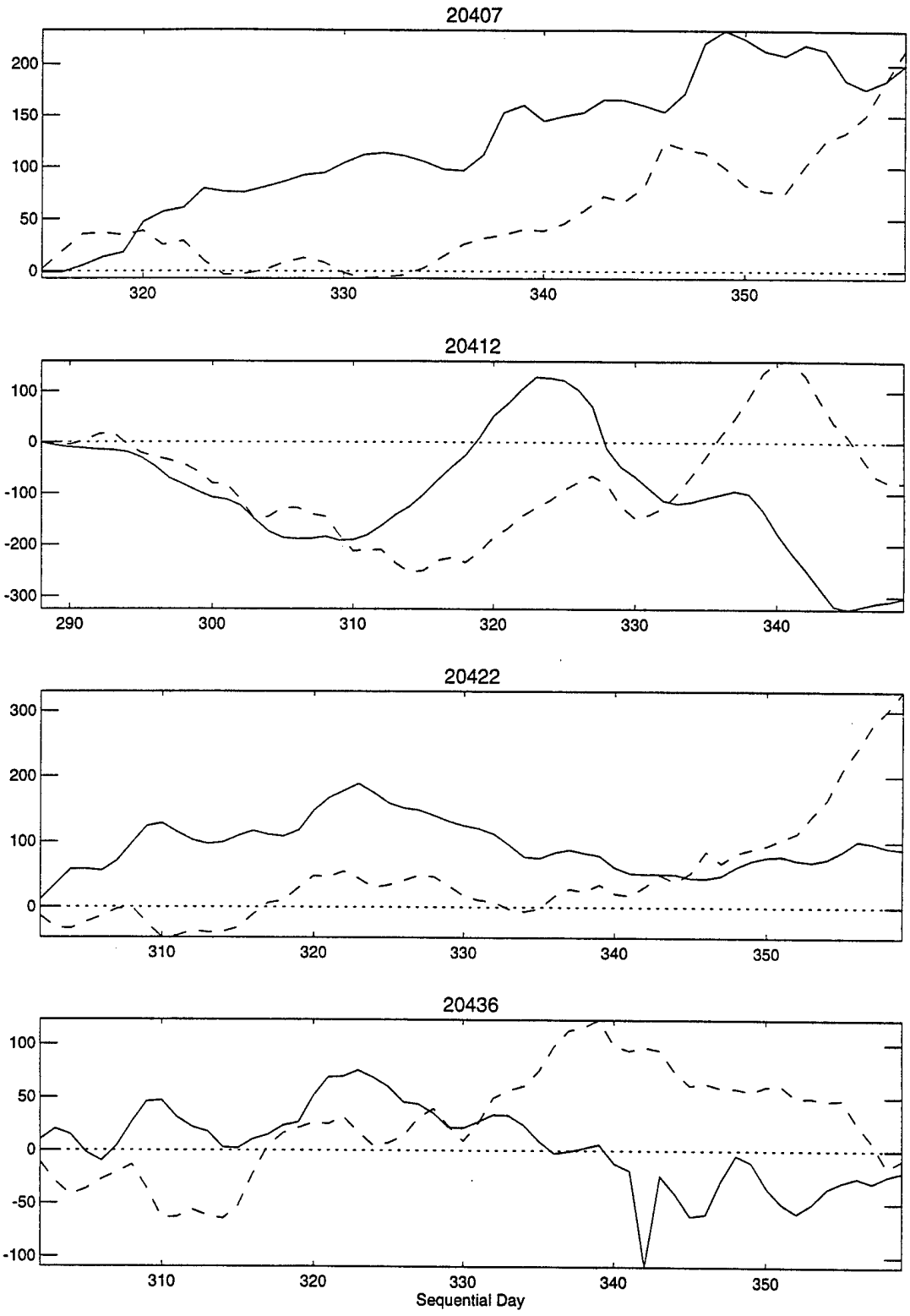

Figure 9: Position errors for drifters 20407 - 20436.

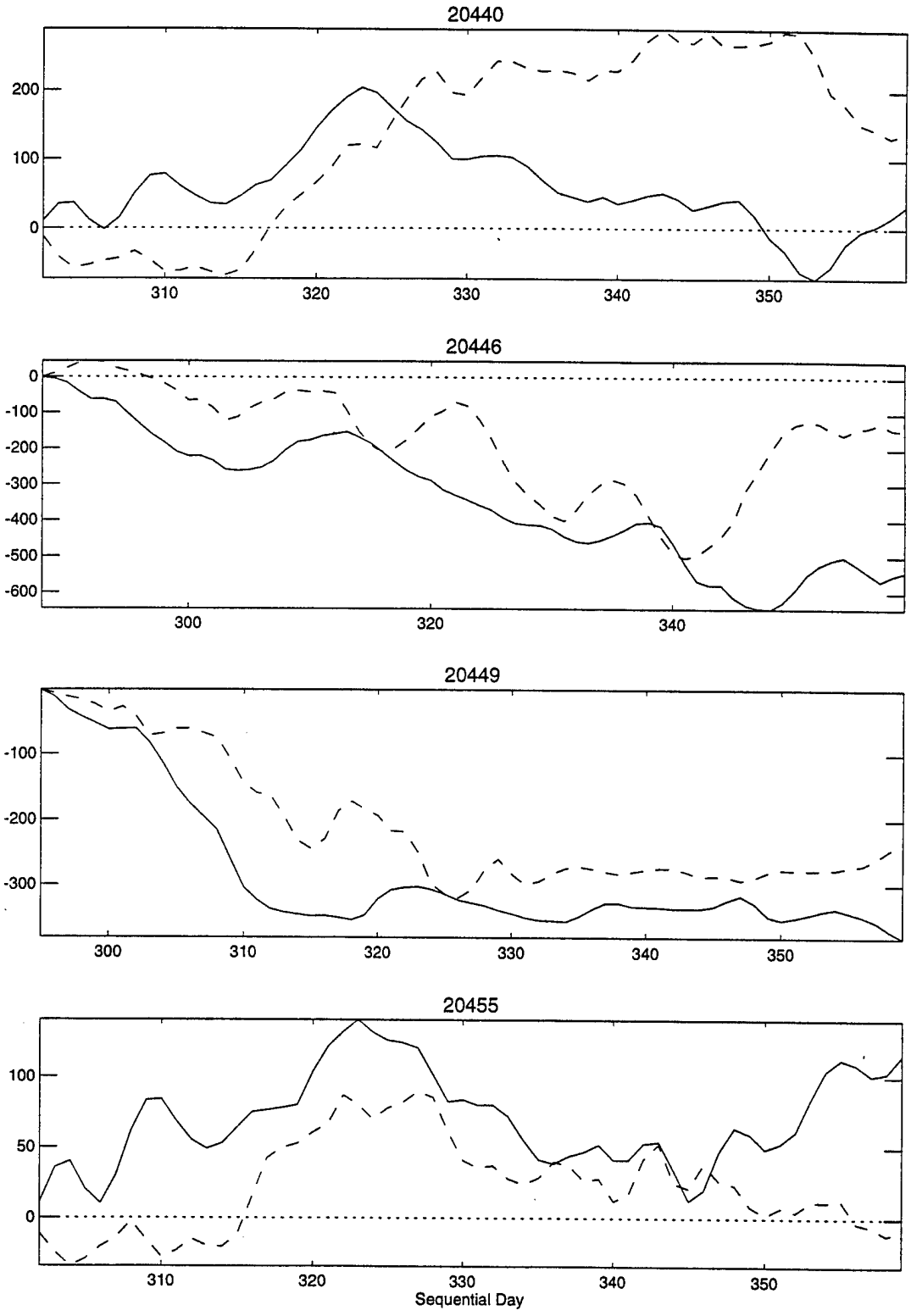

Figure 10: Position errors for drifters 20440 – 20455.

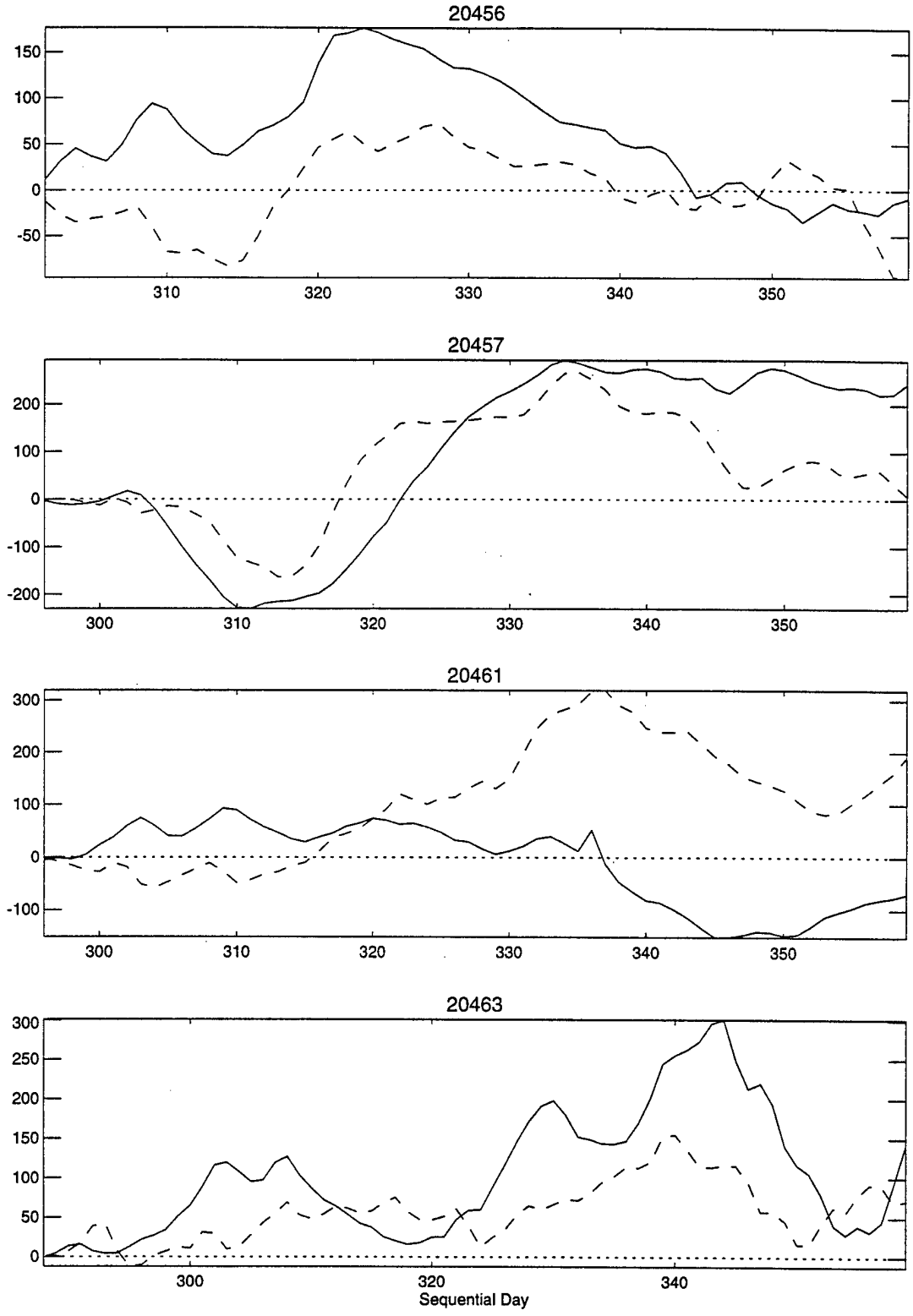

Figure 11: Position errors for drifters 20456 – 20463.

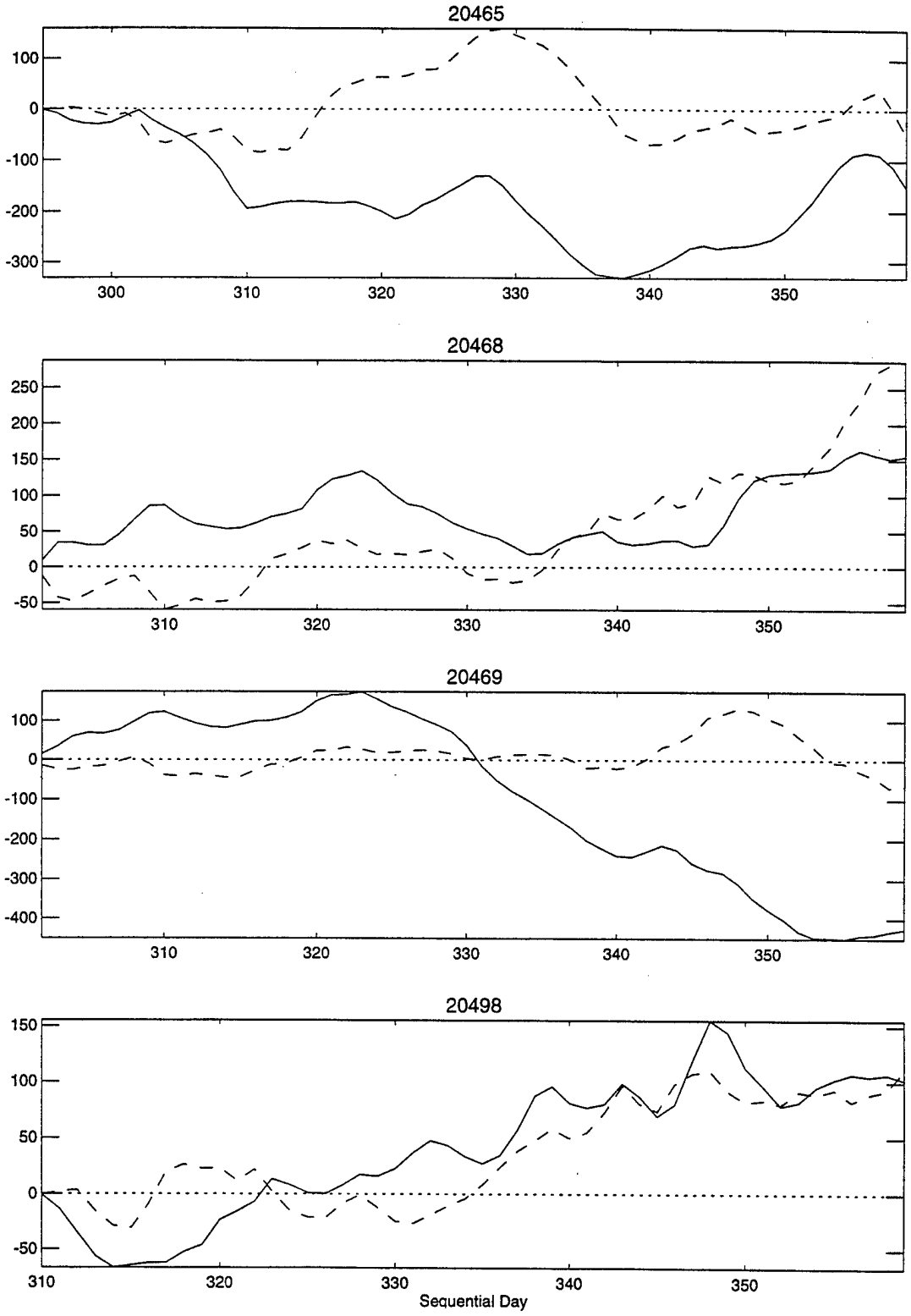

Figure 12: Position errors for drifters 20465 – 20498.

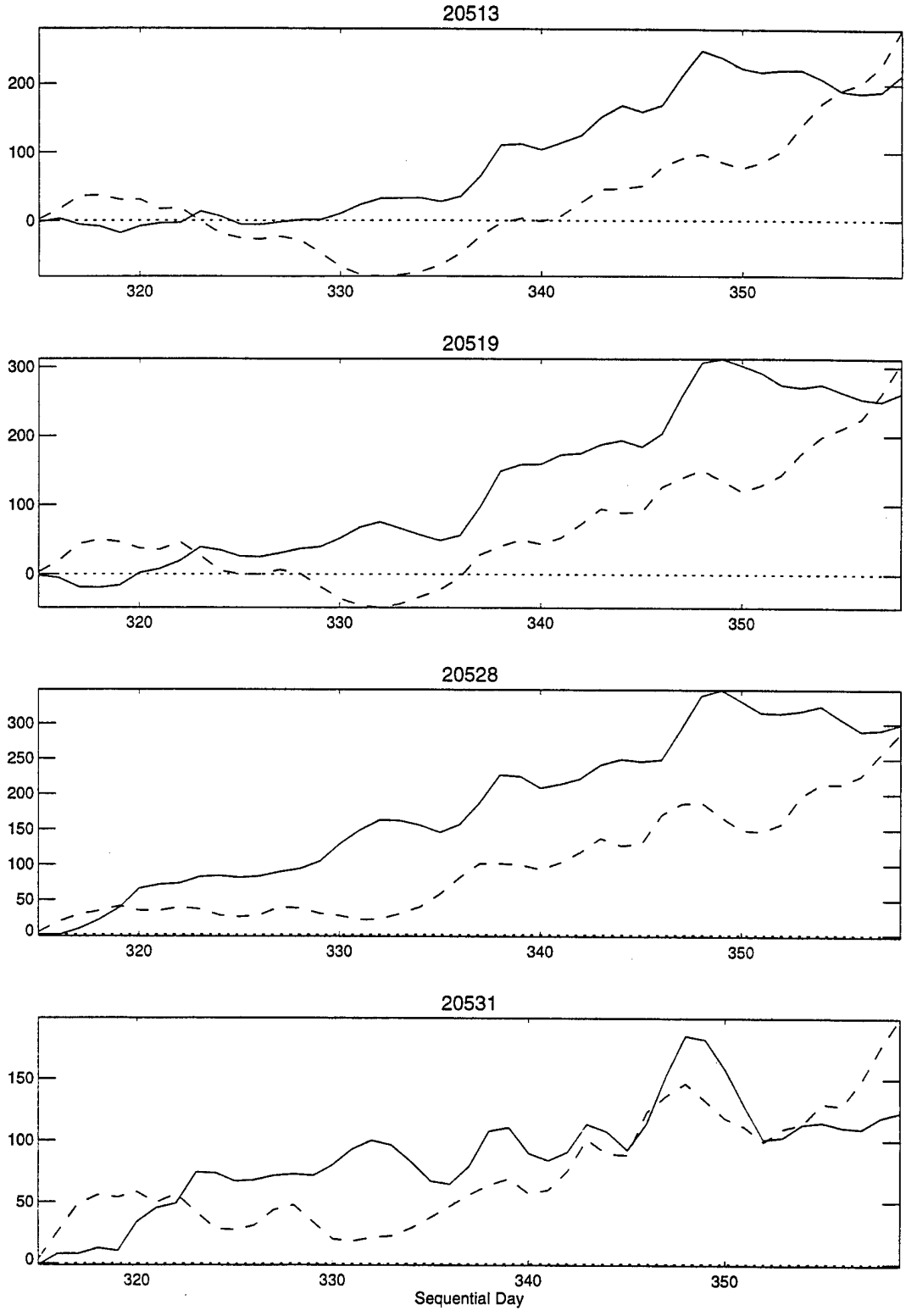

Figure 13: Position errors for drifters 20513 – 20531.

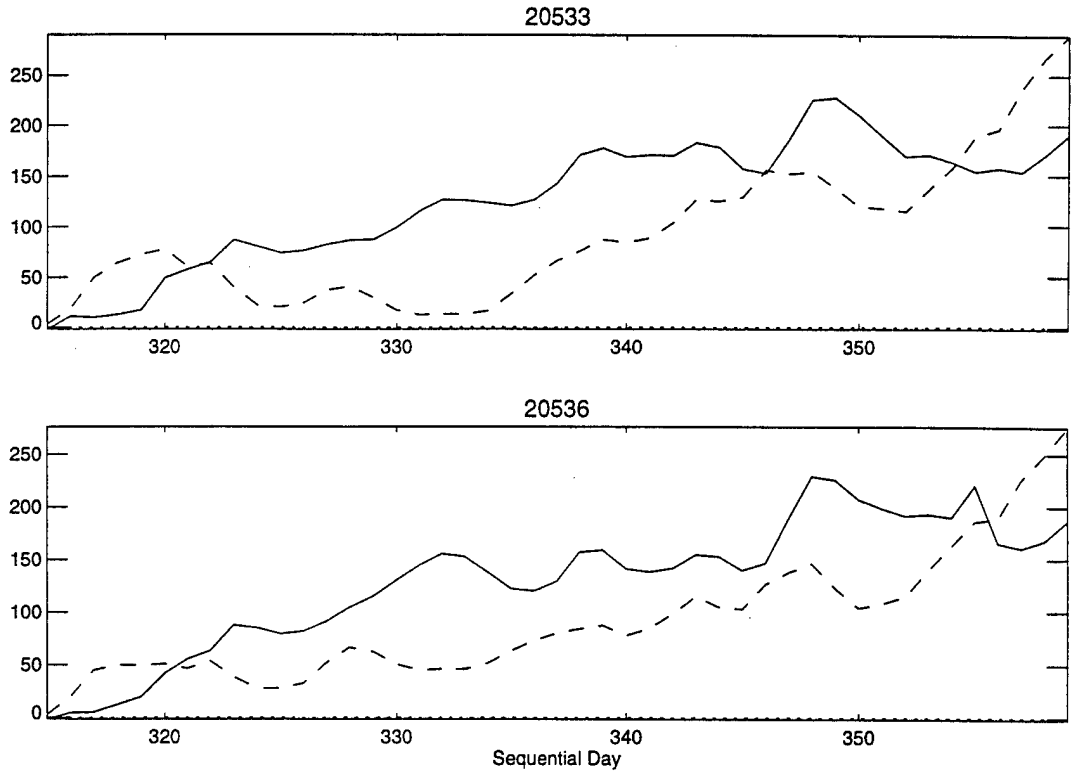

Figure 14: Position errors for drifters 20533 and 20536.

A.2 Velocity correlations

The correlation of the observed and modeled drifter velocity components over time were compared by calculating the lag correlations between each velocity component. Velocity correlations were calculated from daily perturbation velocity estimates, derived from daily positions. Perturbation velocity components u_i were calculated as:

$$u_i = U_i - \bar{u}_i, \qquad i = 1, 2$$

where U_i is the estimated daily velocity, and $\bar{u}_i$ is the mean daily velocity for the drifter record.

The velocity lag correlation for component i with respect to component j is expressed as:

$$C_{ij}(\tau) = \frac{\int_0^{T-\tau} u_i(t) u_j(t+\tau) dt}{||u_i|| ||u_j||}$$

where

$$||u|| = \sqrt{\frac{1}{T} \int_0^T u^2(t) dt}.$$

and T is the length of the drifter record.

Time series of observed and modeled drifter C_{ij} are shown in figures 15 – 40. Correlations for the observed trajectory are shown as solid lines, and correlations for the model trajectory are shown as dashed lines.

One measure of a drifter's correlation time scale is the lag time where C_{ij} first reaches zero, $\hat{\tau}_{ij}$. Table 3 shows values of $\hat{\tau}_{11}$ and $\hat{\tau}_{22}$ for each observed and modeled drifter. The zero crossings for the C_{11} and C_{22} correlations are also marked with a diamond in the top and bottom panels of figures 15 – 40.

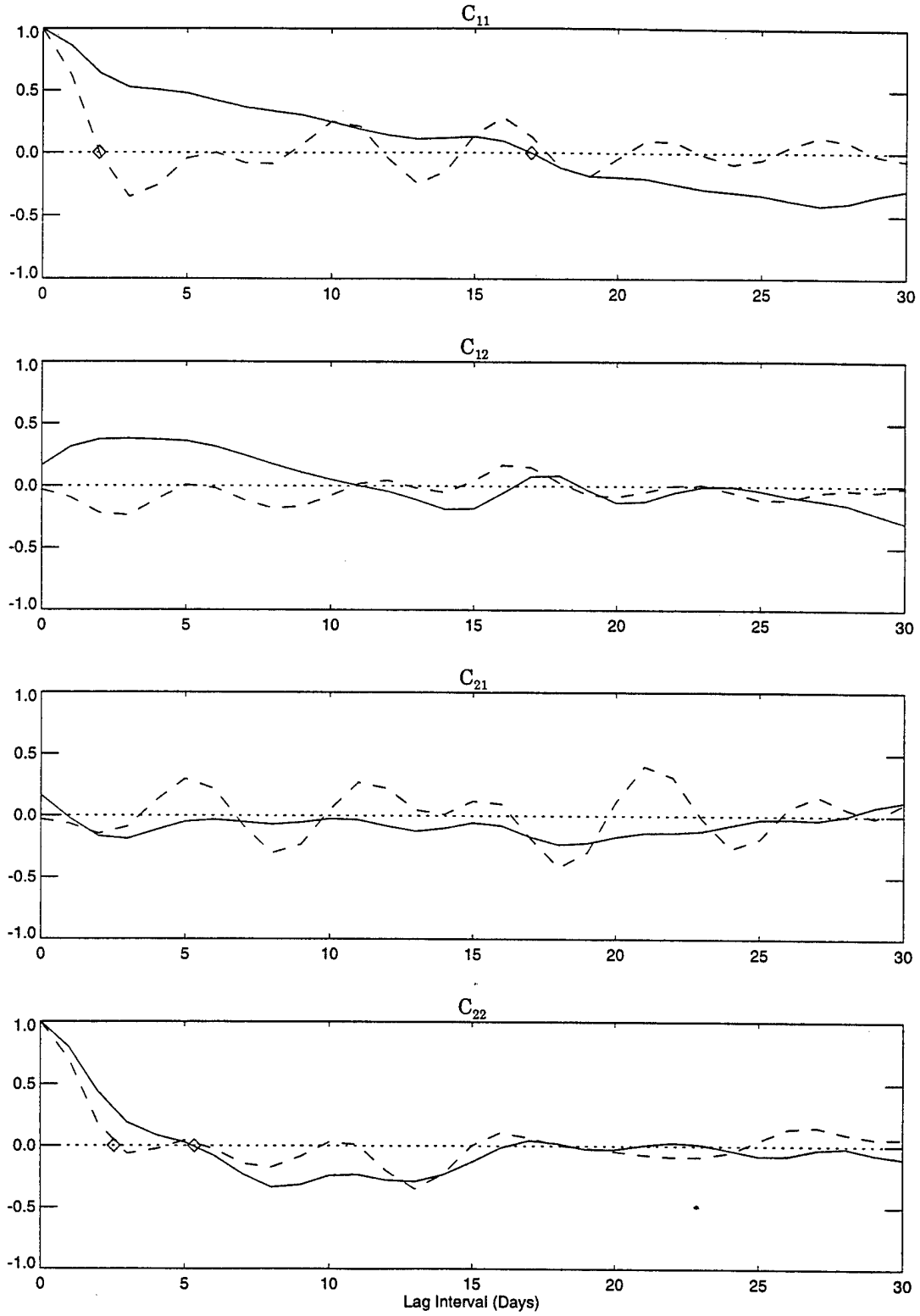

Figure 15: Comparison of C_{ij} for drifter 20383.

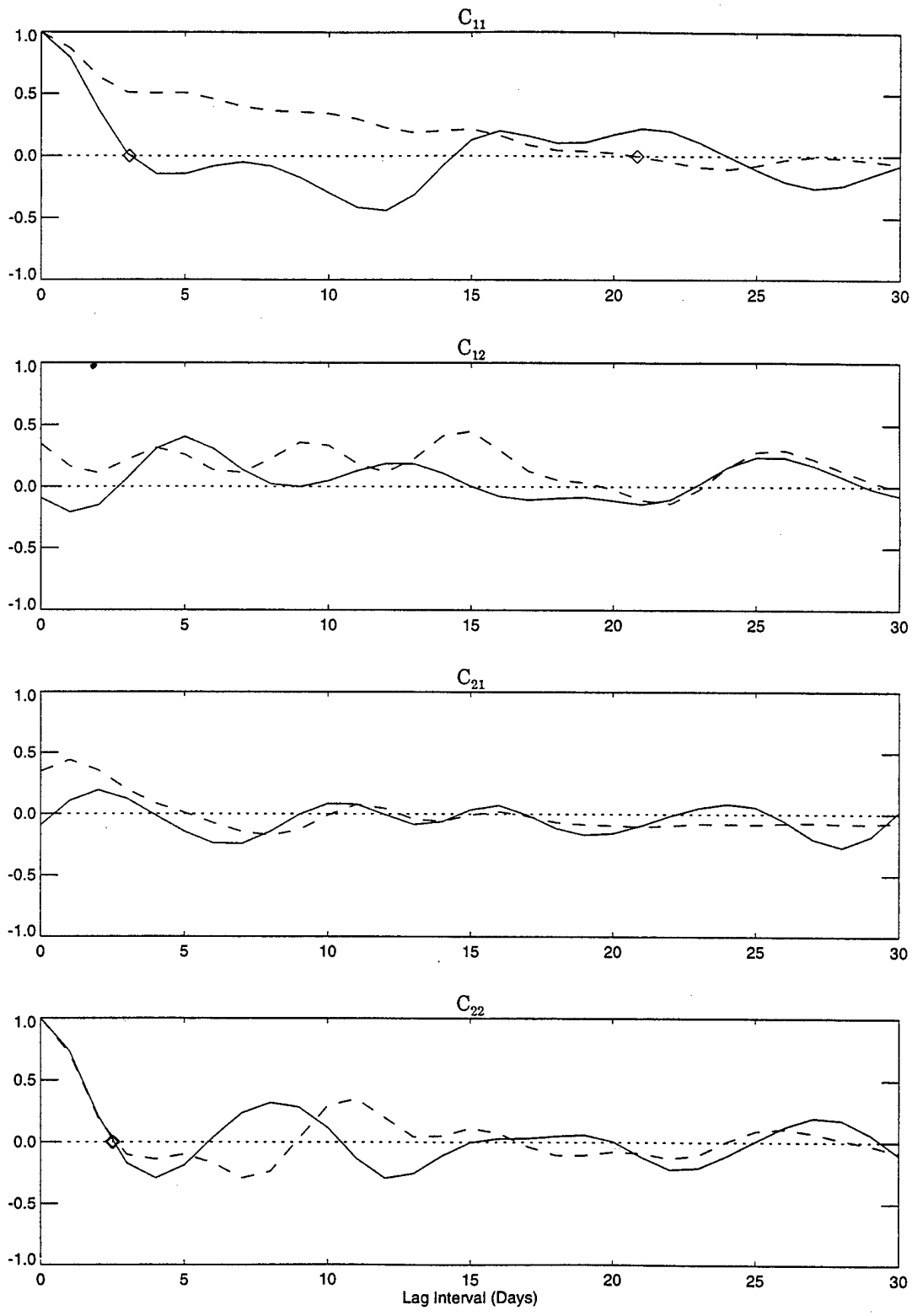

Figure 16: Comparison of C_{ij} for drifter 20386.

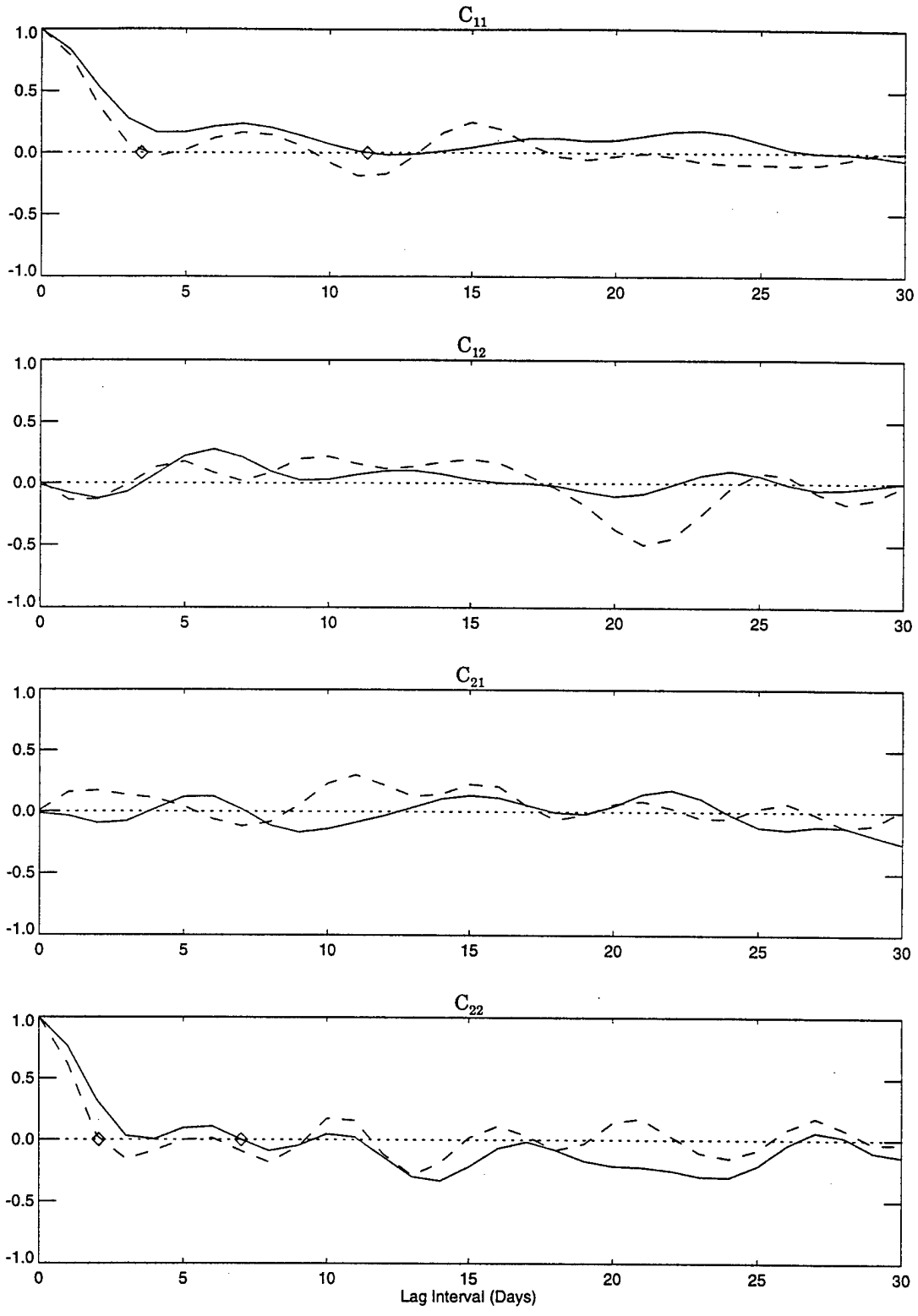

Figure 17: Comparison of C_{ij} for drifter 20396.

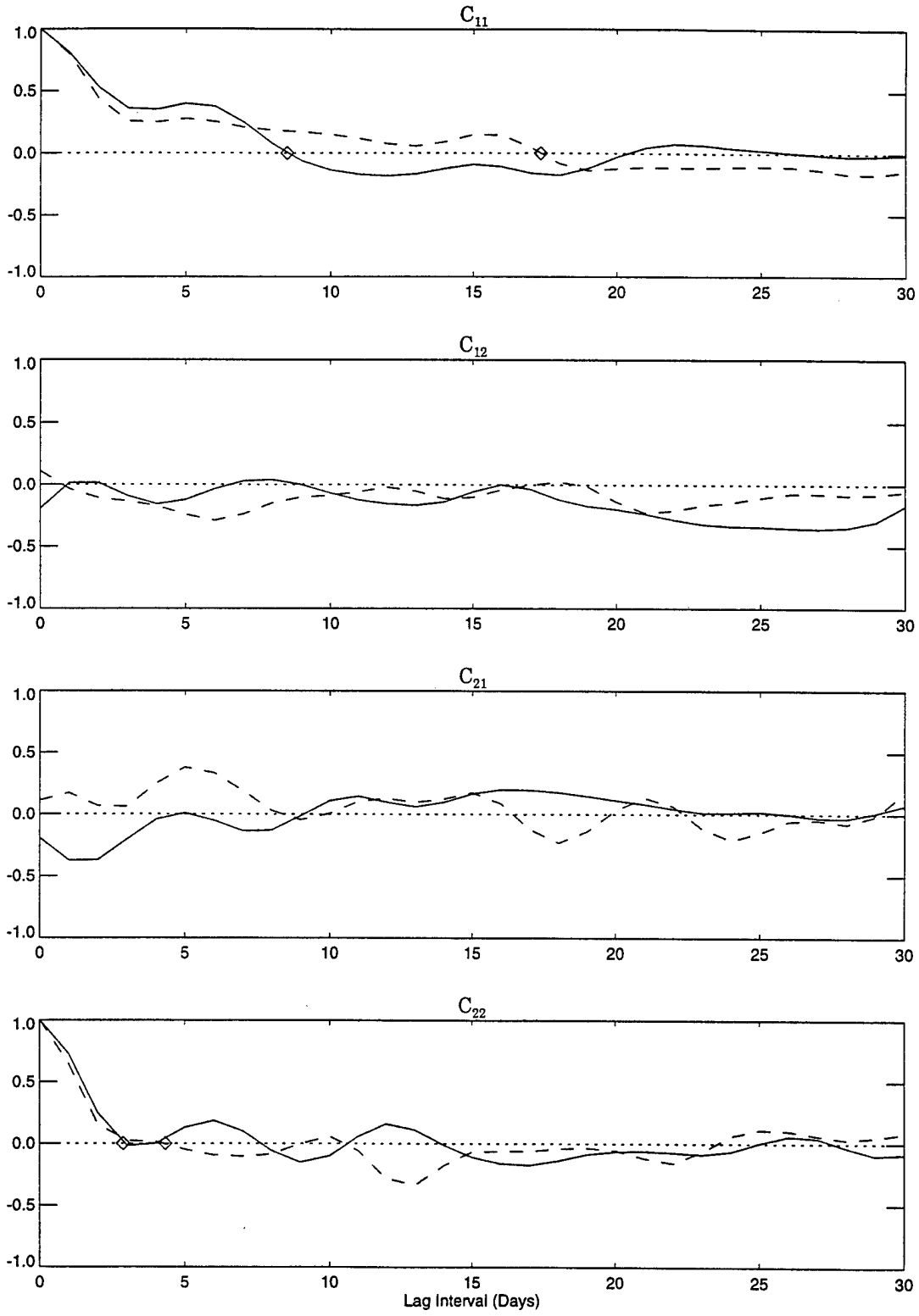

Figure 18: Comparison of C_{ij} for drifter 20402.

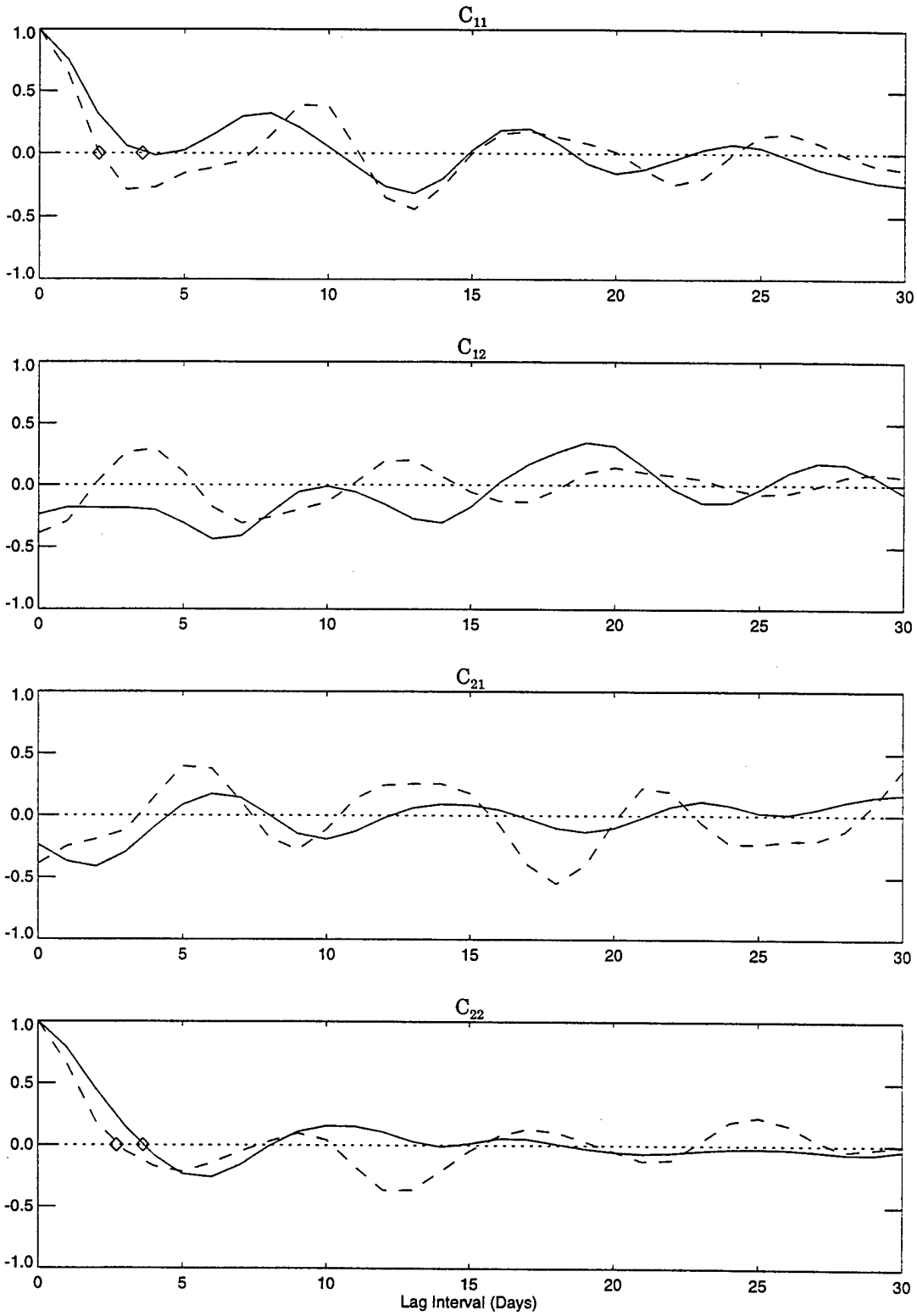

Figure 19: Comparison of C_{ij} for drifter 20407.

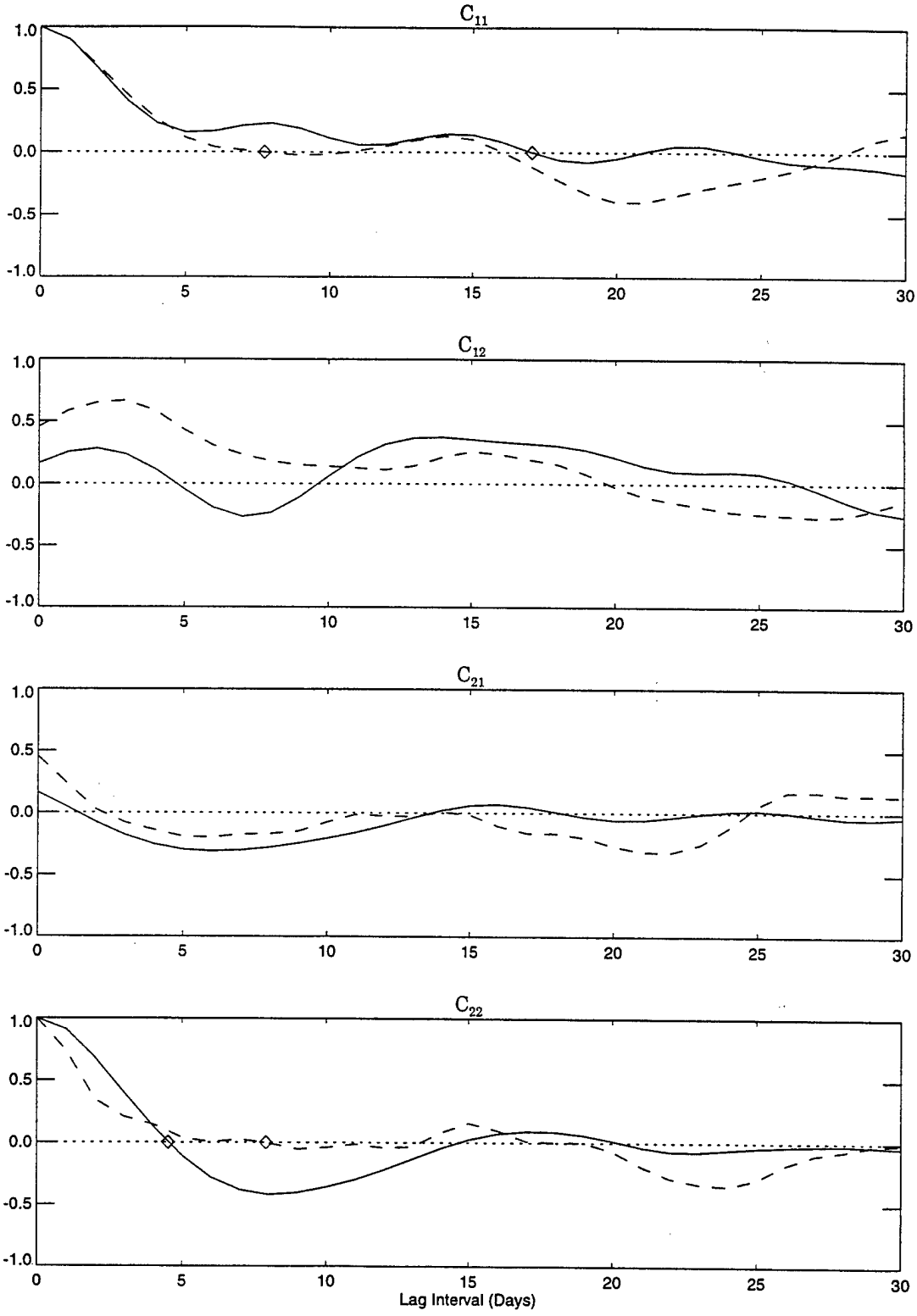

Figure 20: Comparison of C_{ij} for drifter 20412.

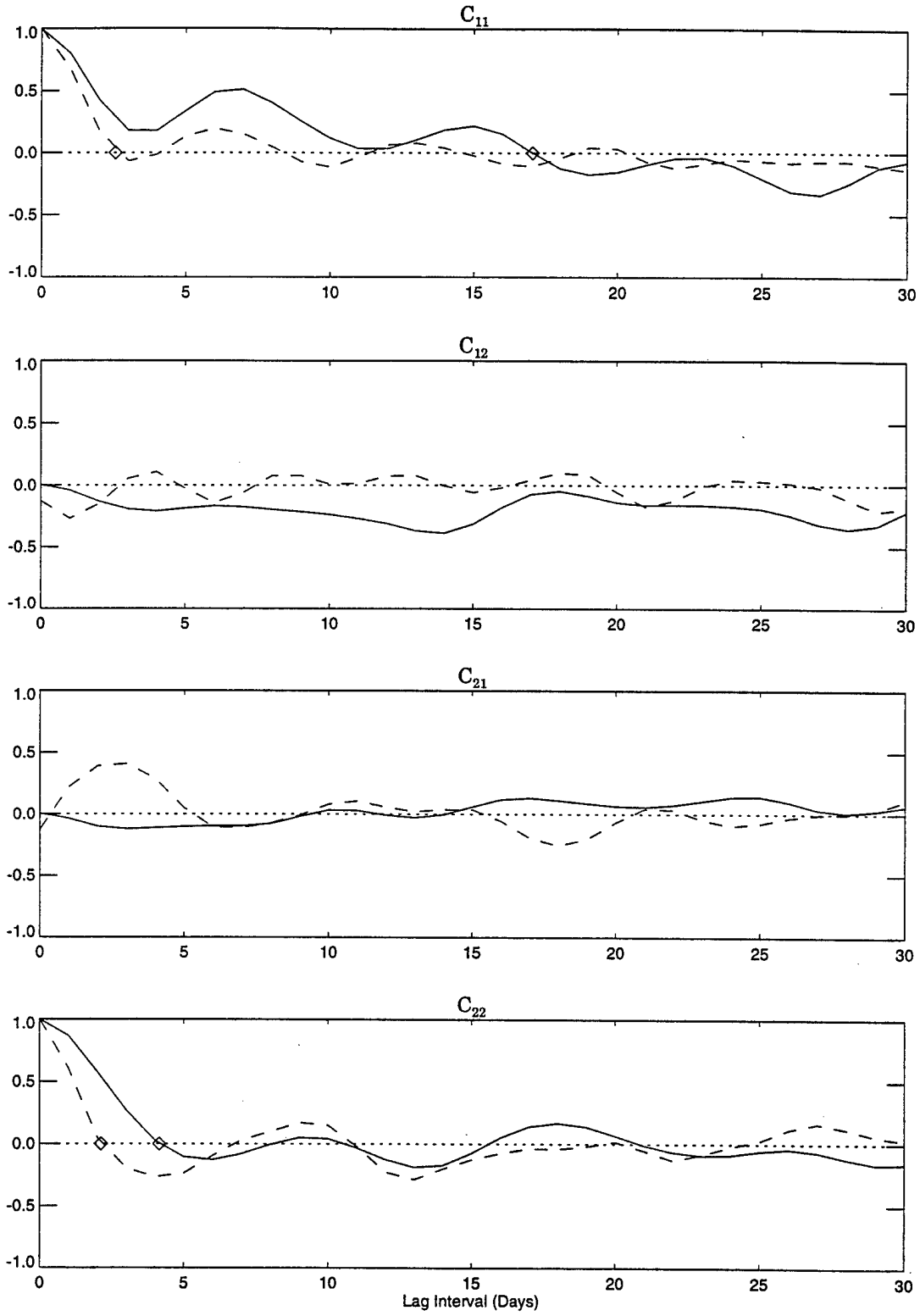

Figure 21: Comparison of C_{ij} for drifter 20422.

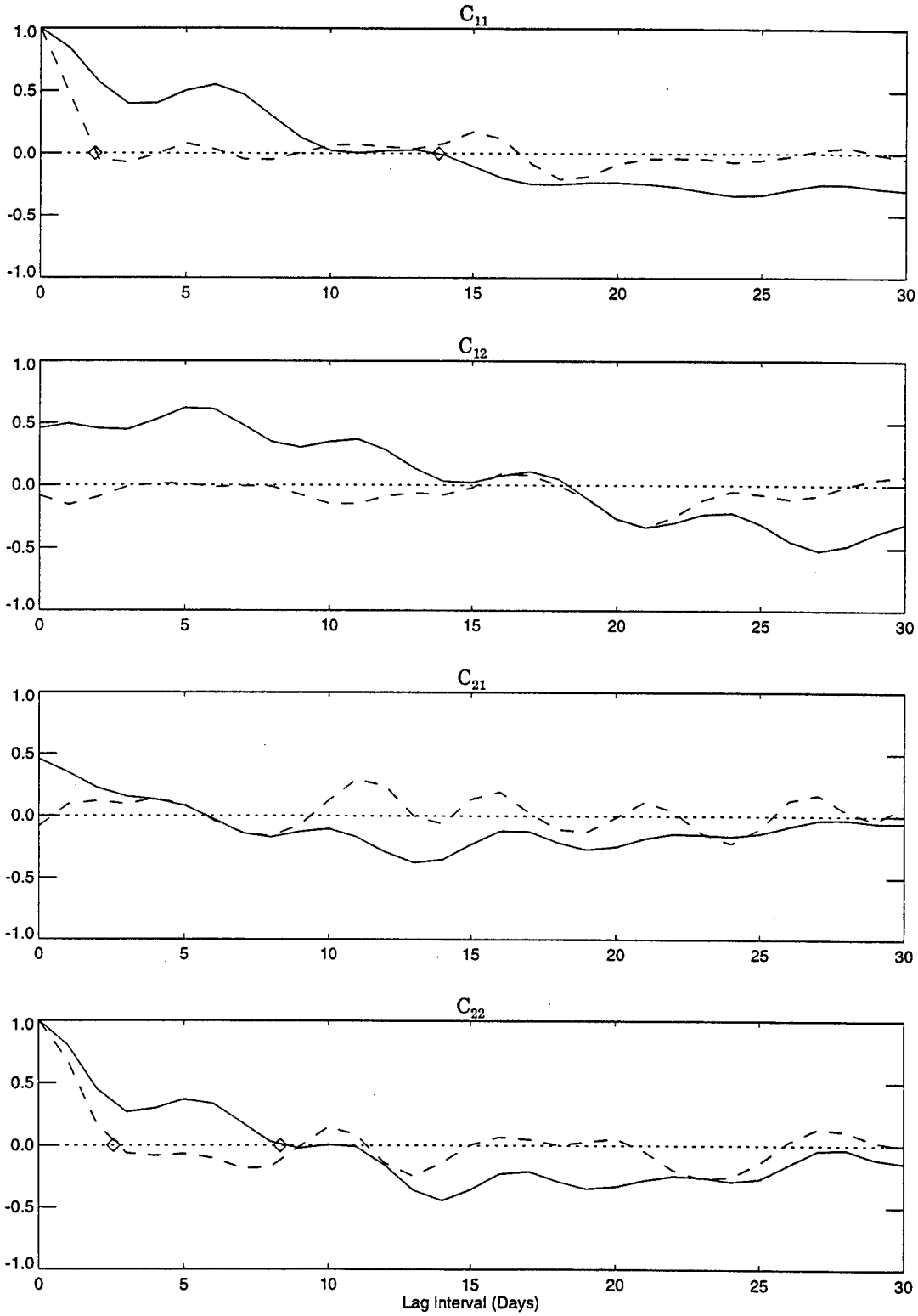

Figure 22: Comparison of C_{ij} for drifter 20436.

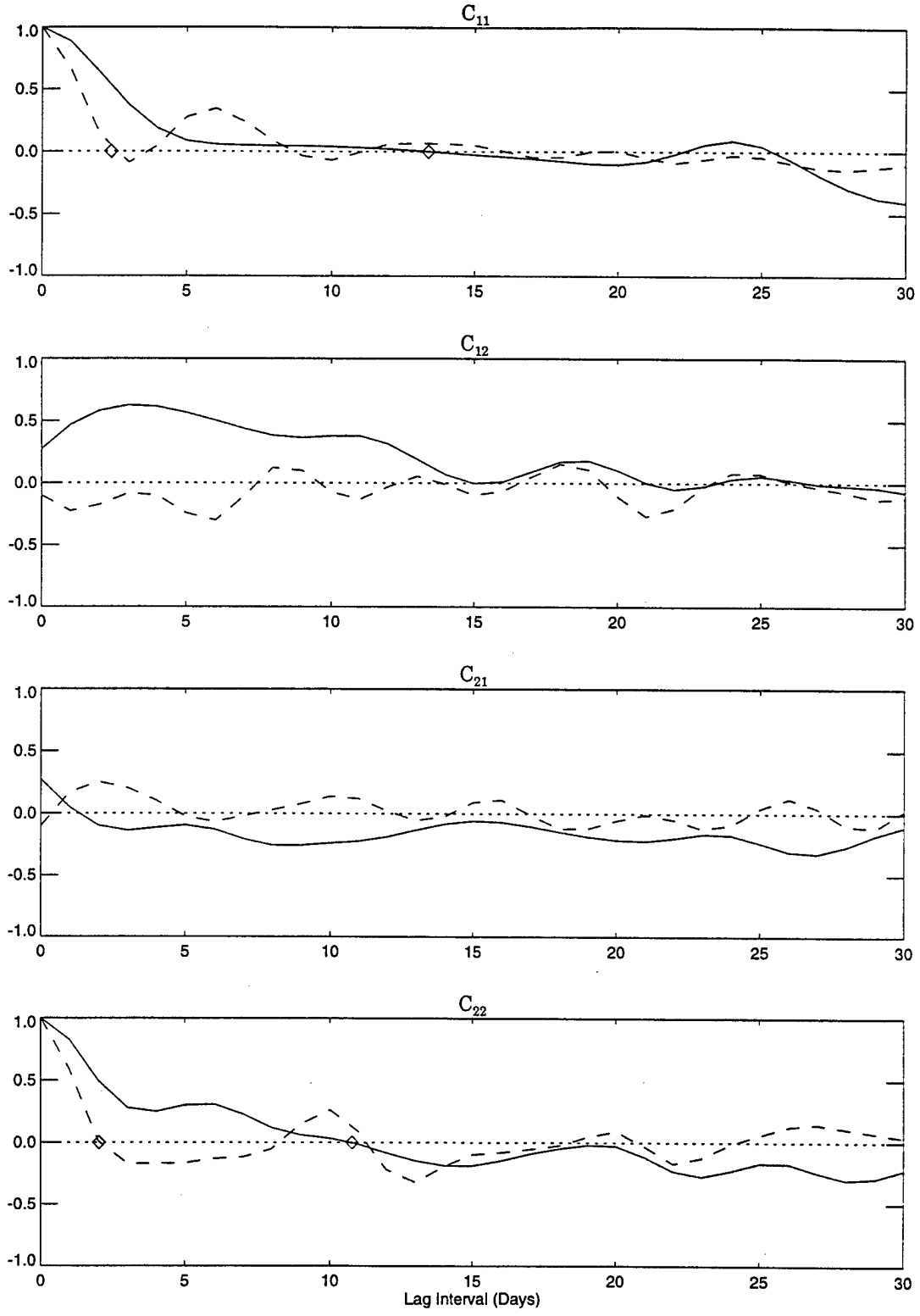

Figure 23: Comparison of C_{ij} for drifter 20440.

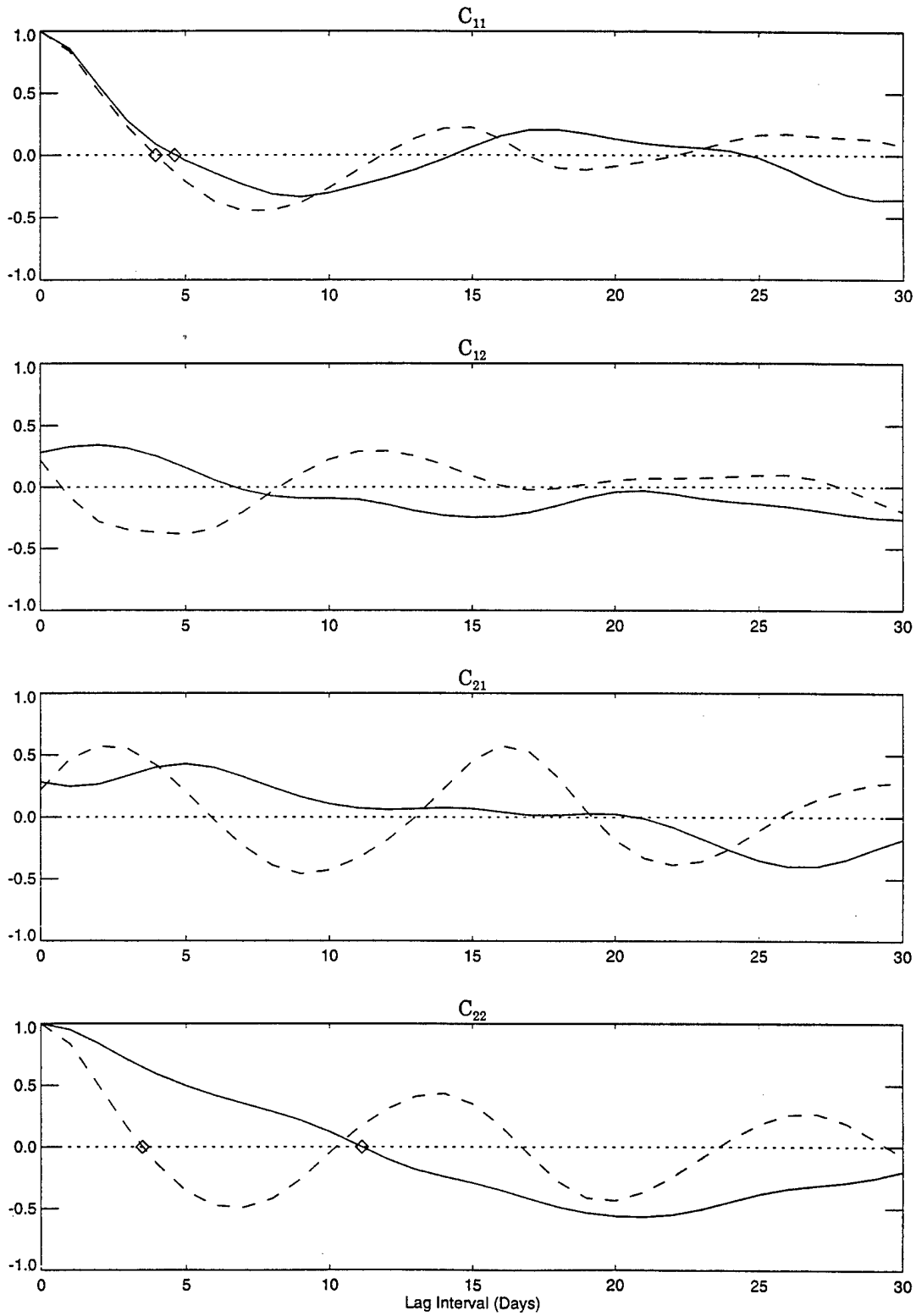

Figure 24: Comparison of C_{ij} for drifter 20446.

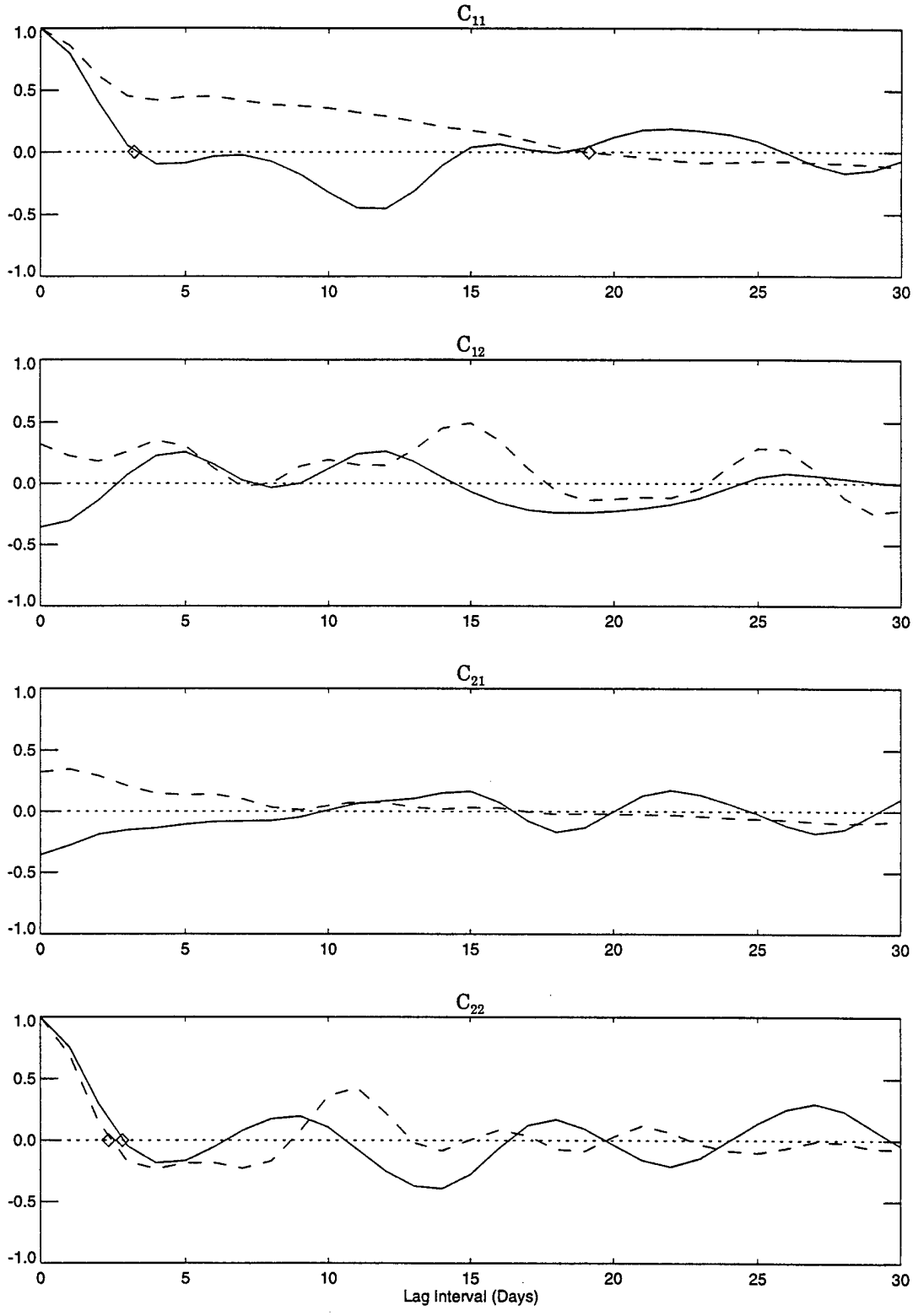

Figure 25: Comparison of C_{ij} for drifter 20449.

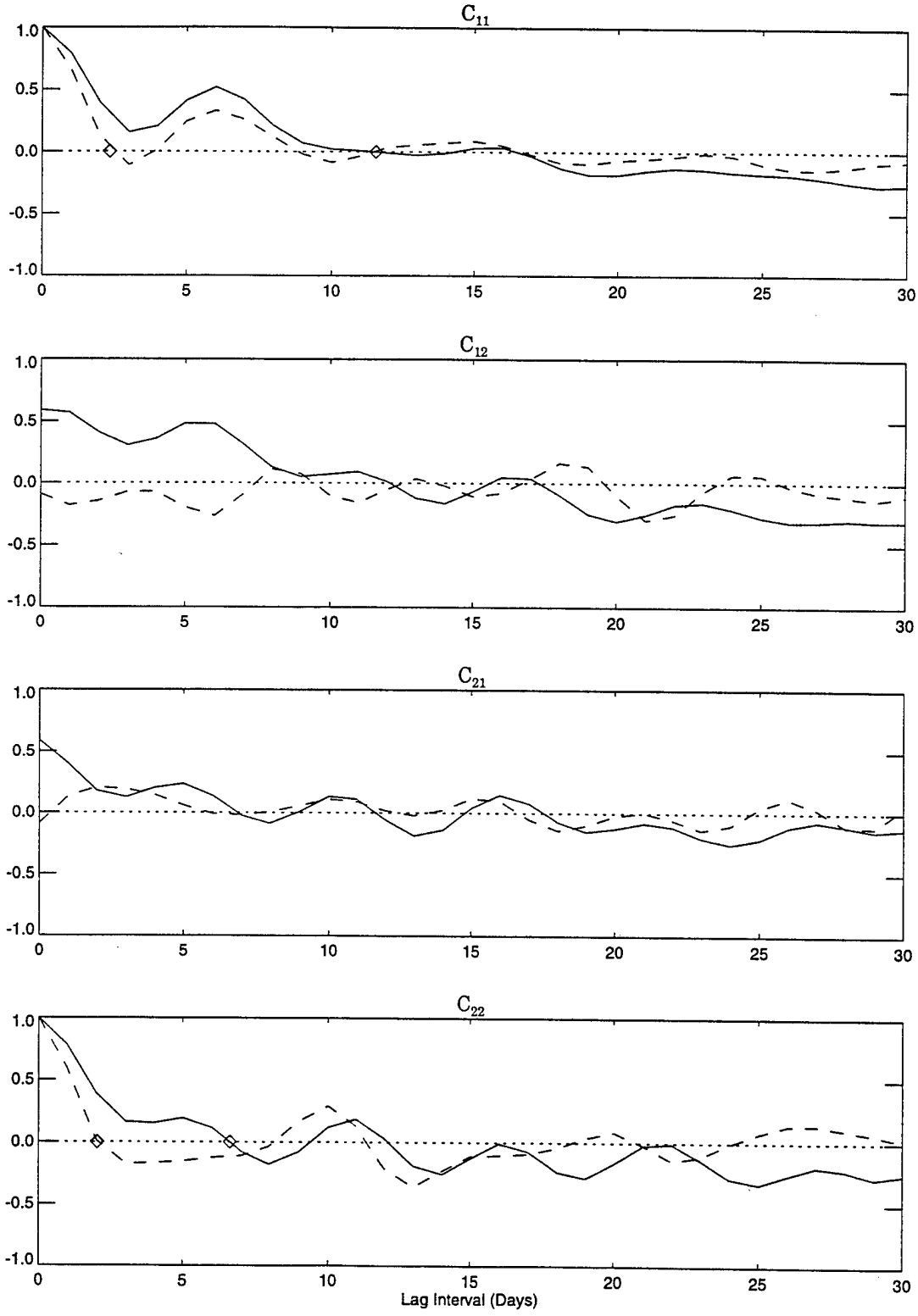

Figure 26: Comparison of C_{ij} for drifter 20455.

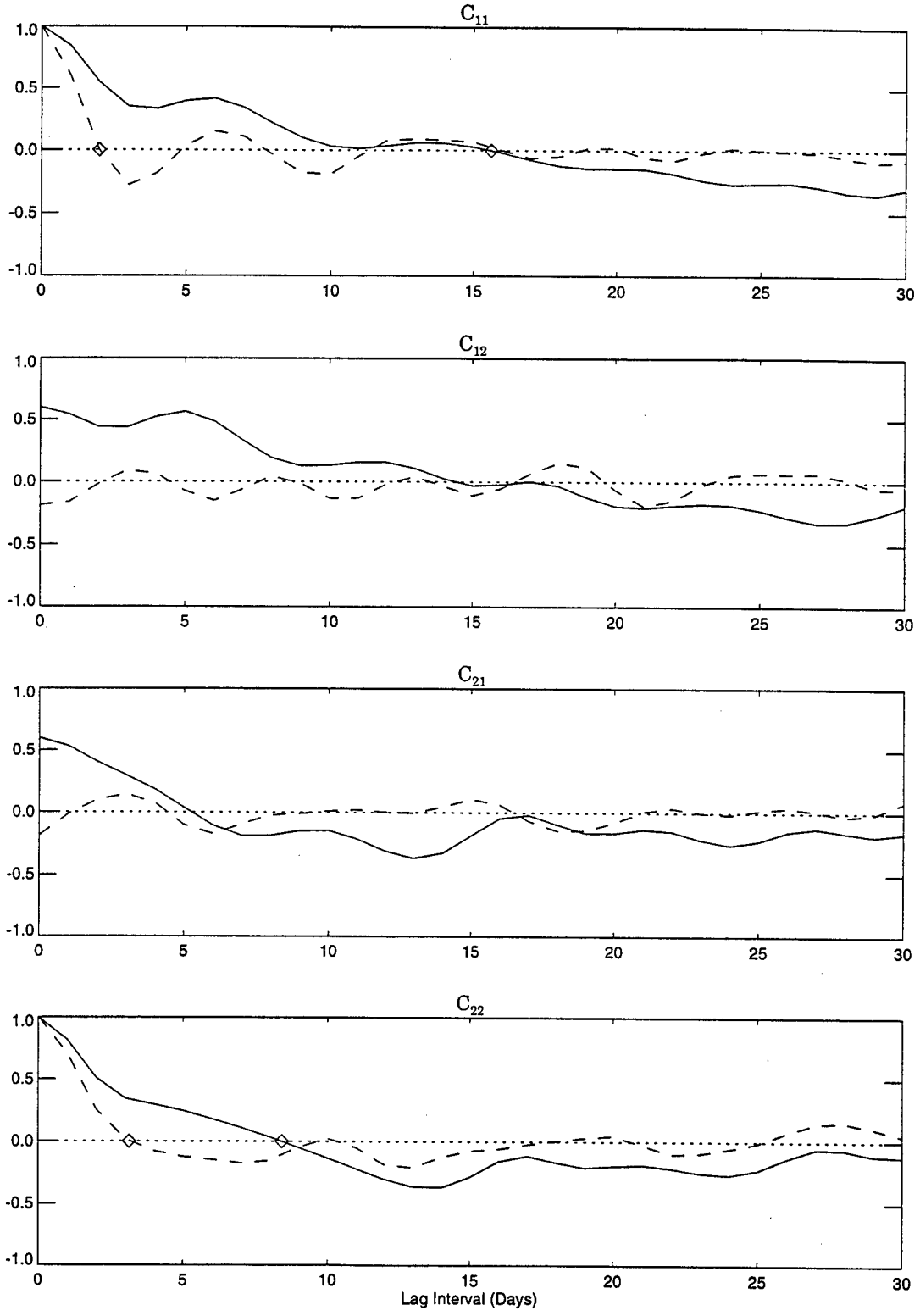

Figure 27: Comparison of C_{ij} for drifter 20456.

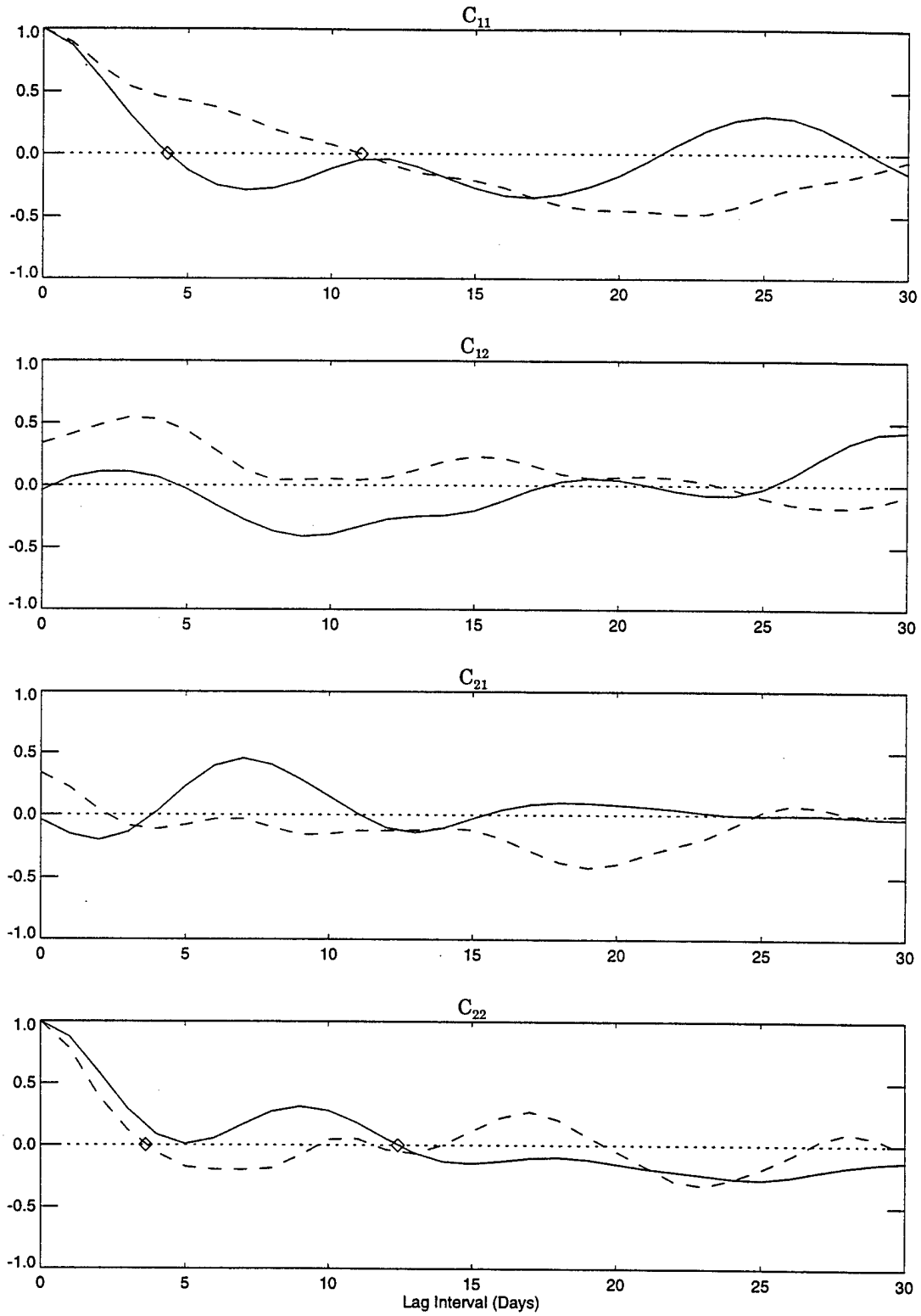

Figure 28: Comparison of C_{ij} for drifter 20457.

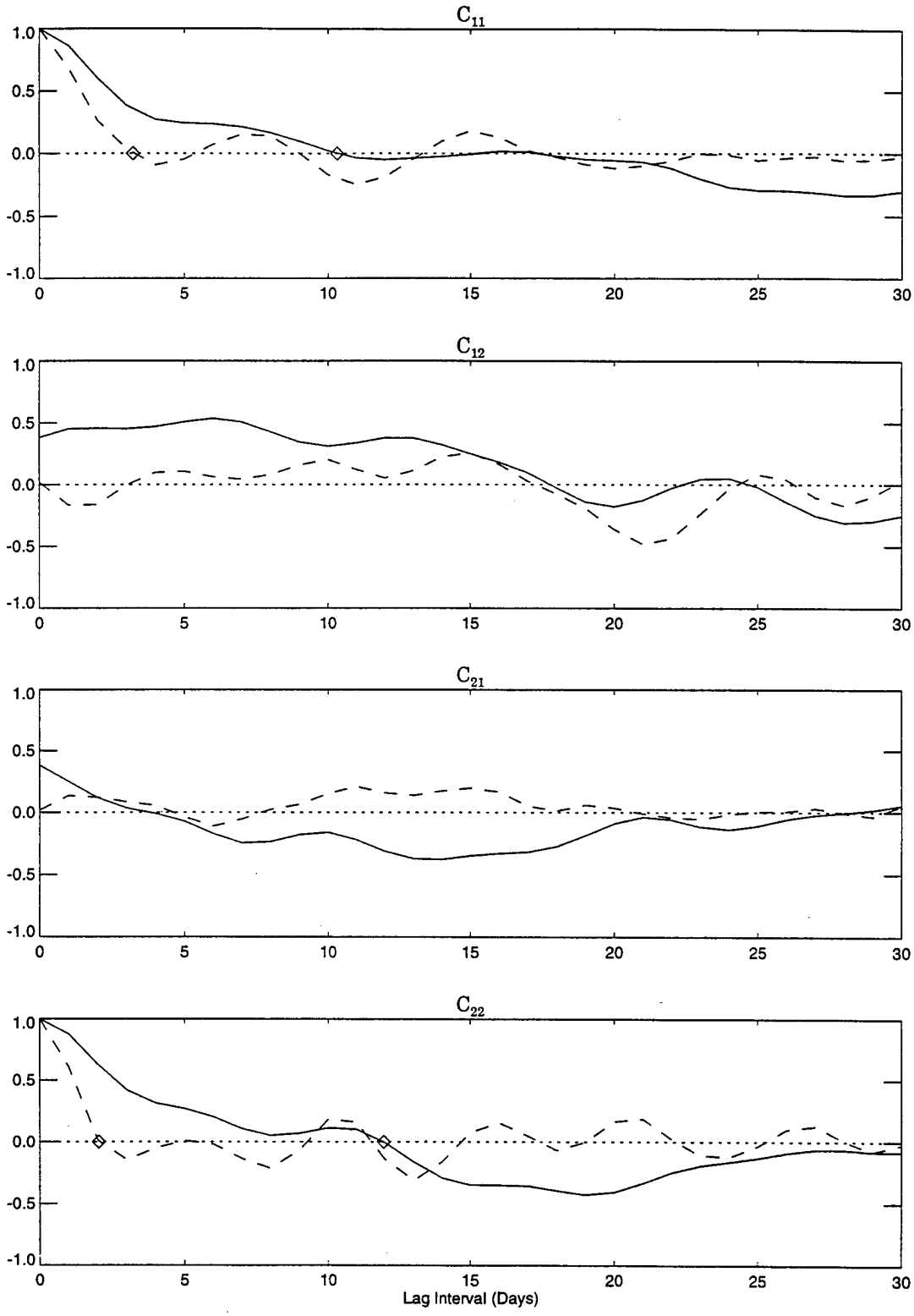

Figure 29: Comparison of C_{ij} for drifter 20461.

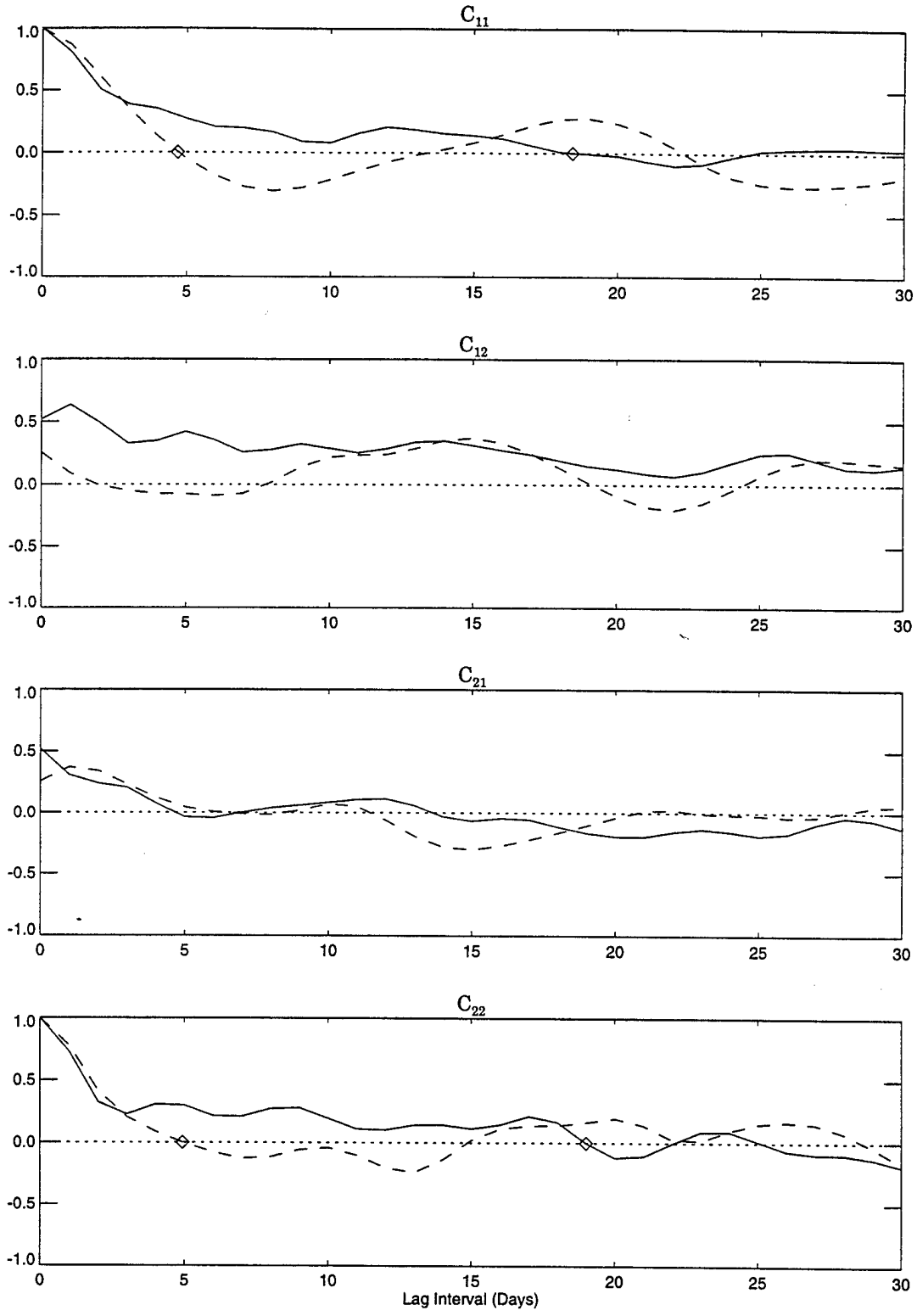

Figure 30: Comparison of C_{ij} for drifter 20463.

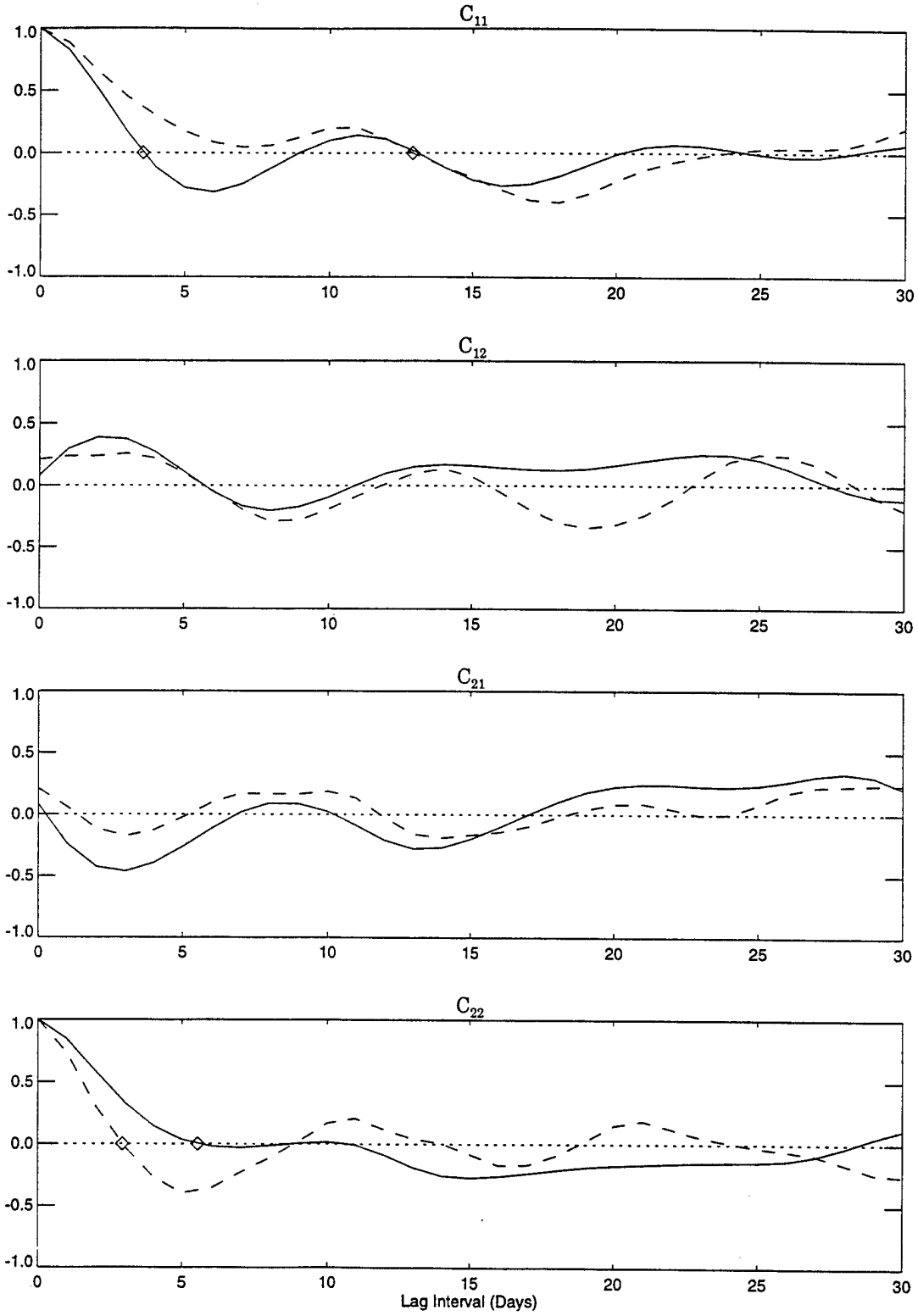

Figure 31: Comparison of C_{ij} for drifter 20465.

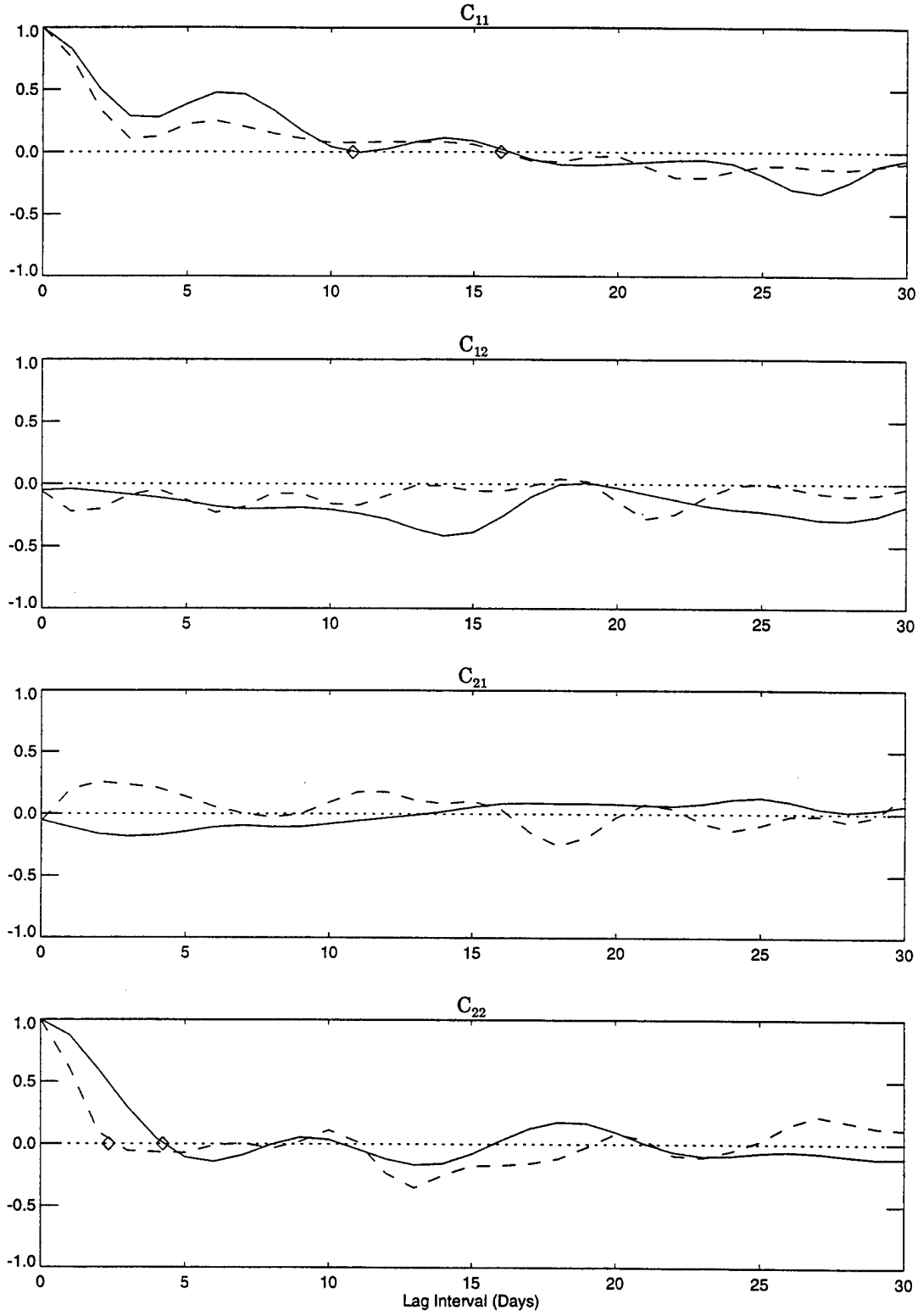

Figure 32: Comparison of C_{ij} for drifter 20468.

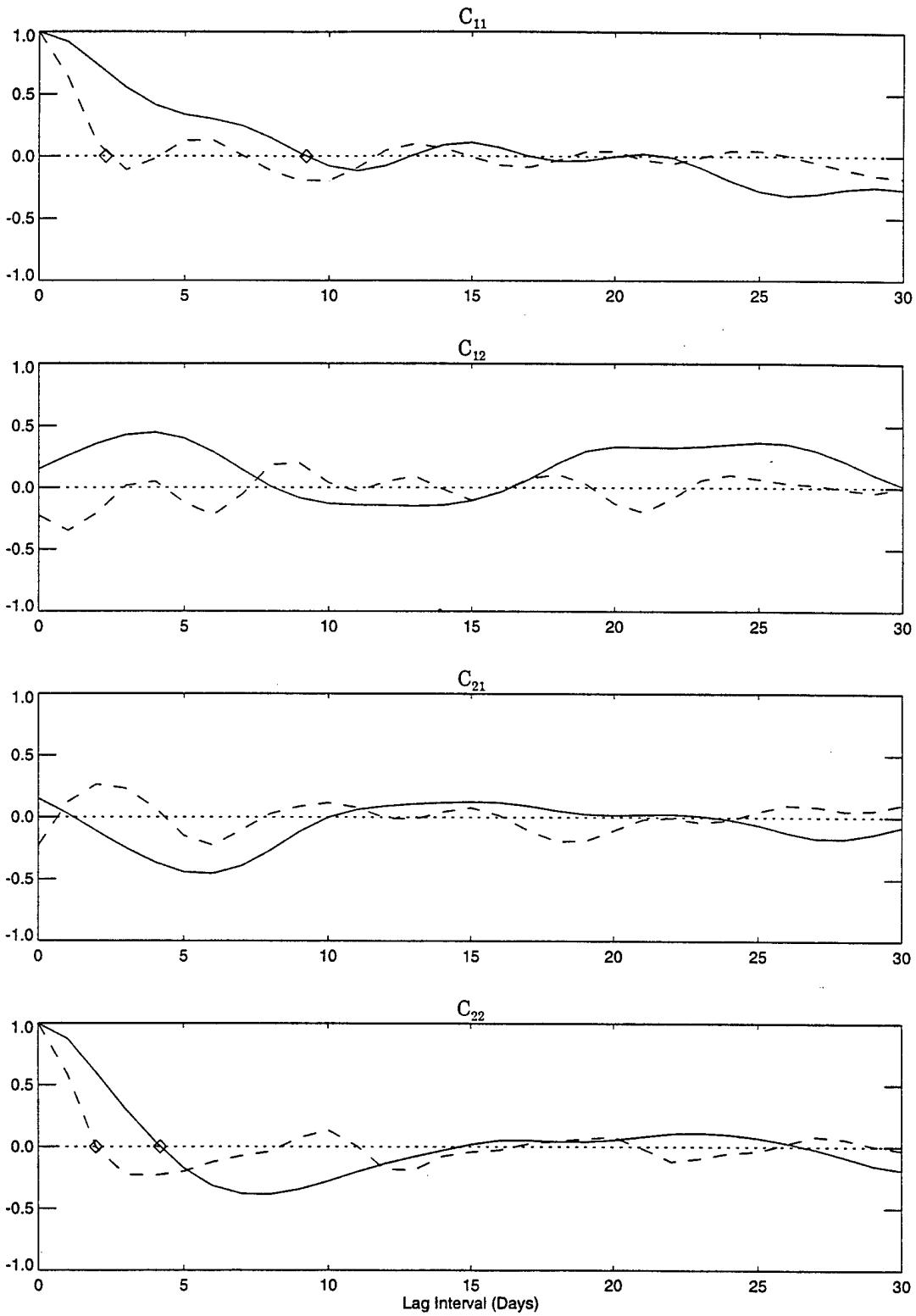

Figure 33: Comparison of C_{ij} for drifter 20469.

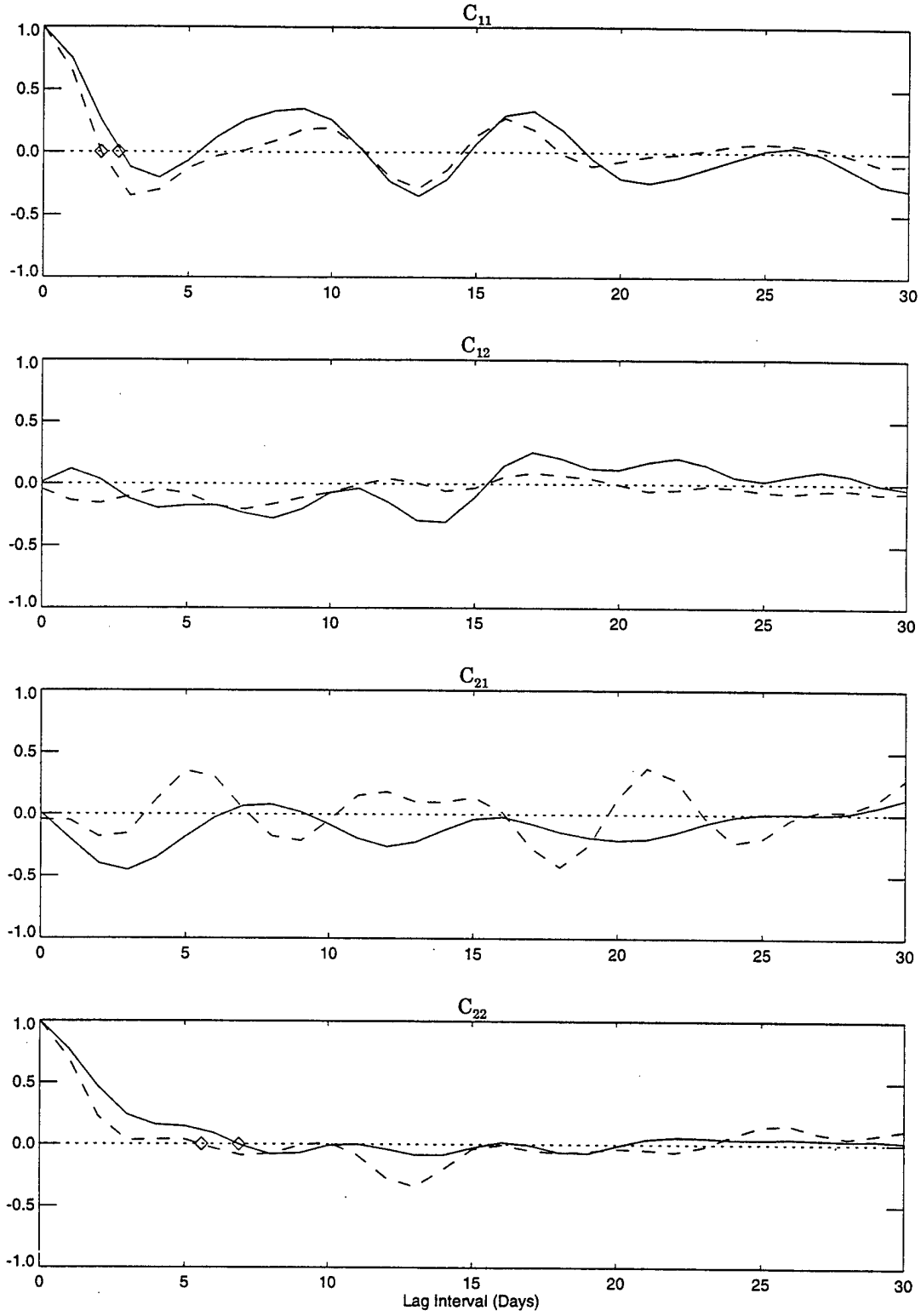

Figure 34: Comparison of C_{ij} for drifter 20498.

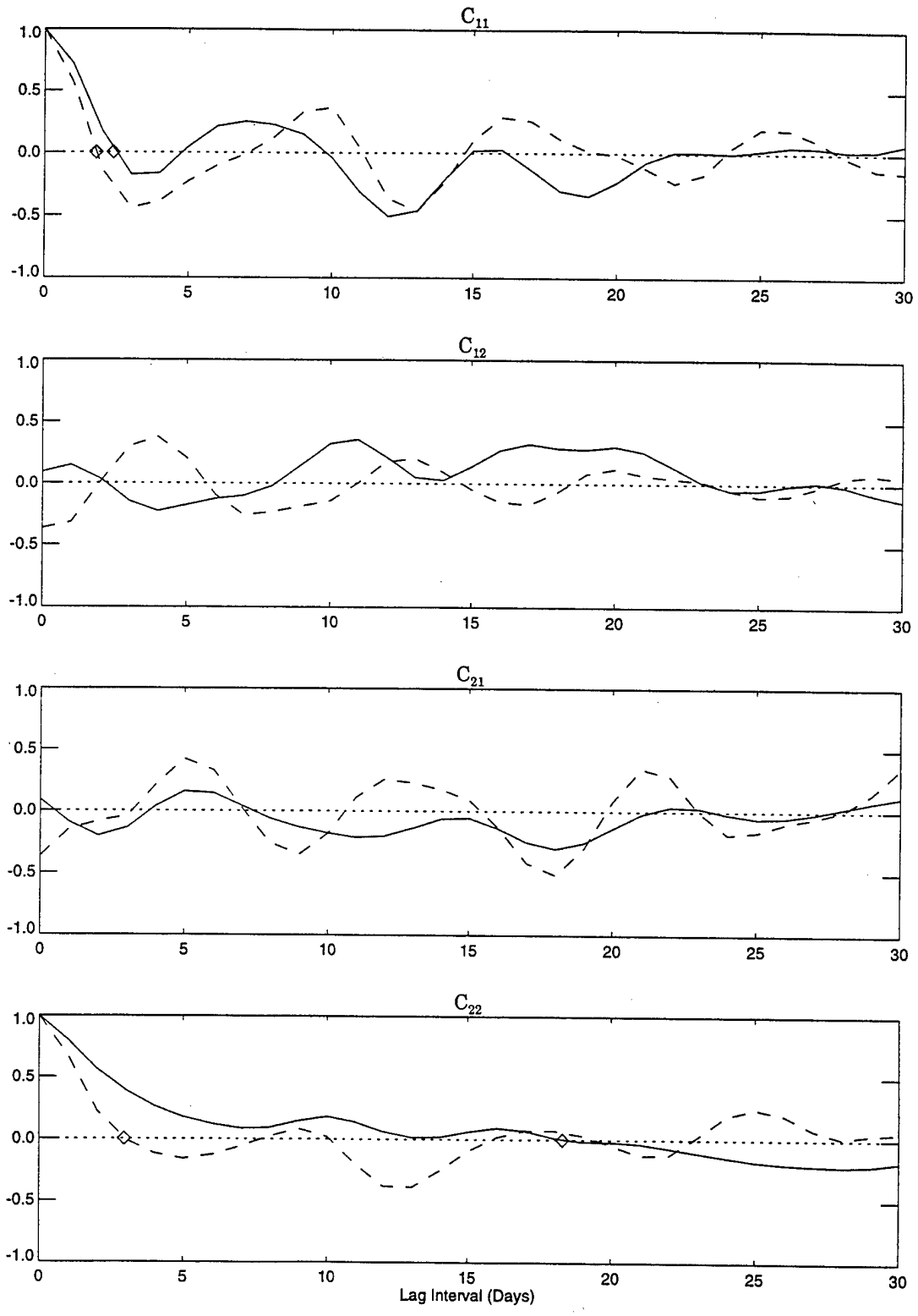

Figure 35: Comparison of C_{ij} for drifter 20513.

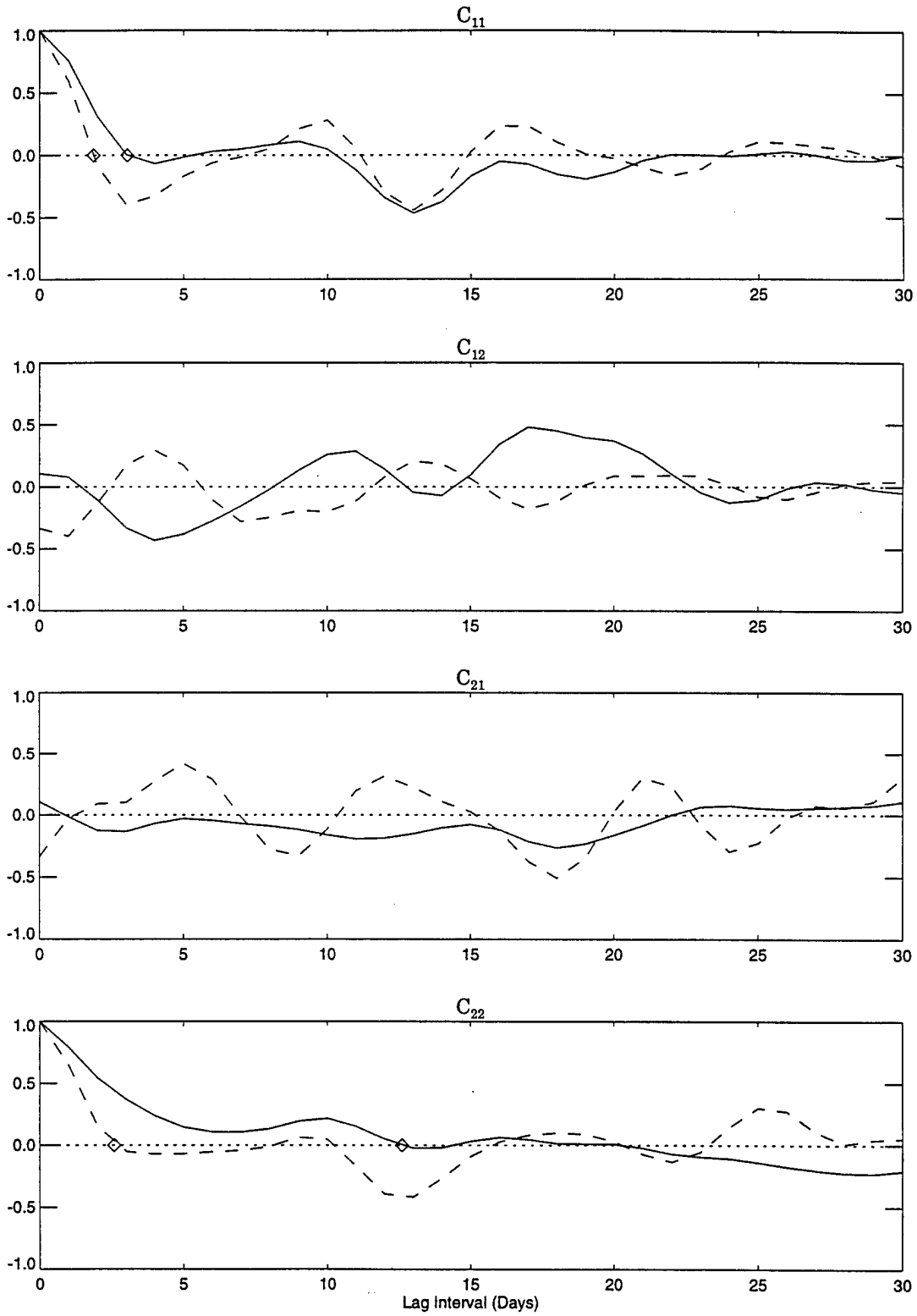

Figure 36: Comparison of C_{ij} for drifter 20519.

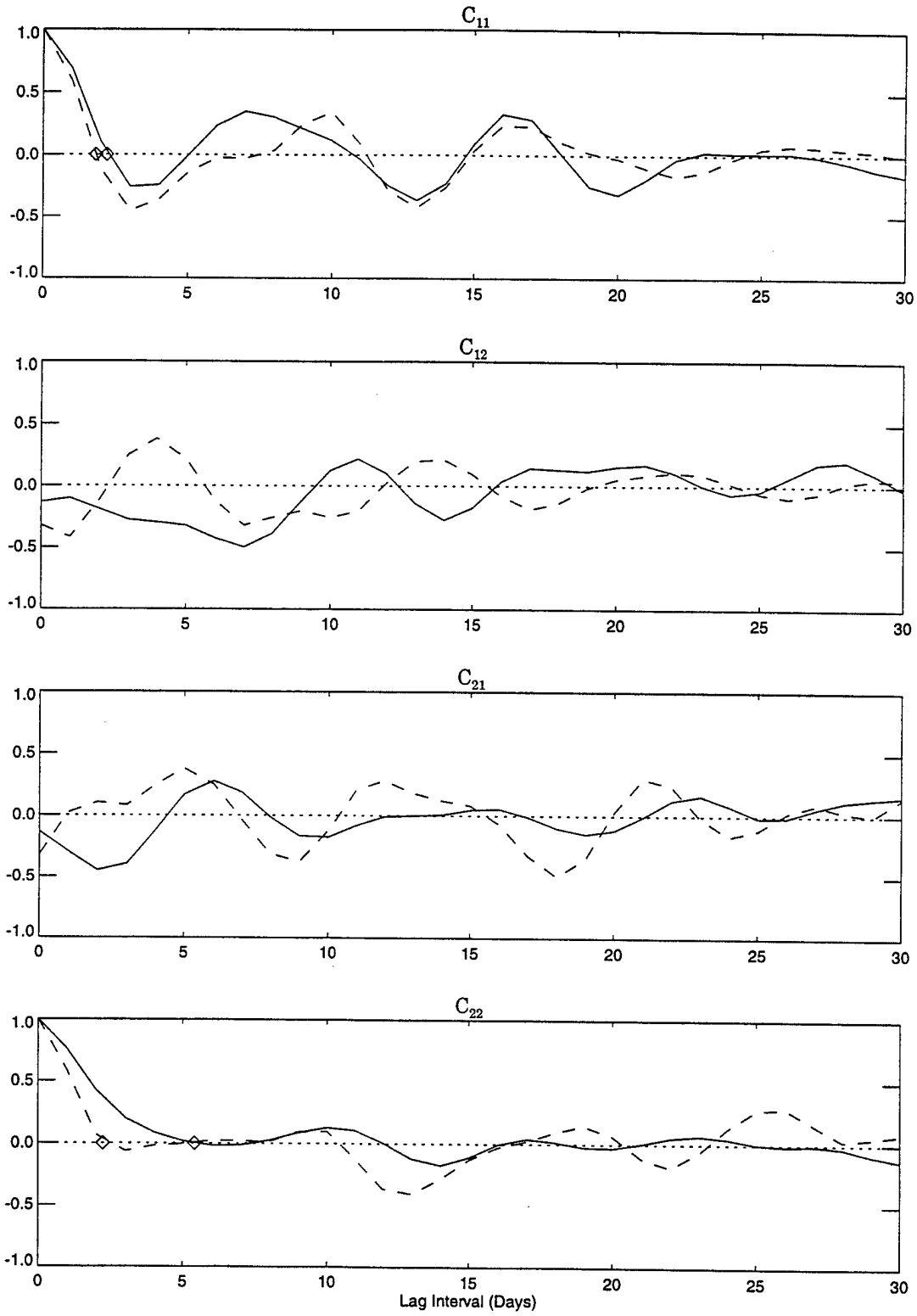

Figure 37: Comparison of C_{ij} for drifter 20528.

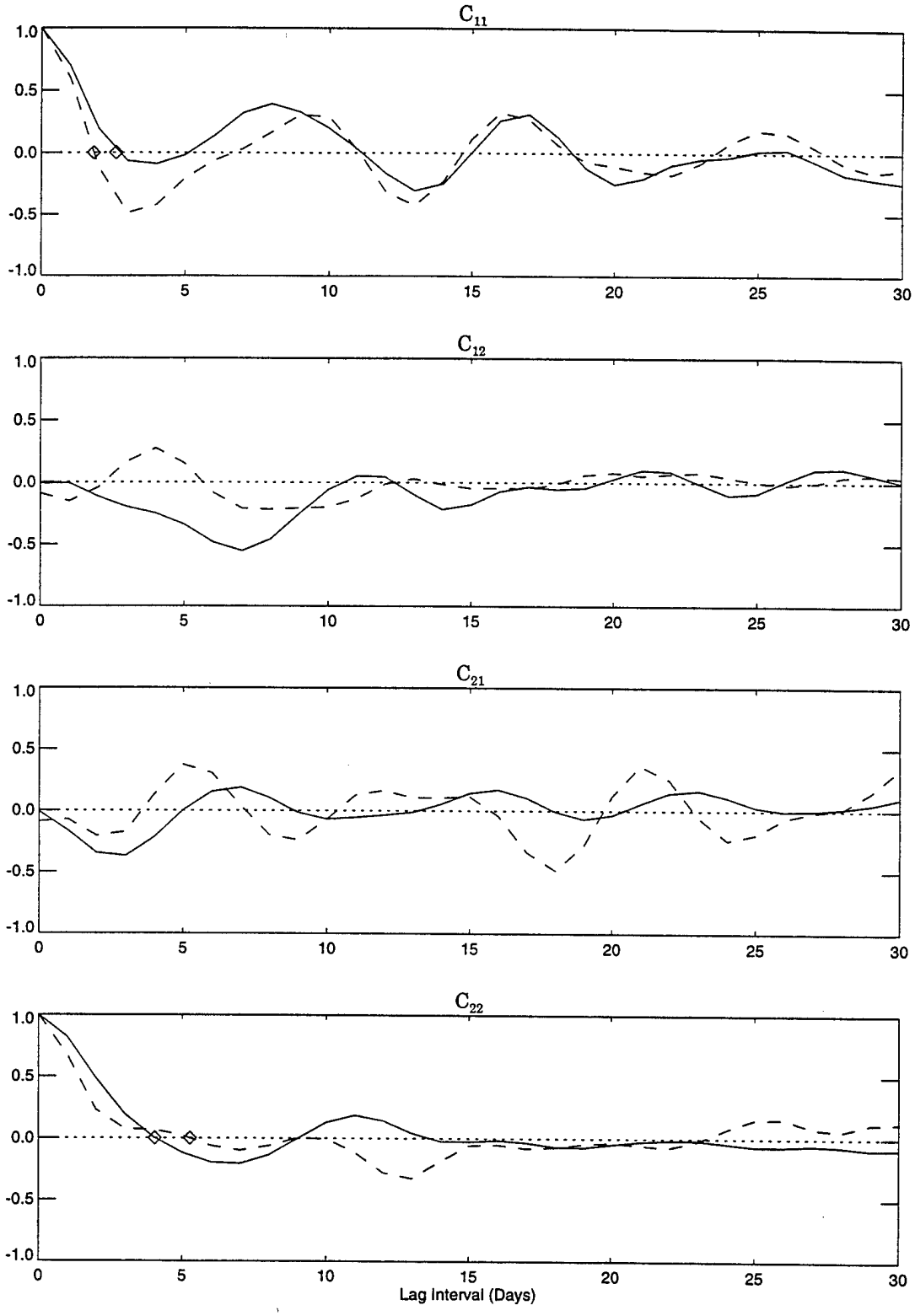

Figure 38: Comparison of C_{ij} for drifter 20531.

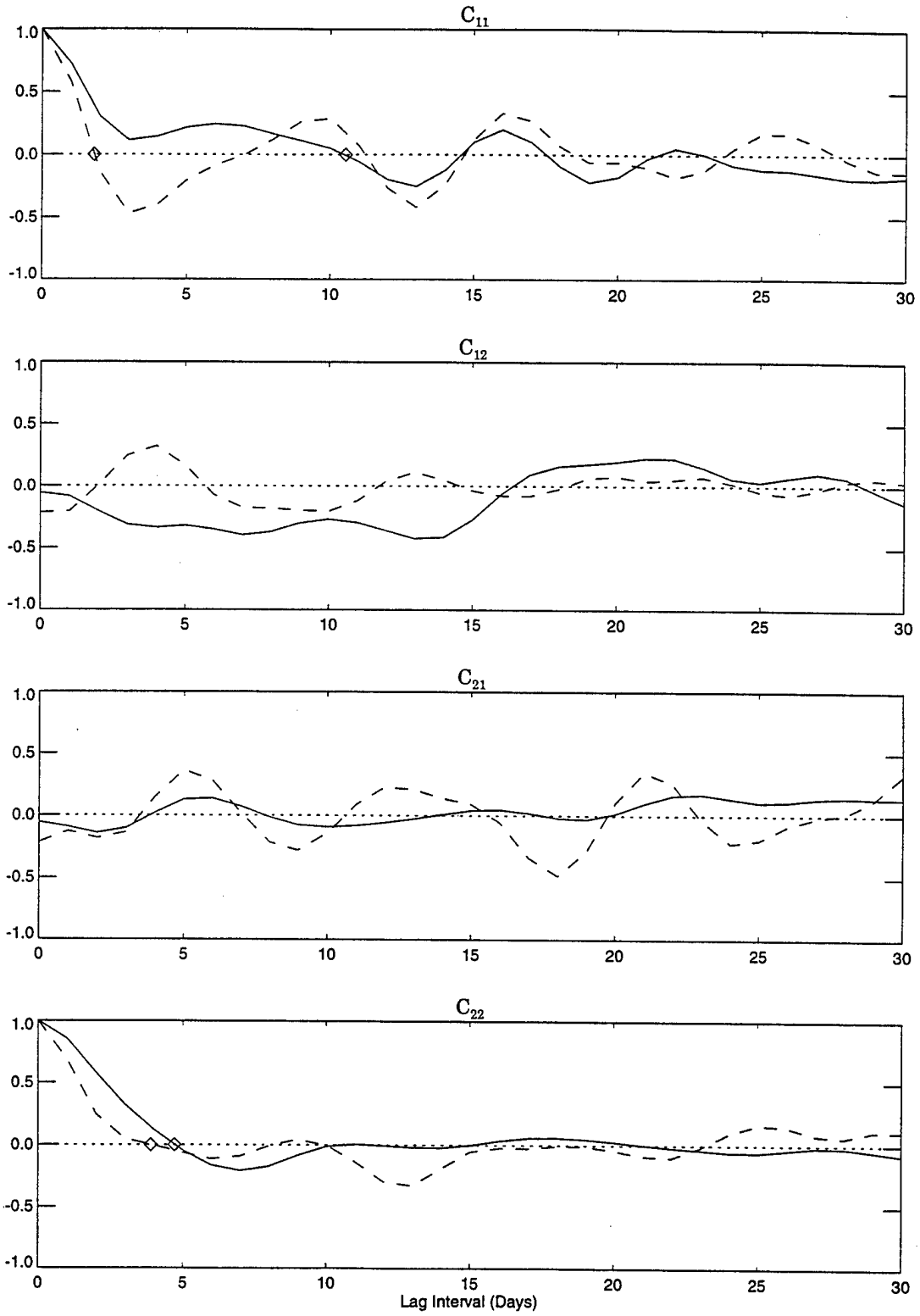

Figure 39: Comparison of C_{ij} for drifter 20533.

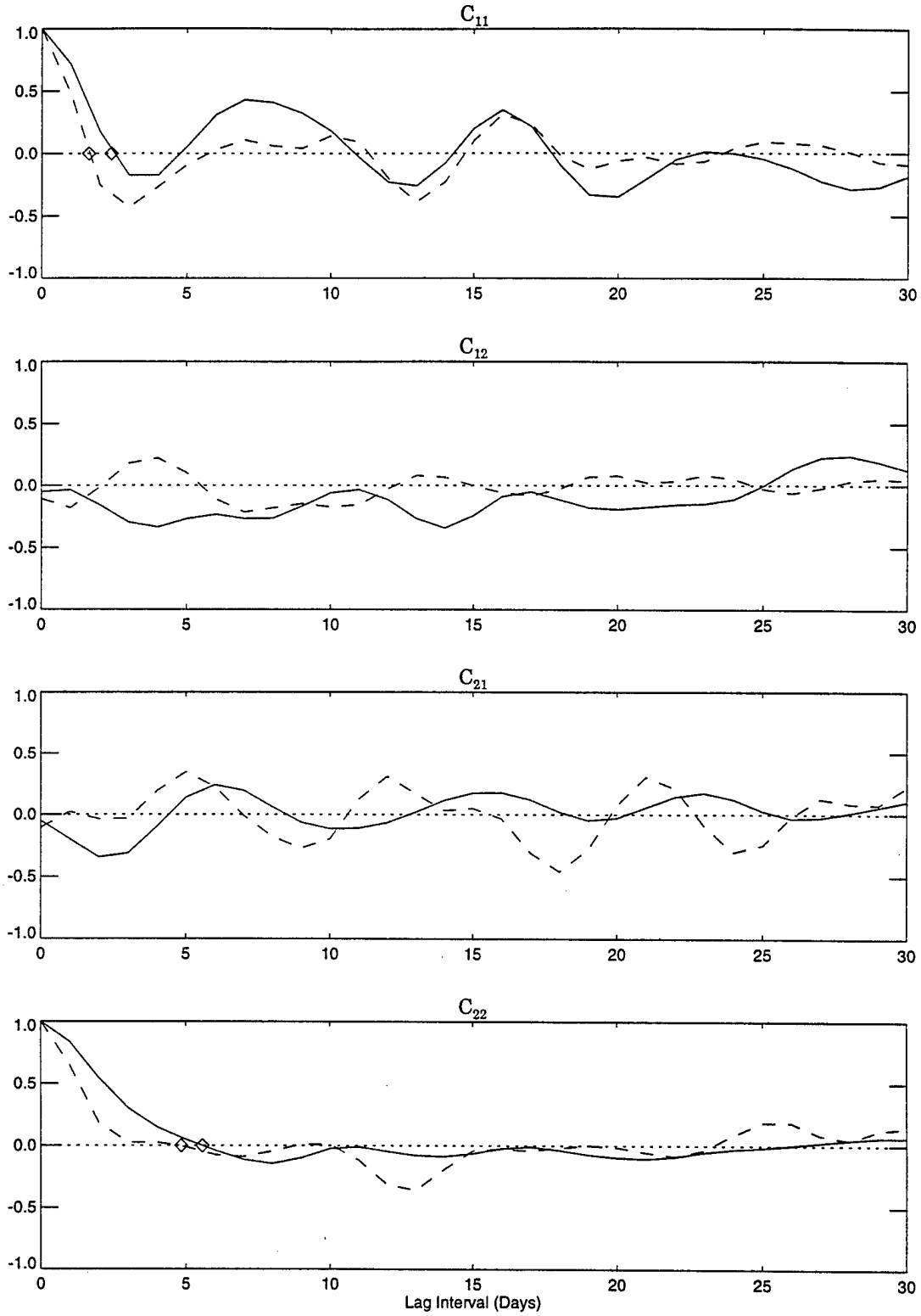

Figure 40: Comparison of C_{ij} for drifter 20536.

Table 3: $\hat{\tau}_{11}$ and $\hat{\tau}_{22}$ for each observed and modeled drifter

Drifter	$\hat{\tau}_{11}^{obs}$	$\hat{\tau}_{11}^{mod}$	$\hat{\tau}_{22}^{obs}$	$\hat{\tau}_{22}^{mod}$
20383	16.97	1.96	5.34	2.56
20386	3.06	20.81	2.47	2.53
20396	11.34	3.45	7.02	2.07
20402	8.51	17.33	2.86	4.32
20407	3.54	2.05	3.61	2.70
20412	17.06	7.72	4.52	7.92
20422	17.05	2.55	4.15	2.11
20436	13.80	1.87	8.36	2.56
20440	13.37	2.39	10.78	2.03
20446	4.63	3.97	11.13	3.50
20449	3.24	19.12	2.82	2.33
20455	11.58	2.33	6.61	2.03
20456	15.62	2.00	8.44	3.13
20457	4.28	11.05	12.43	3.62
20461	10.32	3.23	11.96	2.03
20463	18.43	4.69	19.00	4.94
20465	3.54	12.90	5.52	2.89
20468	10.76	15.92	4.22	2.35
20469	9.22	2.30	4.18	1.99
20498	2.59	1.98	6.90	5.58
20513	2.37	1.78	18.29	2.92
20519	3.03	1.85	12.61	2.56
20528	2.20	1.82	5.41	2.23
20531	2.60	1.83	4.04	5.27
20533	10.53	1.79	4.71	3.89
20536	2.39	1.62	5.57	4.84

A.3 Reynolds stresses

The Reynolds stress components for a drifter trajectory are expressed as:

$$R_{ij} = \frac{1}{T}\int_0^T u_i(t)u_j(t)dt$$

where T is the length of the drifter record. Since $R_{12} = R_{21}$, there are three unique stress components. Table 4 shows the three Reynolds stress components for each observed and modeled drifter.

Figure 41 shows scatter plots for each R_{ij}, with one data point for each of the 26 modeled drifters. The X axis represents *observed* R_{ij} and the Y axis shows *modeled* R_{ij}. The dashed line in each panel represents the line of correlation between the observed and modeled data.

Table 4: Observed and modeled drifter R_{ij} (in $10^{-2}\ m^2 s^{-2}$)

Drifter	R_{11}^{obs}	R_{11}^{mod}	R_{12}^{obs}	R_{12}^{mod}	R_{22}^{obs}	R_{22}^{mod}
20383	1.43	1.77	0.25	-0.05	1.67	1.35
20386	0.96	1.02	-0.04	0.56	0.23	2.54
20396	3.25	1.62	-0.04	0.02	2.58	1.60
20402	2.37	1.87	-0.34	0.18	1.35	1.36
20407	1.16	1.46	-0.45	-0.51	3.13	1.14
20412	3.93	3.41	0.62	1.35	3.66	2.59
20422	1.27	1.40	0.01	-0.18	2.91	1.43
20436	1.52	2.86	0.52	-0.20	0.85	2.06
20440	4.00	1.50	0.97	-0.14	3.15	1.31
20446	2.48	4.15	1.07	1.33	5.76	8.67
20449	1.18	1.01	-0.22	0.54	0.31	2.82
20455	1.54	1.68	0.68	-0.14	0.86	1.43
20456	1.90	1.24	0.75	-0.30	0.84	2.11
20457	1.83	3.36	-0.12	0.99	4.76	2.60
20461	2.54	1.85	1.27	0.03	4.36	1.70
20463	2.56	4.16	1.12	0.79	1.82	2.31
20465	2.53	3.23	0.22	0.53	2.93	1.94
20468	1.24	2.19	-0.09	-0.11	2.83	1.56
20469	3.98	1.47	0.53	-0.33	3.14	1.43
20498	1.01	2.32	0.01	-0.08	1.22	1.53
20513	1.25	1.29	0.21	-0.47	4.25	1.26
20519	1.17	1.91	0.22	-0.56	3.59	1.47
20528	1.38	2.24	-0.26	-0.54	2.75	1.27
20531	0.84	2.08	-0.01	-0.17	2.42	1.68
20533	1.00	1.73	-0.11	-0.35	3.68	1.55
20536	0.97	2.17	-0.08	-0.19	2.97	1.49

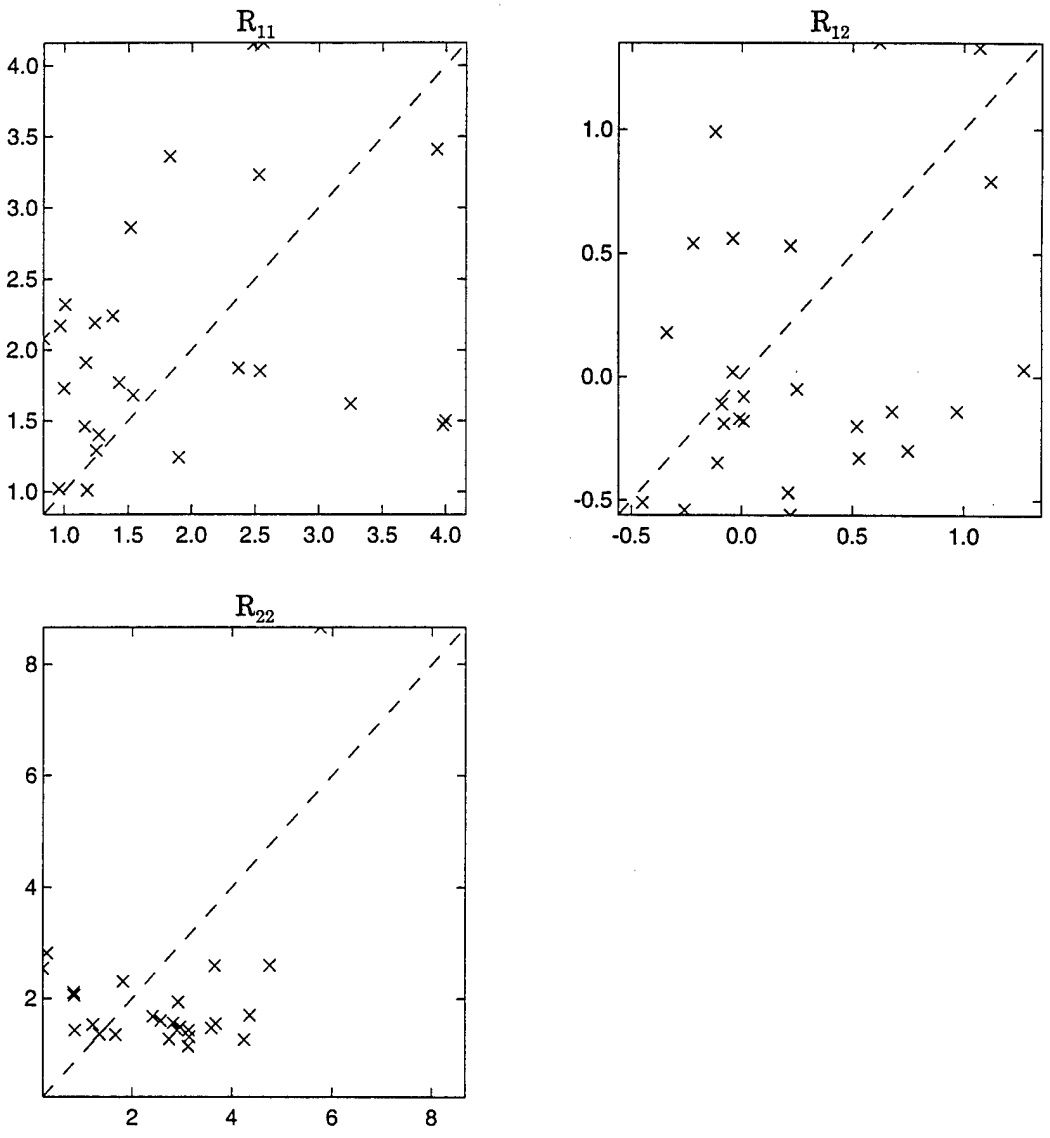

Figure 41: Modeled R_{ij} vs. observed R_{ij} (in 10^{-2} $m^2 s^{-2}$) for each drifter. The dashed line in each panel represents the line of correlation between the observed and modeled data. The data are tabulated in Table 4.

A.4 Lagrangian diffusion tensors

The Lagrangian diffusion tensor (Batchelor; 1949, 1952) provides a measure of the diffusion of fluid parcels over time. The four components of this tensor can be expressed as:

$$L_{ij}^2(t) = 2||u_i||||u_j|| \int_0^t C_{ij}(\tau)(t-\tau)d\tau$$

where τ is the lag time. For the L_{ij}^2 results presented here, each observed and modeled drifter record was truncated after 10 days, and the C_{ij} were calculated from the truncated velocity records, as described in section A.2, after subtracting the 10 day mean from each truncated velocity record.

Figures 42 – 67 show time series of each L_{ij}^2 (in m^2) for the first ten days of each observed and modeled drifter record. Tensor components for the observed trajectory are shown as solid lines, and components for the modeled trajectory are shown as dashed lines.

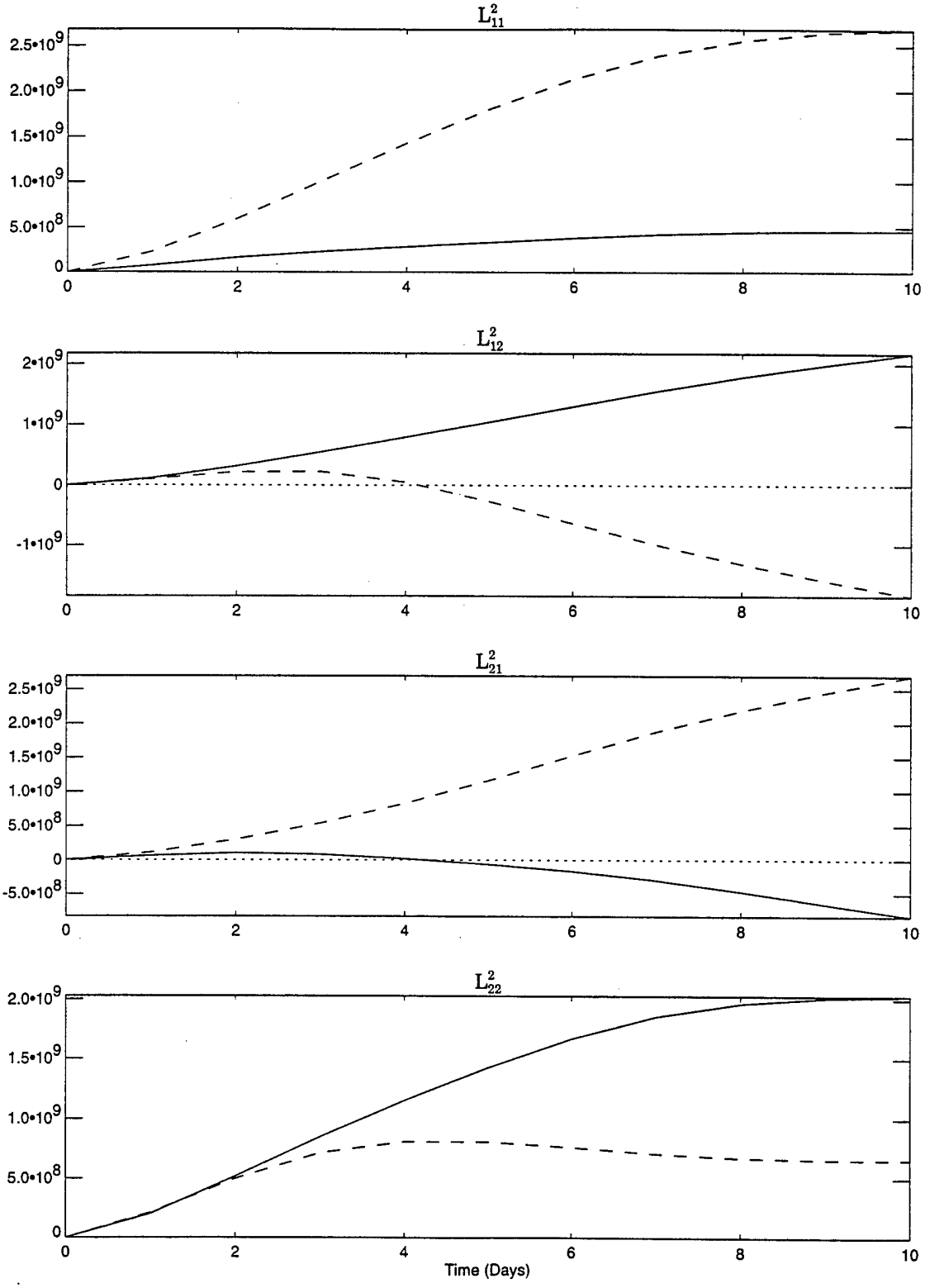

Figure 42: Comparison of L_{ij}^2 (in m^2) for drifter 20383.

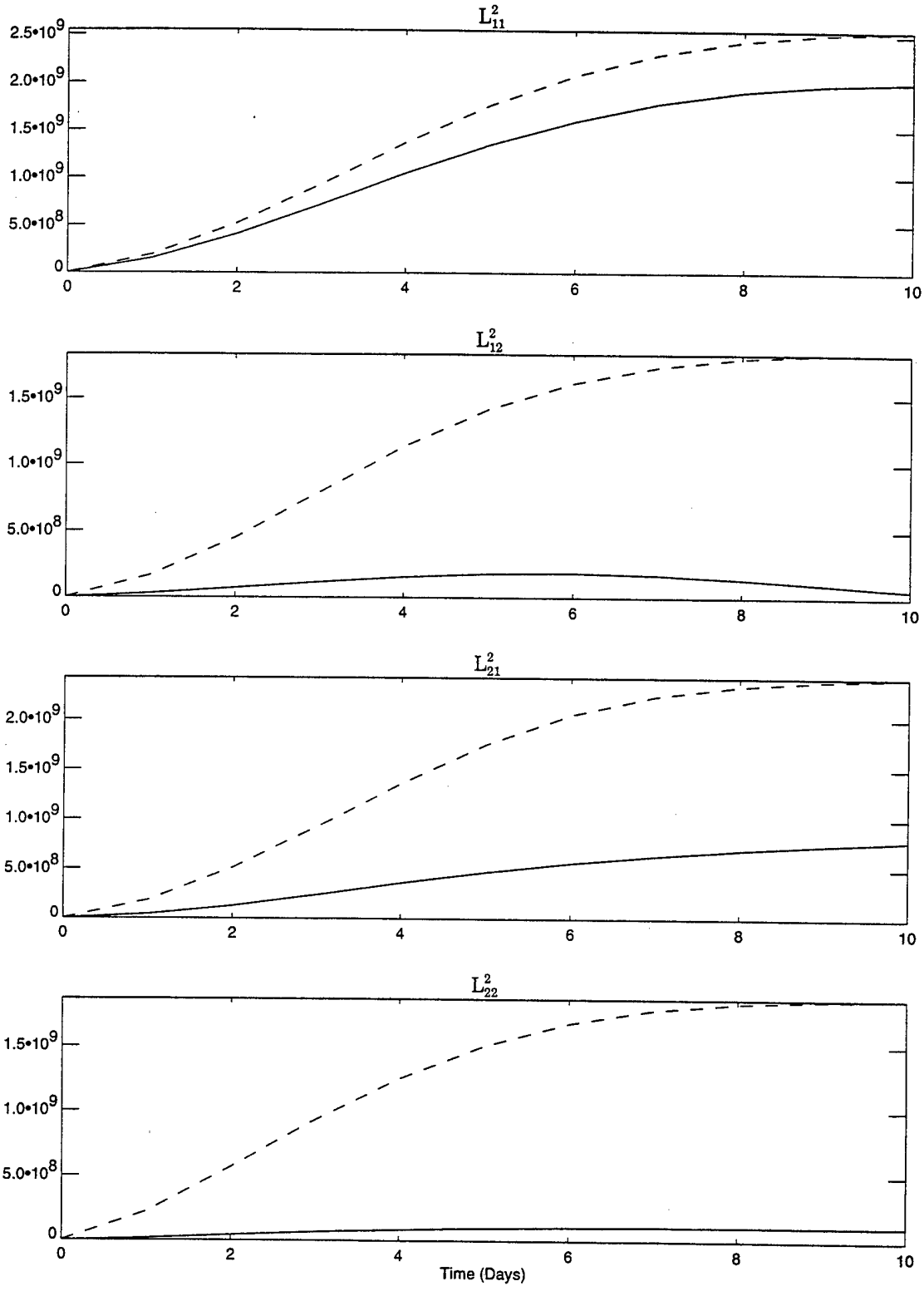

Figure 43: Comparison of L_{ij}^2 (in m^2) for drifter 20386.

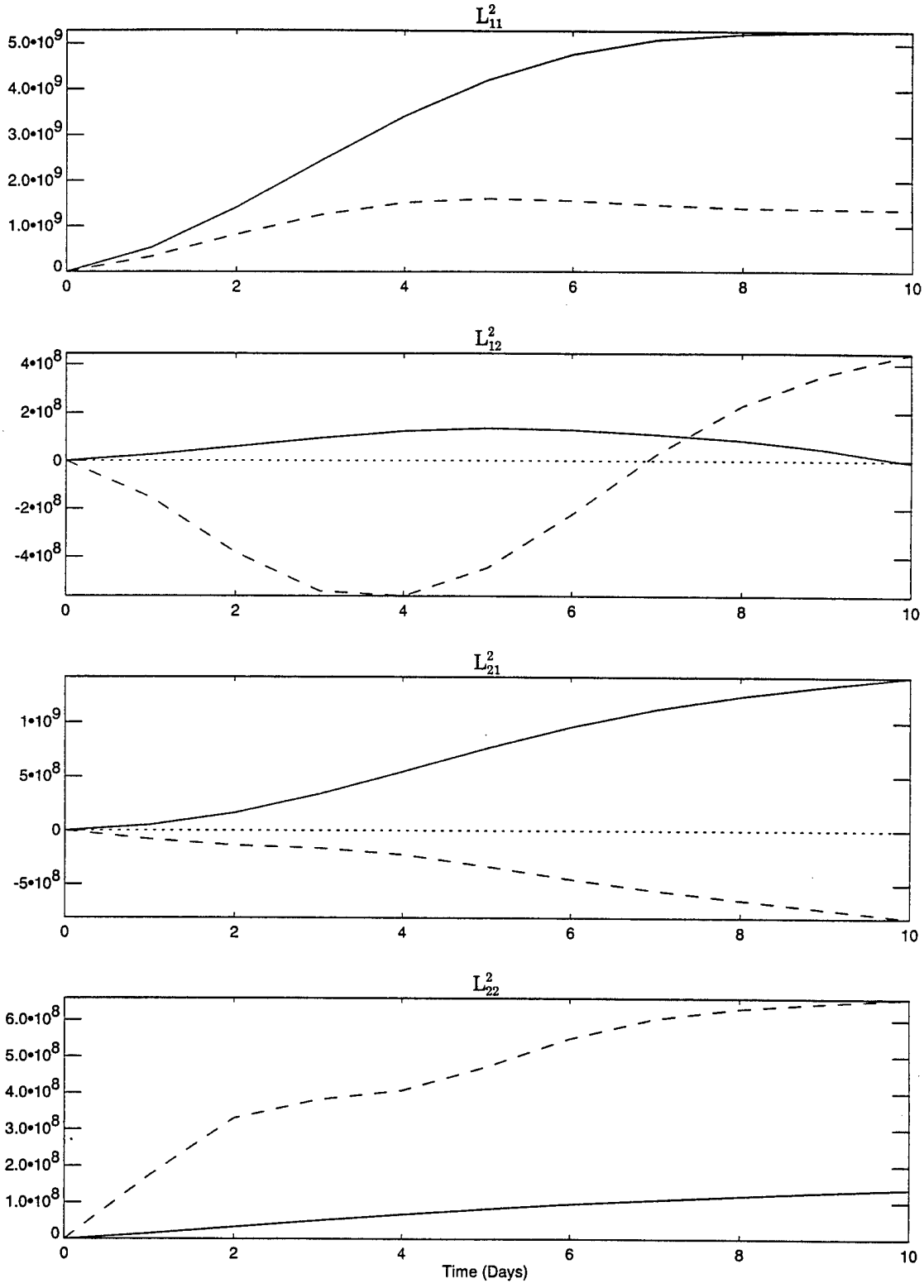

Figure 44: Comparison of L_{ij}^2 (in m^2) for drifter 20396.

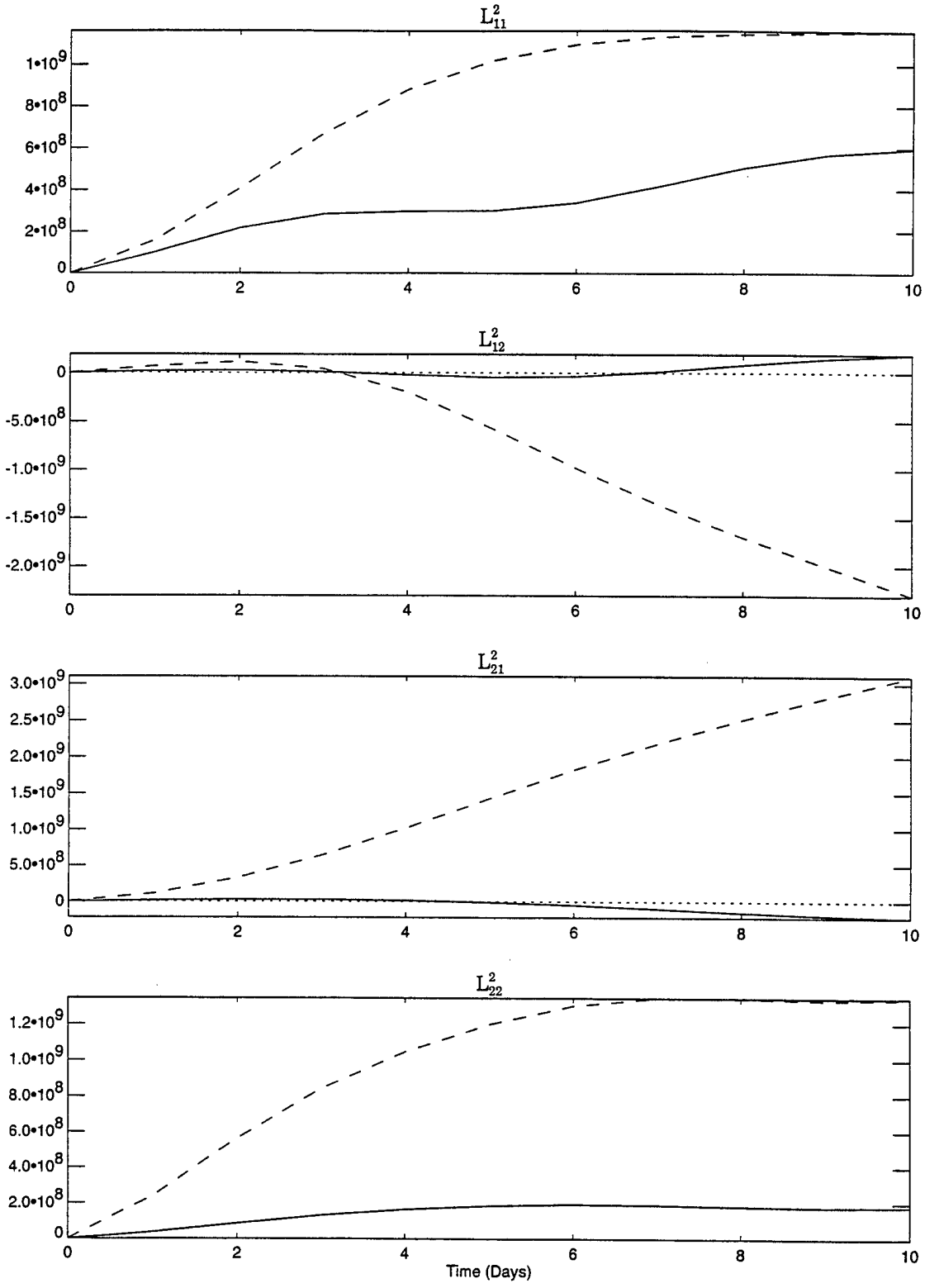

Figure 45: Comparison of L_{ij}^2 (in m^2) for drifter 20402.

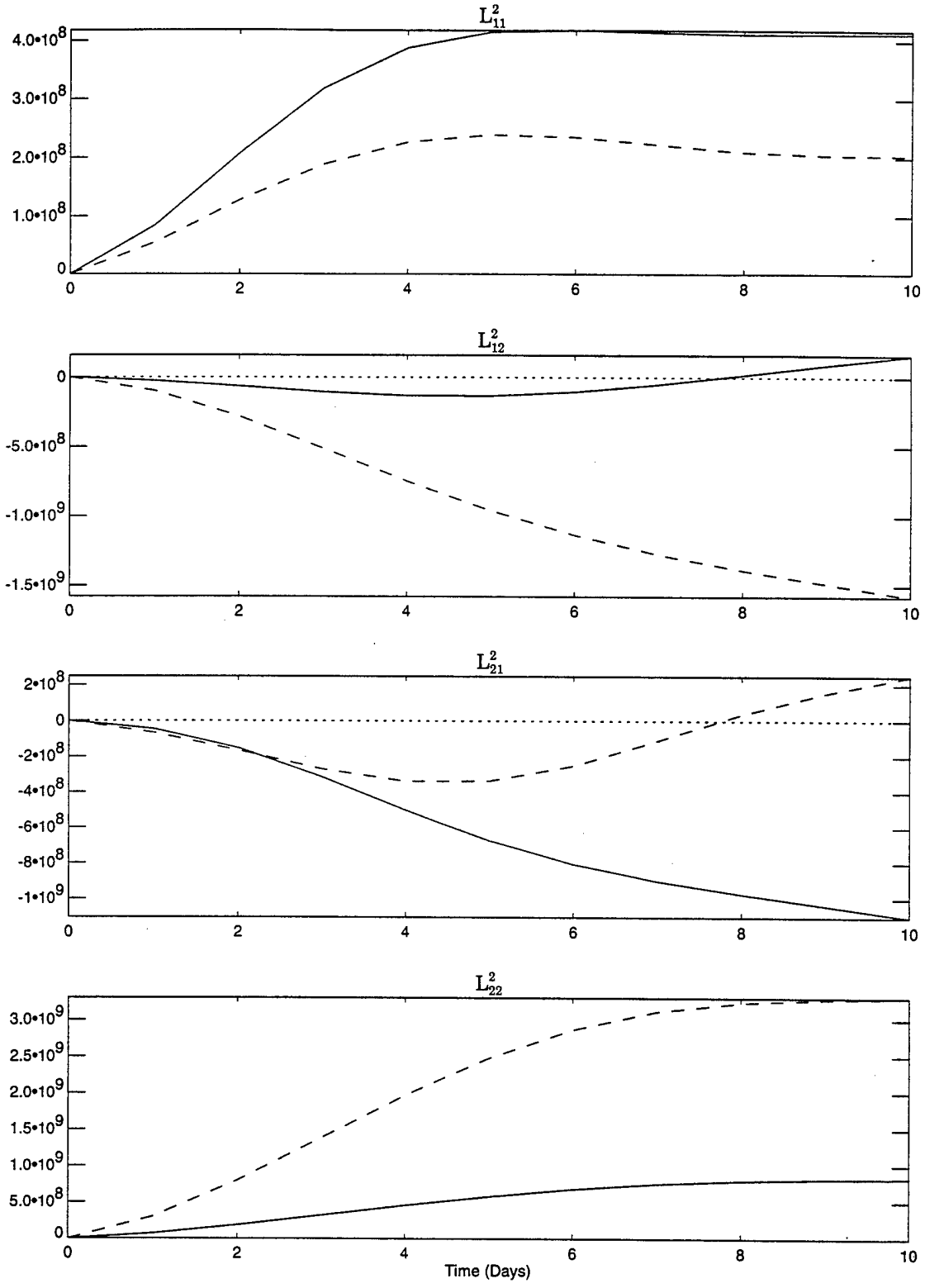

Figure 46: Comparison of L_{ij}^2 (in m^2) for drifter 20407.

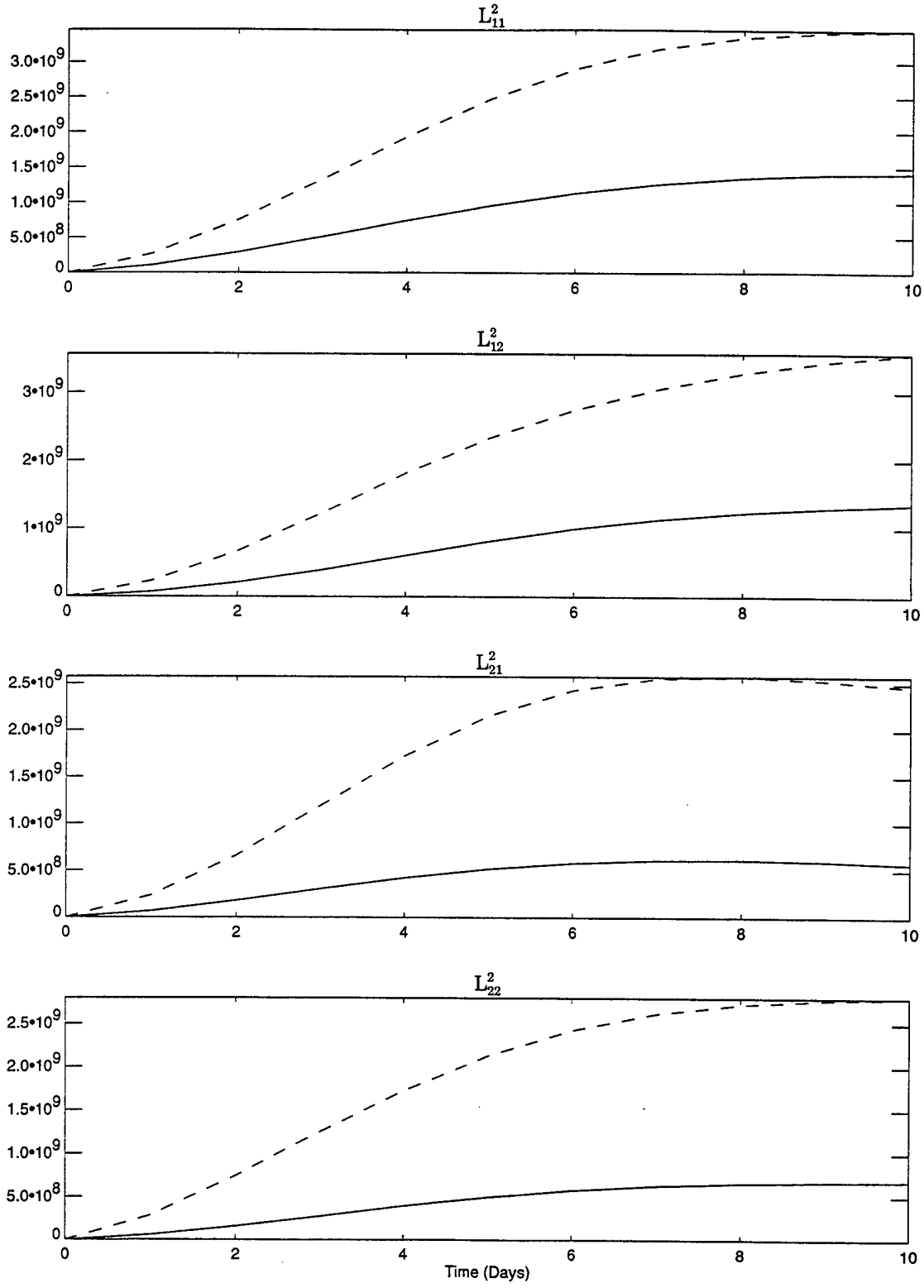

Figure 47: Comparison of L_{ij}^2 (in m^2) for drifter 20412.

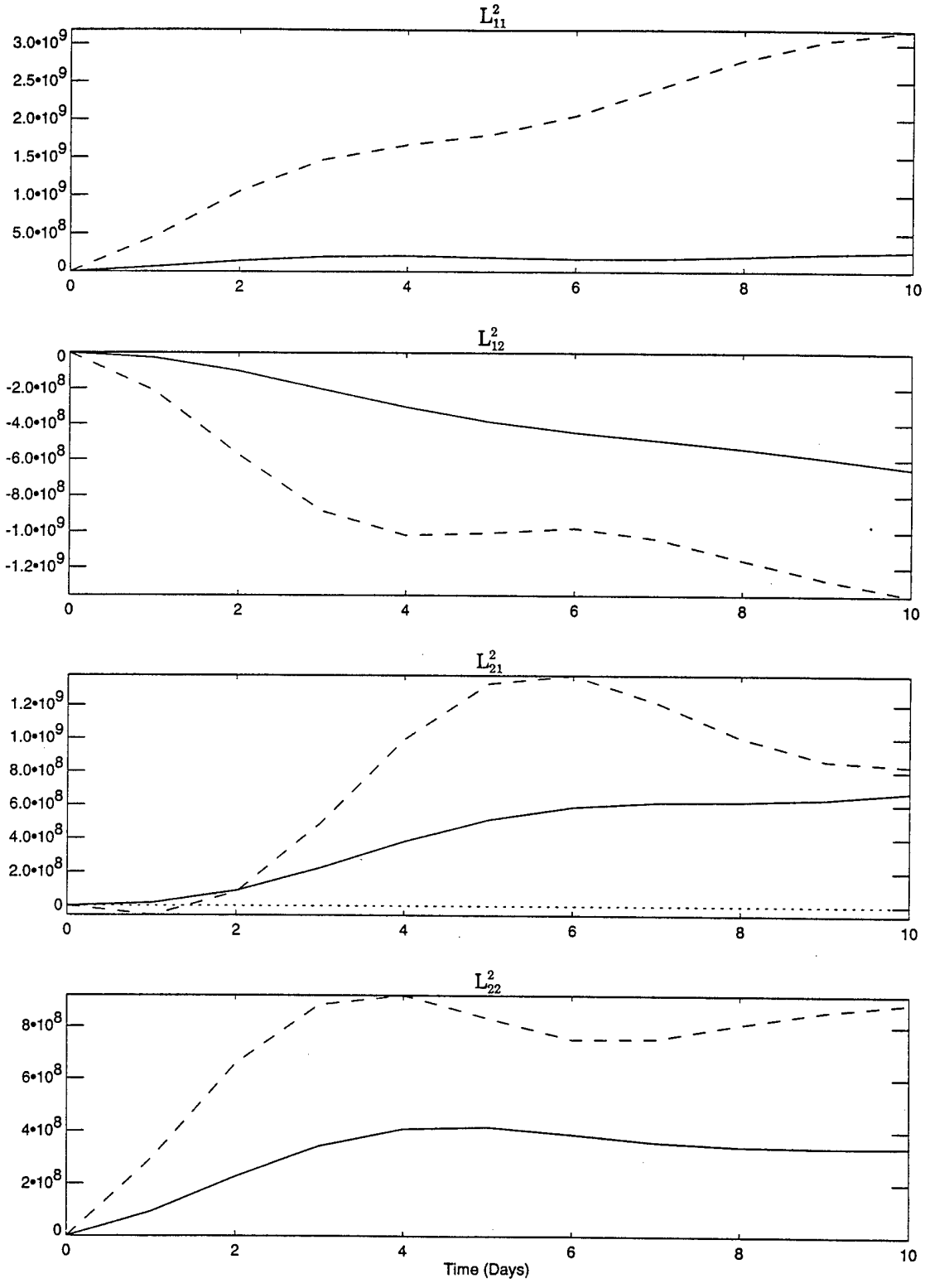

Figure 48: Comparison of L_{ij}^2 (in m^2) for drifter 20422.

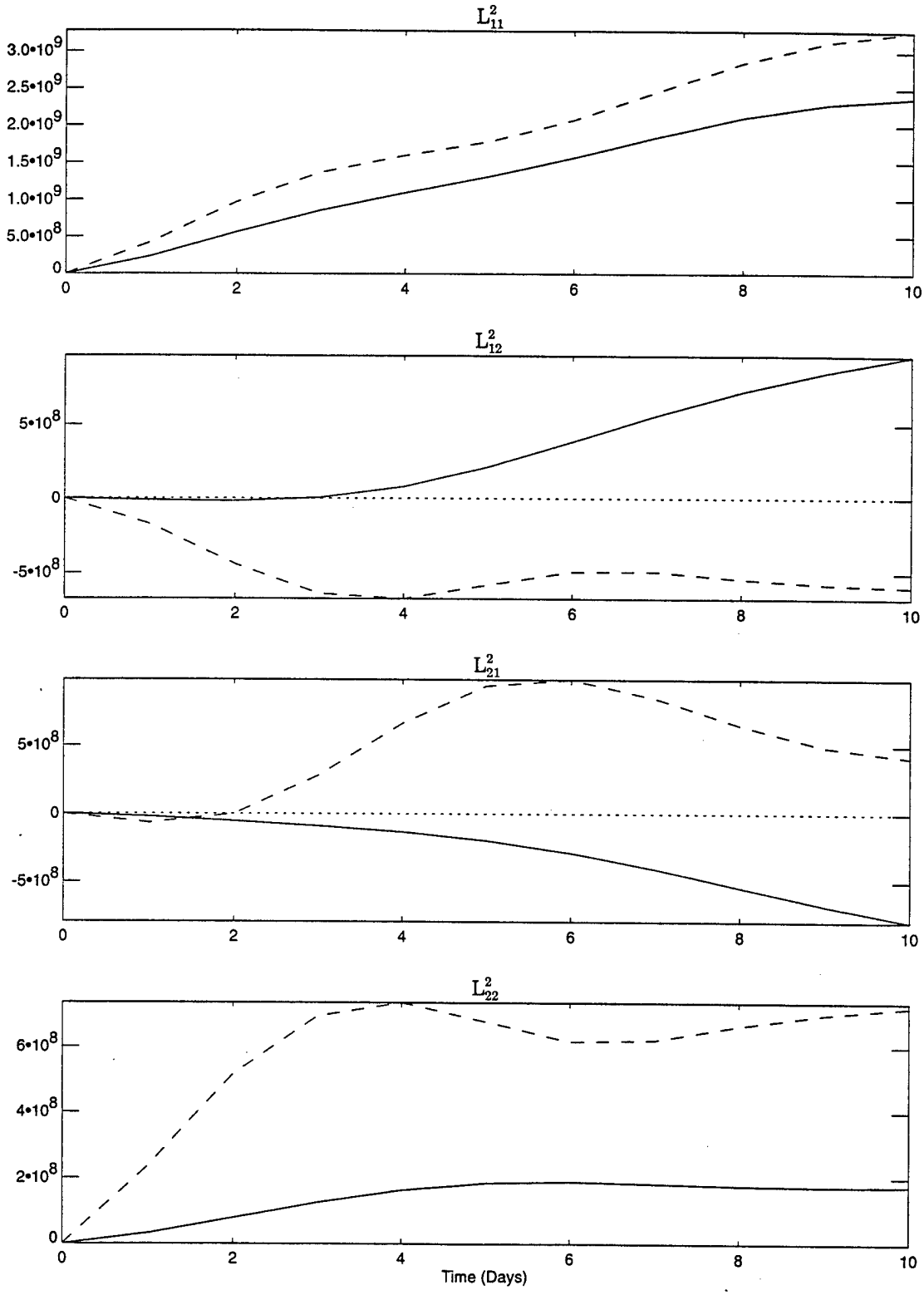

Figure 49: Comparison of L_{ij}^2 (in m^2) for drifter 20436.

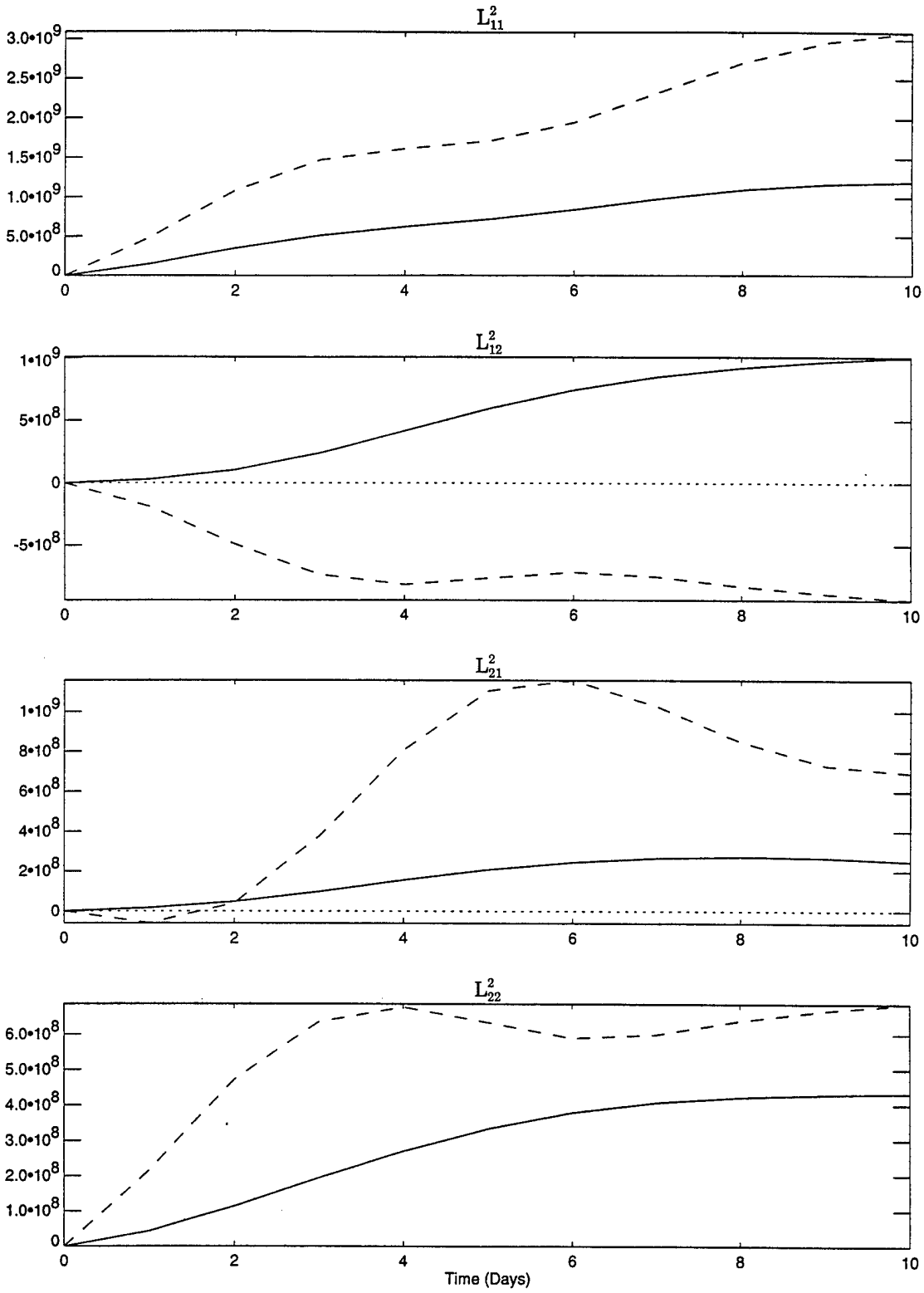

Figure 50: Comparison of L_{ij}^2 (in m^2) for drifter 20440.

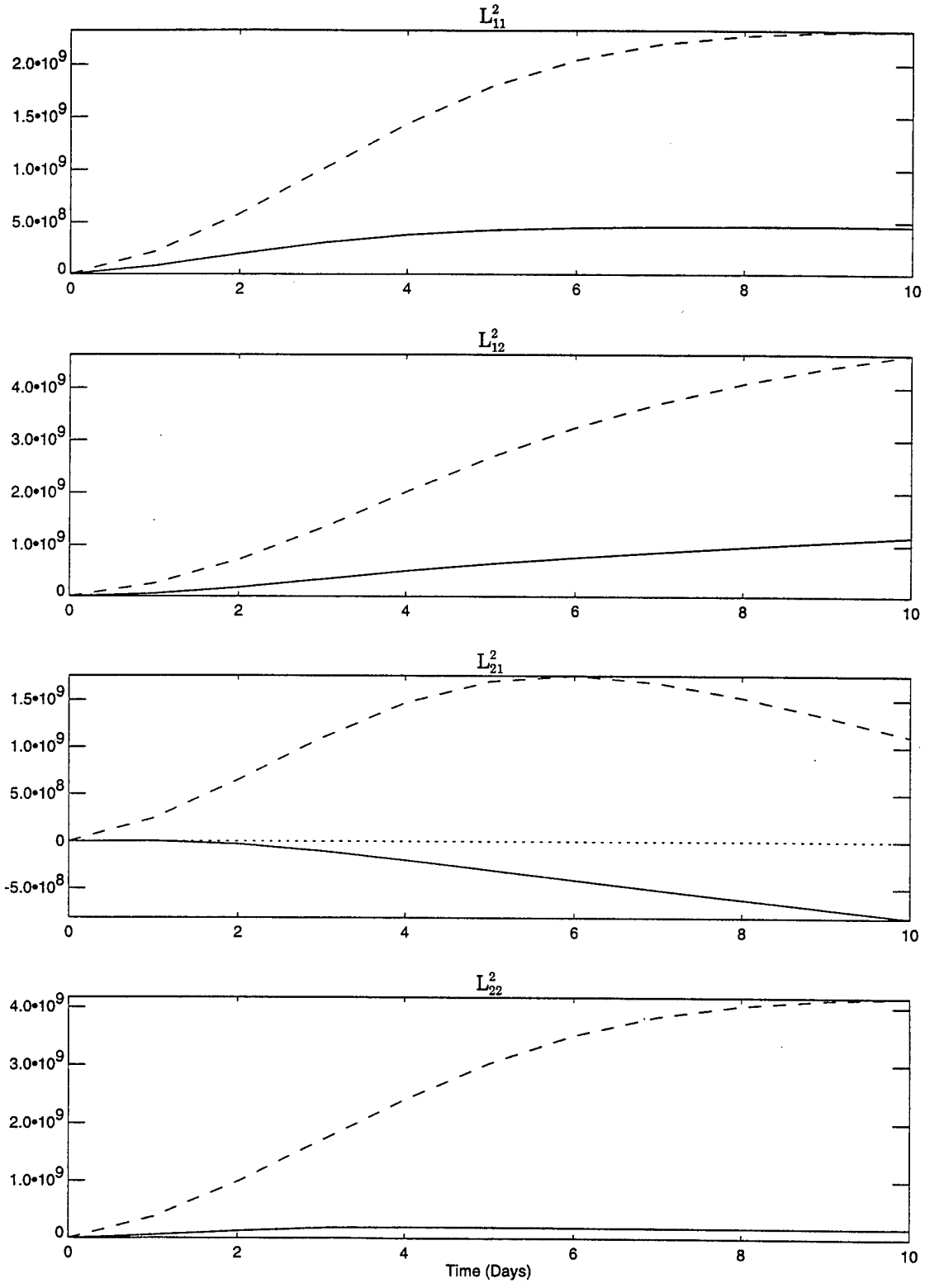

Figure 51: Comparison of L_{ij}^2 (in m^2) for drifter 20446.

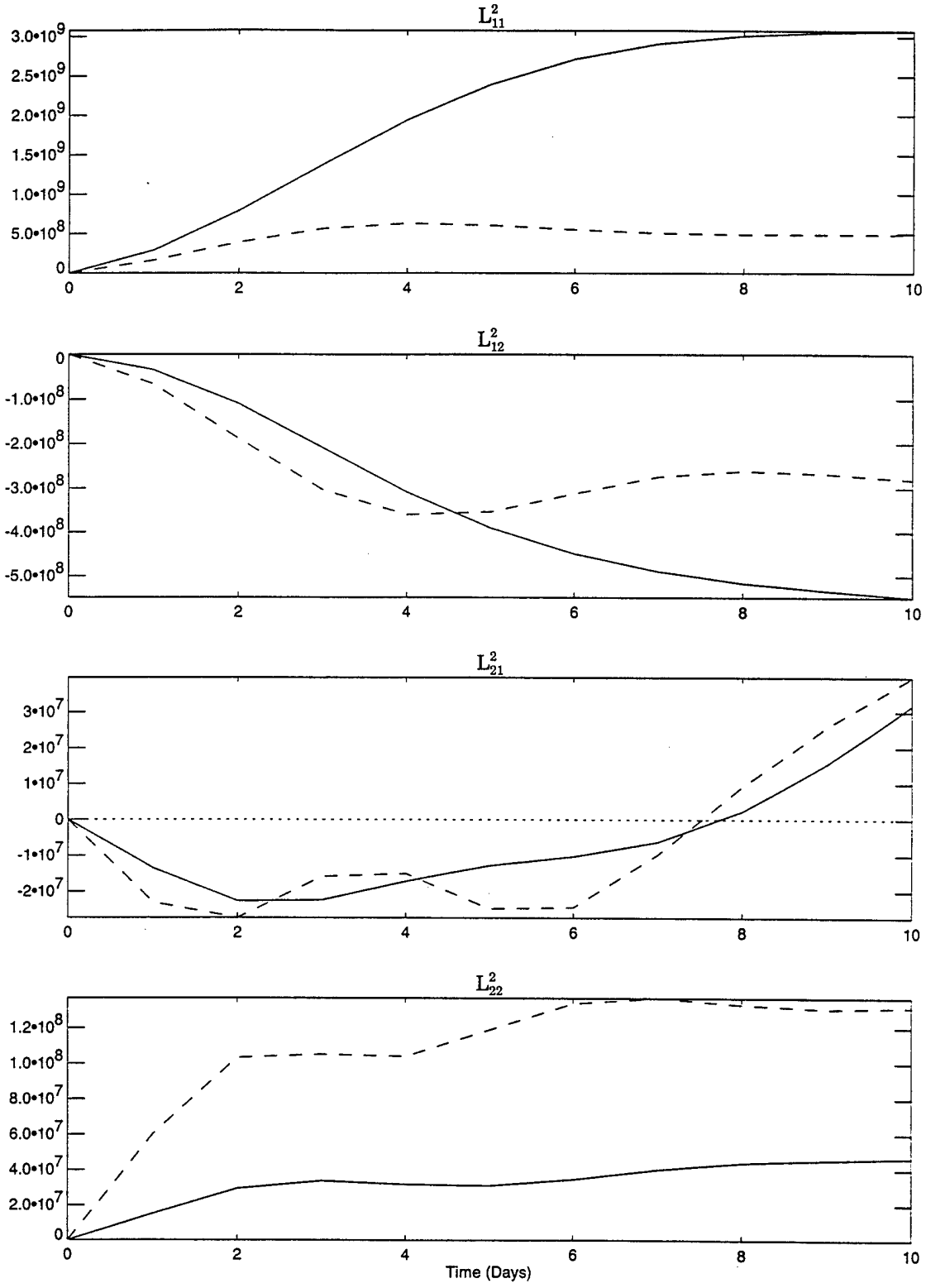

Figure 52: Comparison of L_{ij}^2 (in m^2) for drifter 20449.

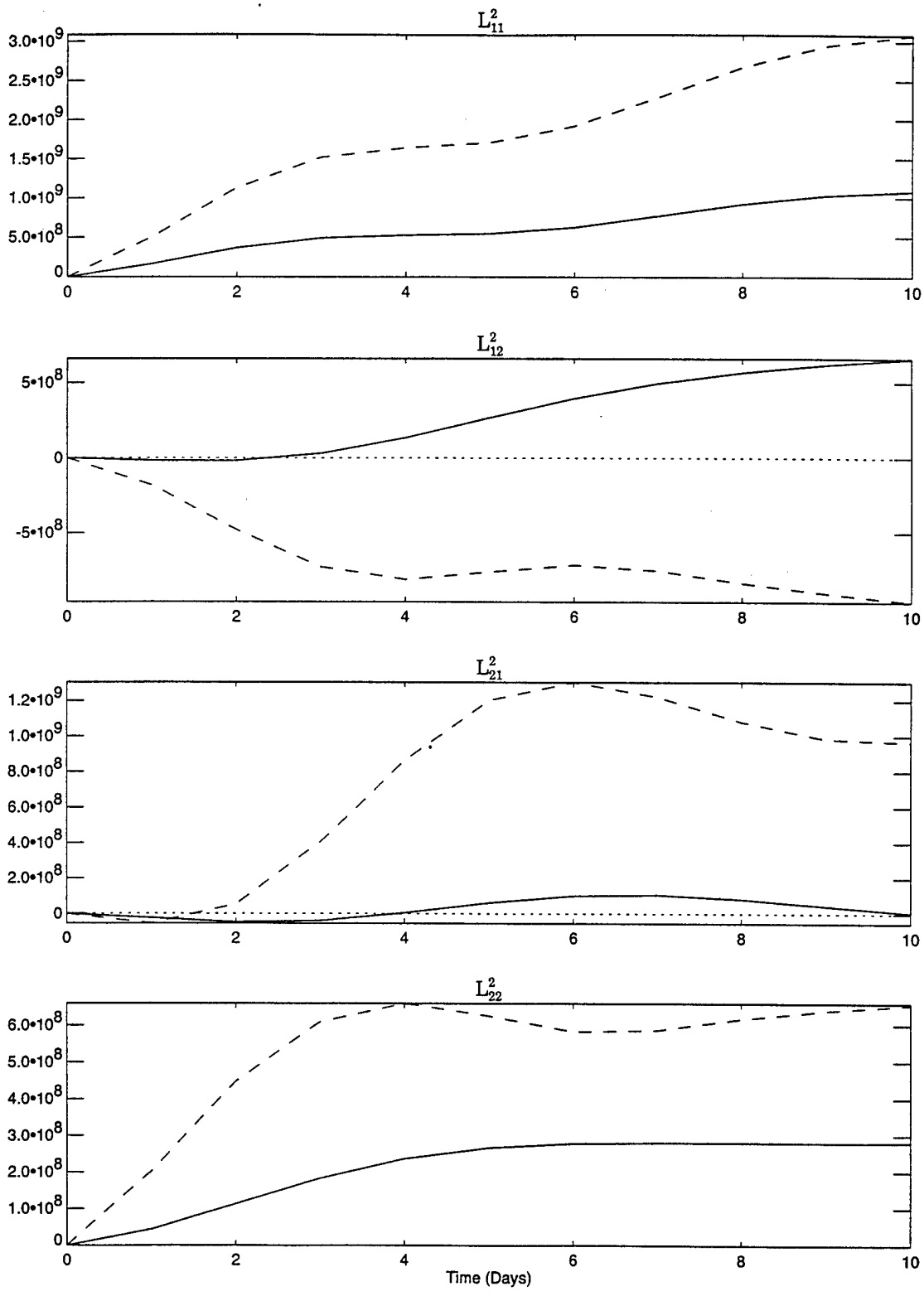

Figure 53: Comparison of L_{ij}^2 (in m^2) for drifter 20455.

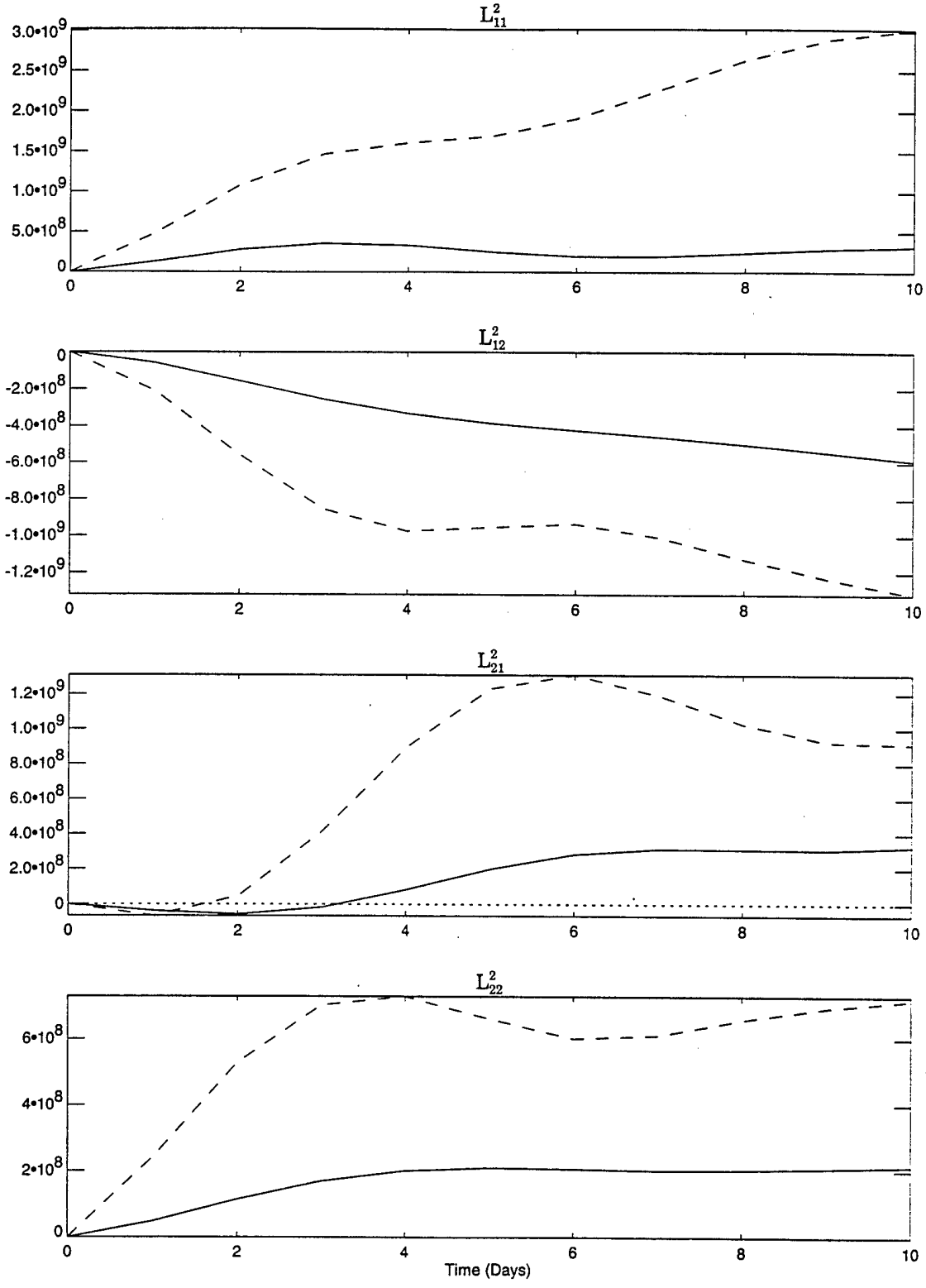

Figure 54: Comparison of L_{ij}^2 (in m^2) for drifter 20456.

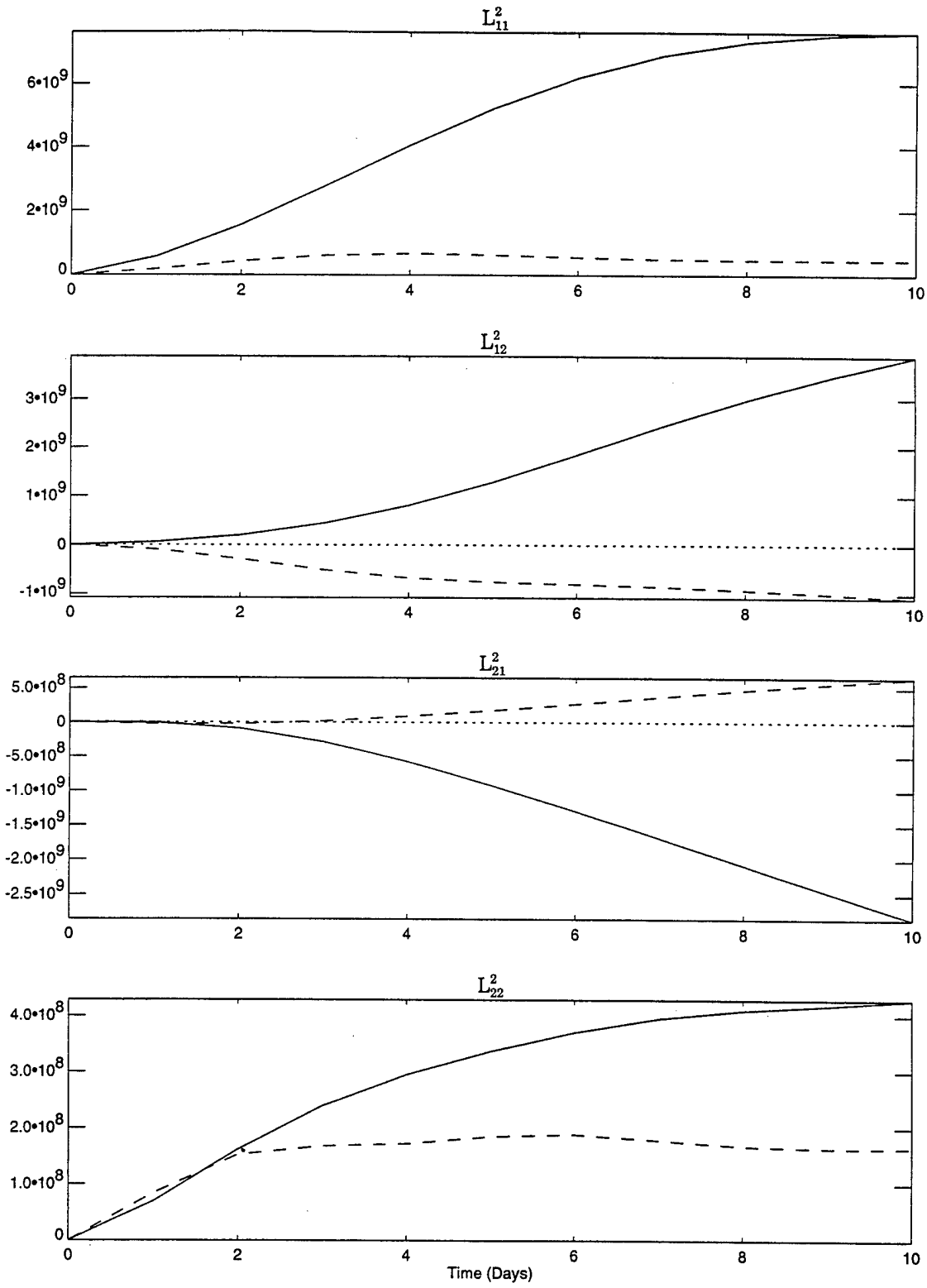

Figure 55: Comparison of L_{ij}^2 (in m^2) for drifter 20457.

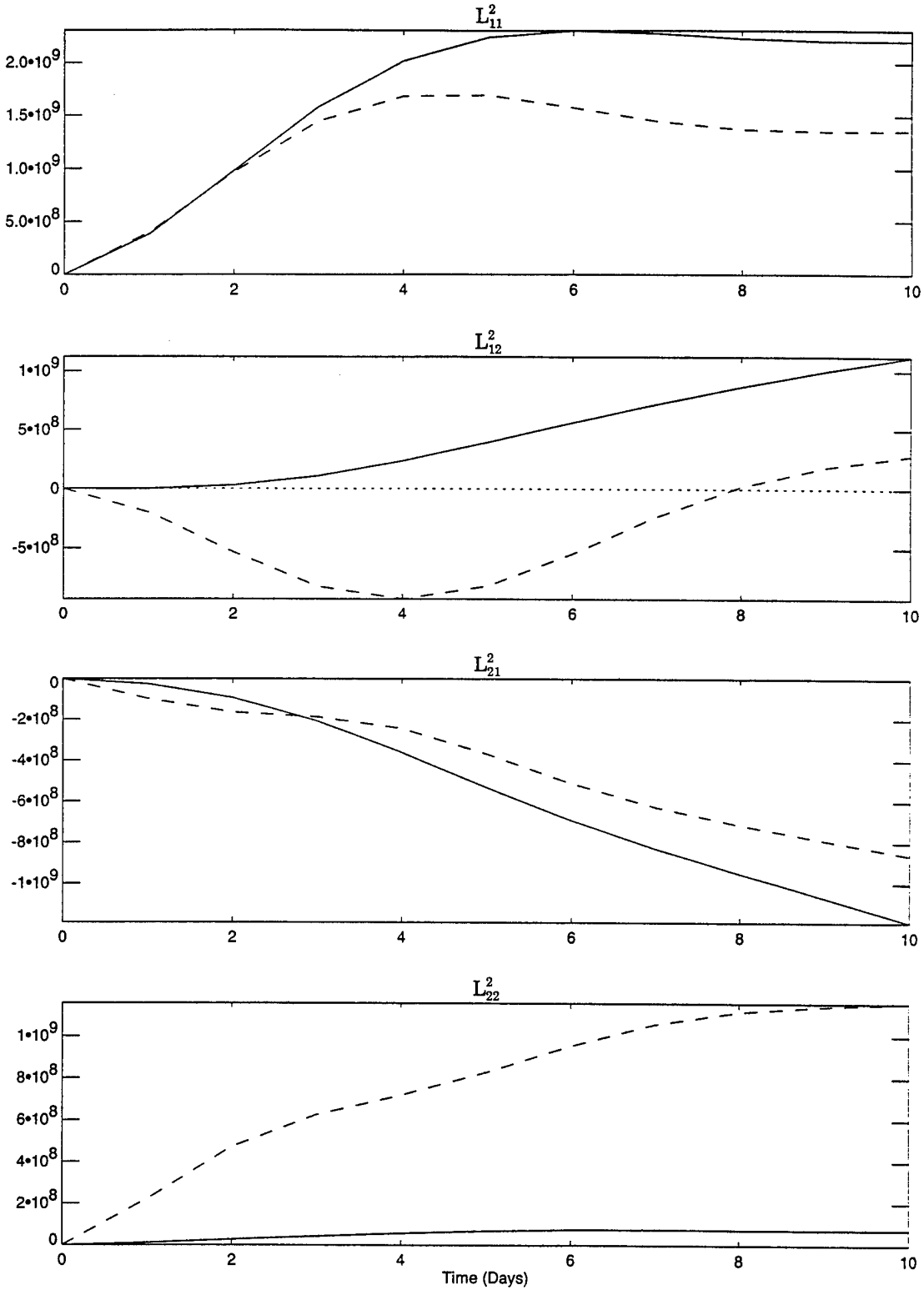

Figure 56: Comparison of L_{ij}^2 (in m^2) for drifter 20461.

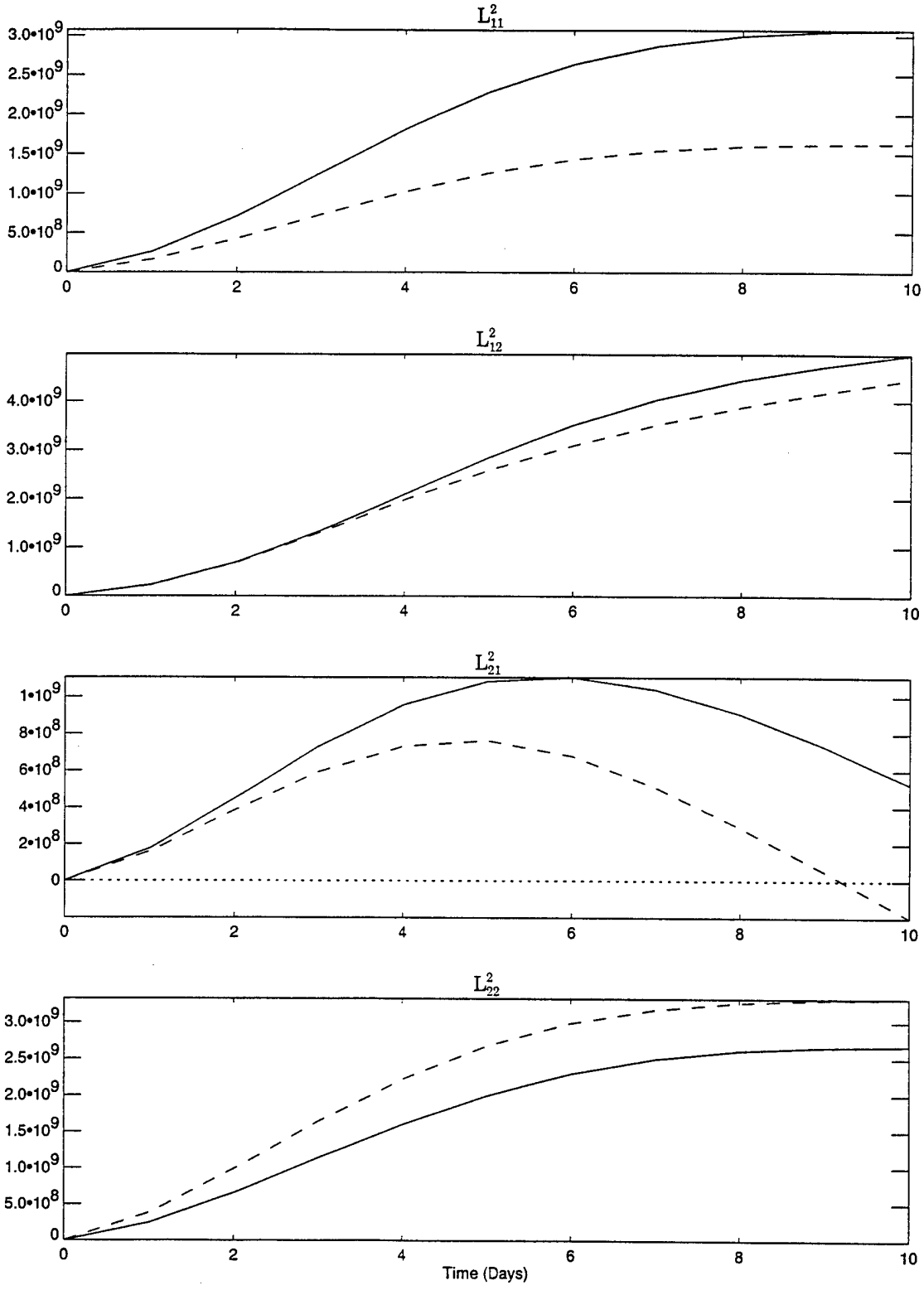

Figure 57: Comparison of L_{ij}^2 (in m^2) for drifter 20463.

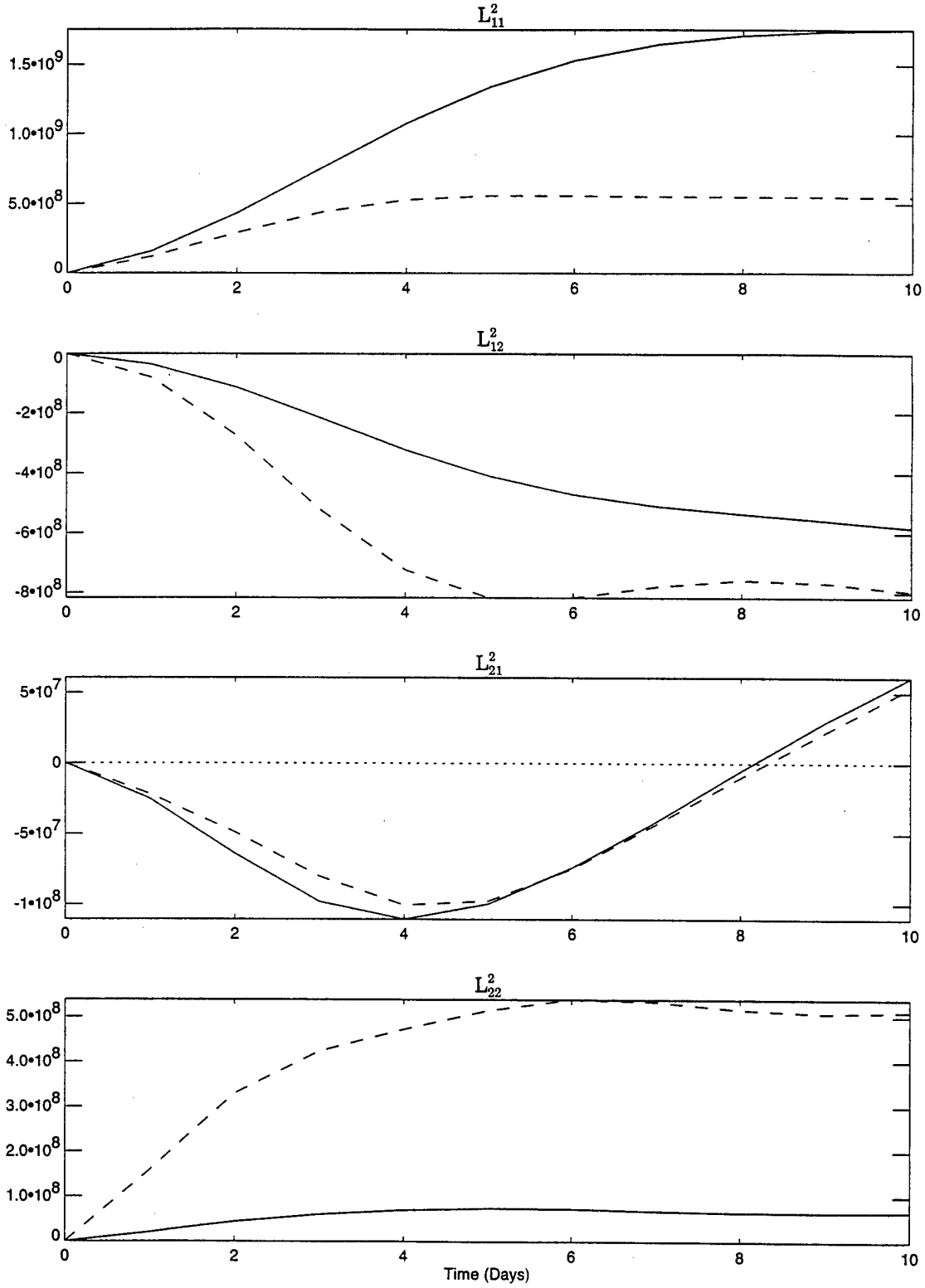

Figure 58: Comparison of L_{ij}^2 (in m^2) for drifter 20465.

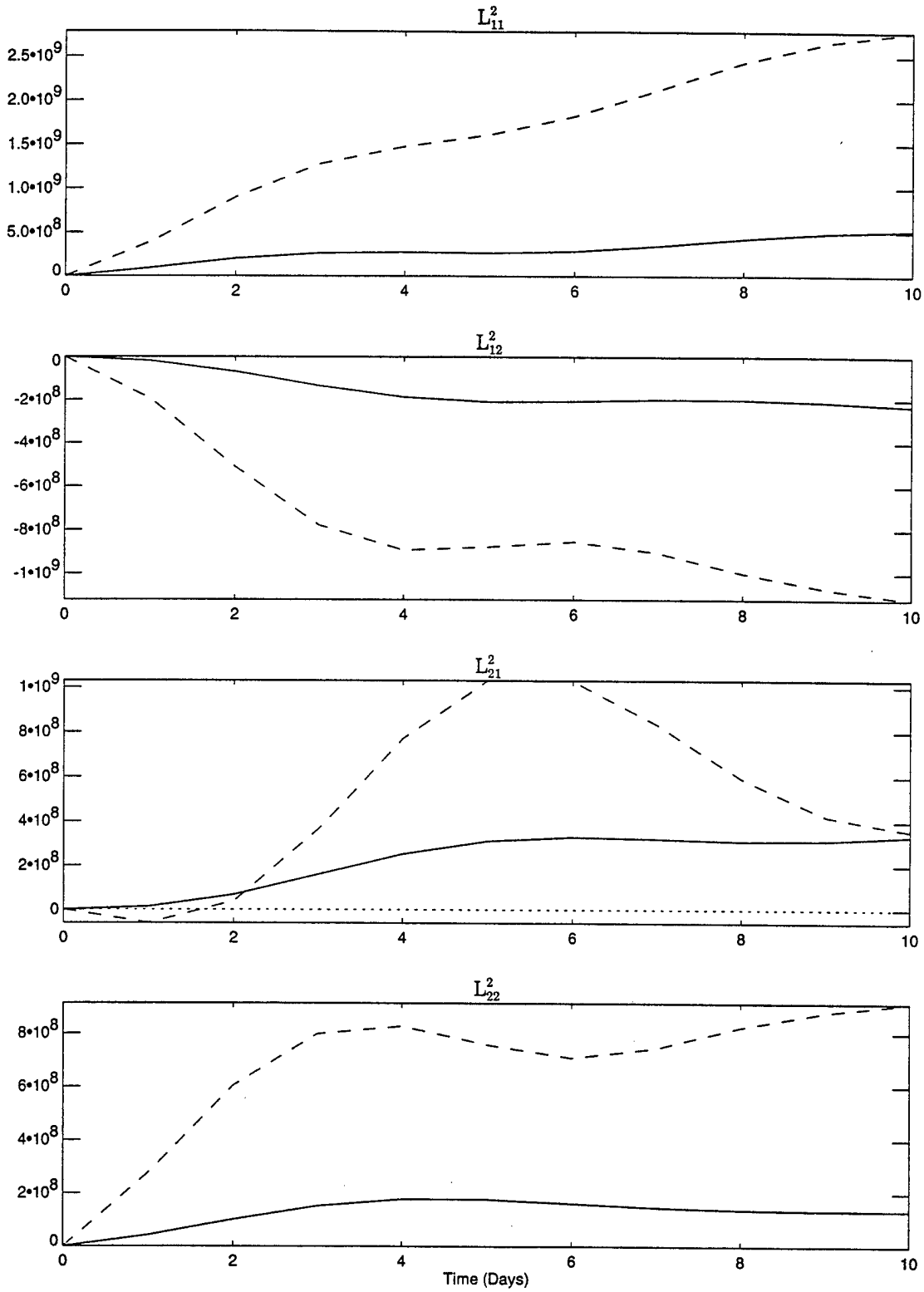

Figure 59: Comparison of L_{ij}^2 (in m^2) for drifter 20468.

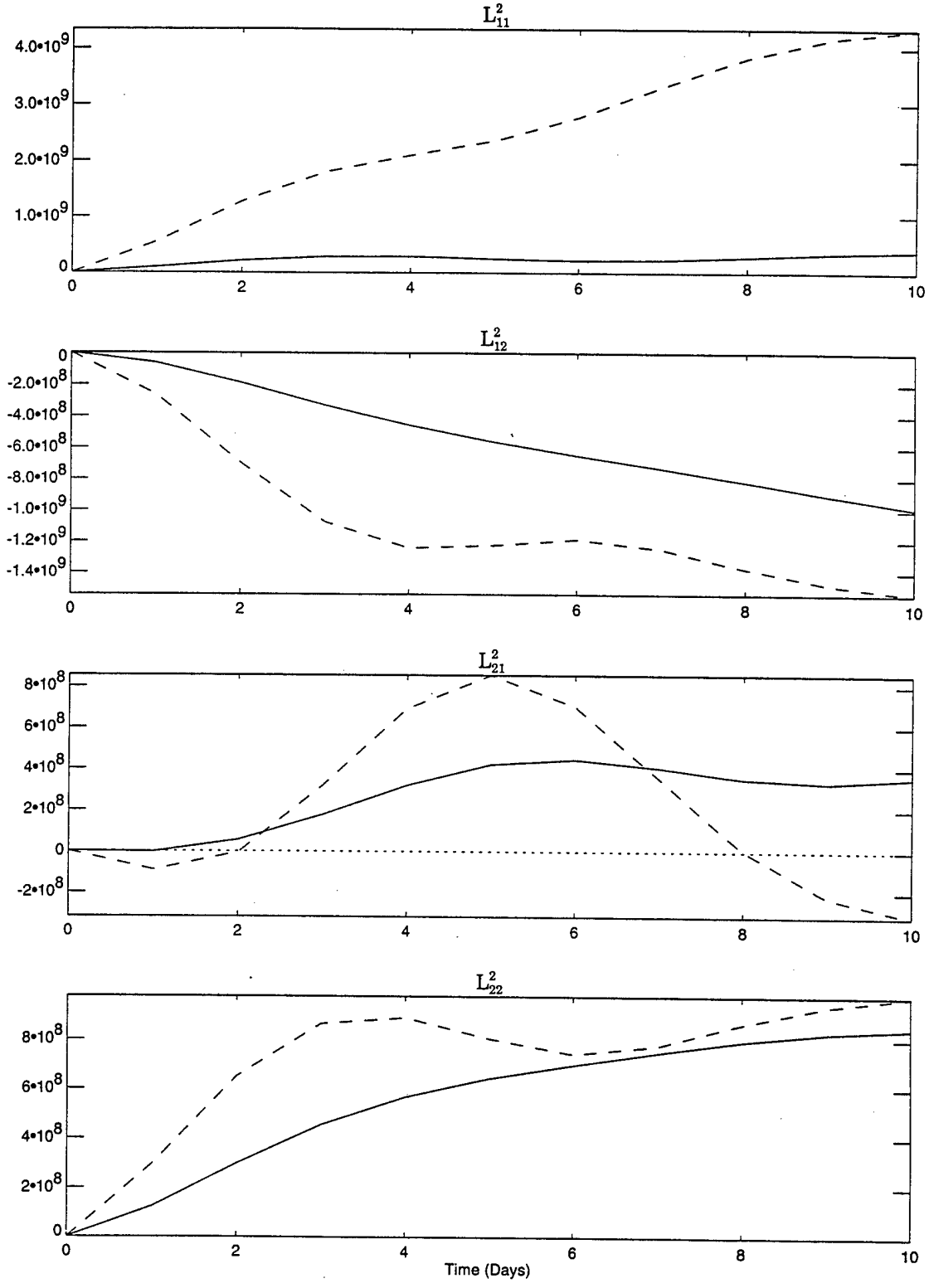

Figure 60: Comparison of L_{ij}^2 (in m^2) for drifter 20469.

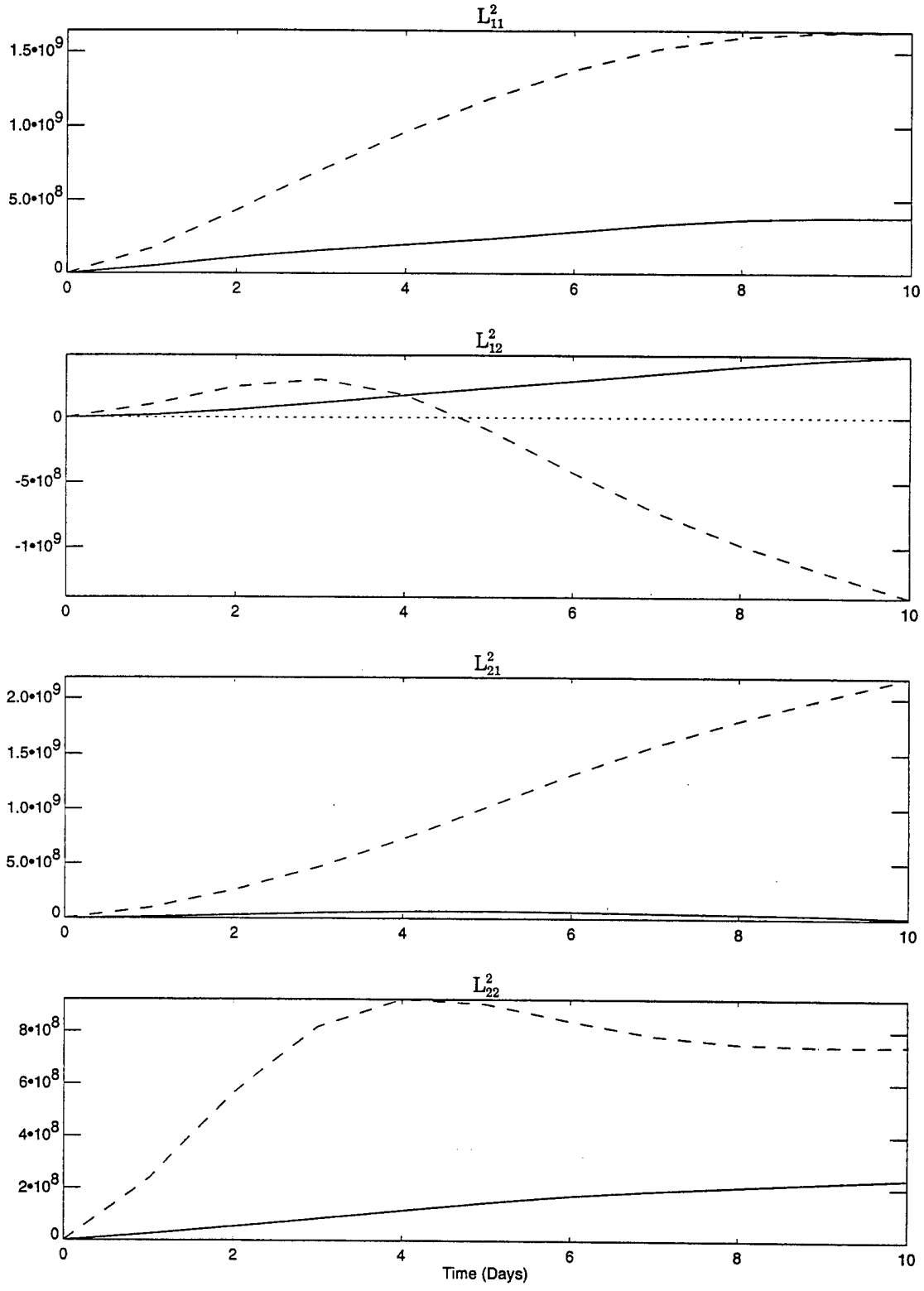

Figure 61: Comparison of L_{ij}^2 (in m^2) for drifter 20498.

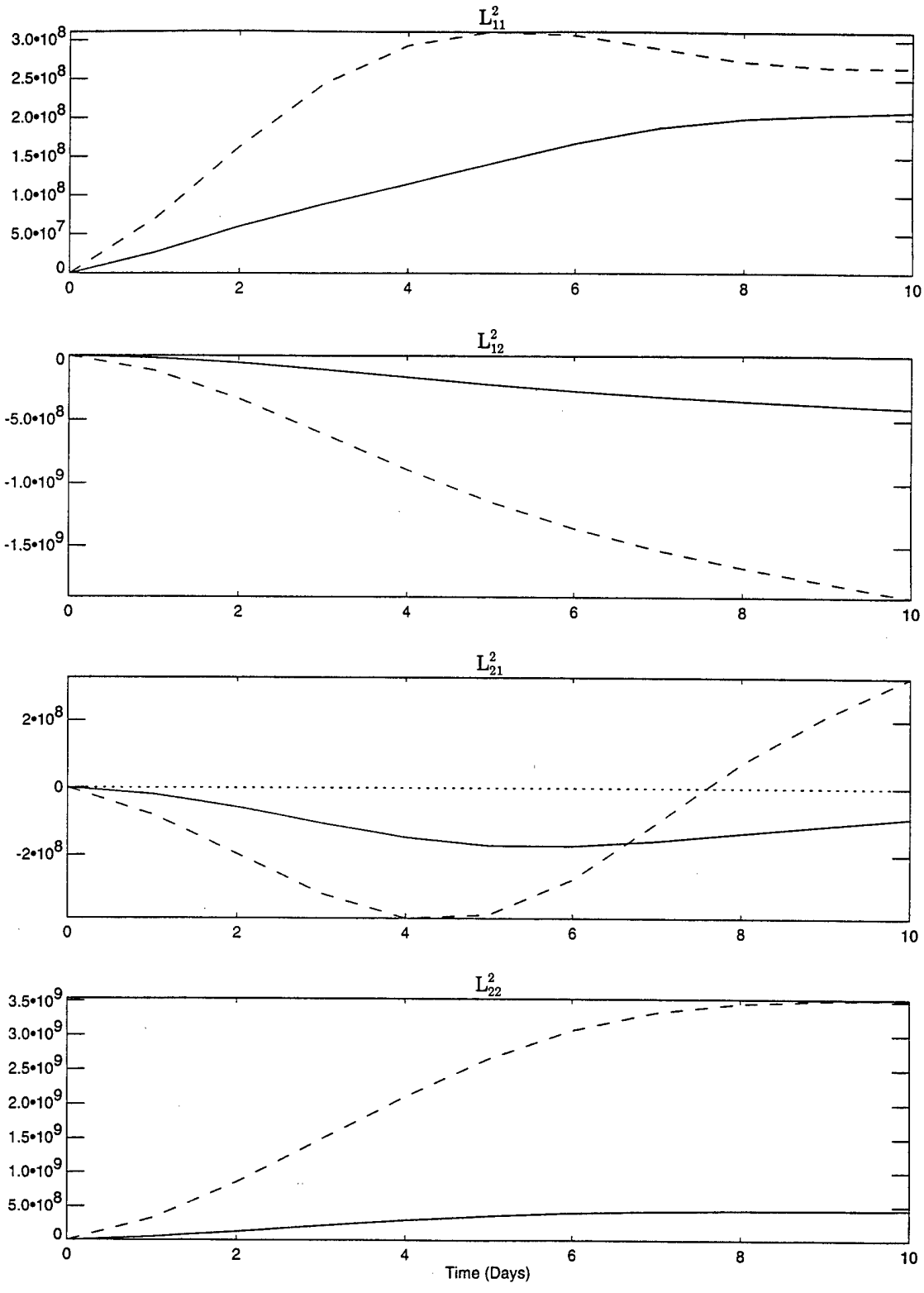

Figure 62: Comparison of L_{ij}^2 (in m^2) for drifter 20513.

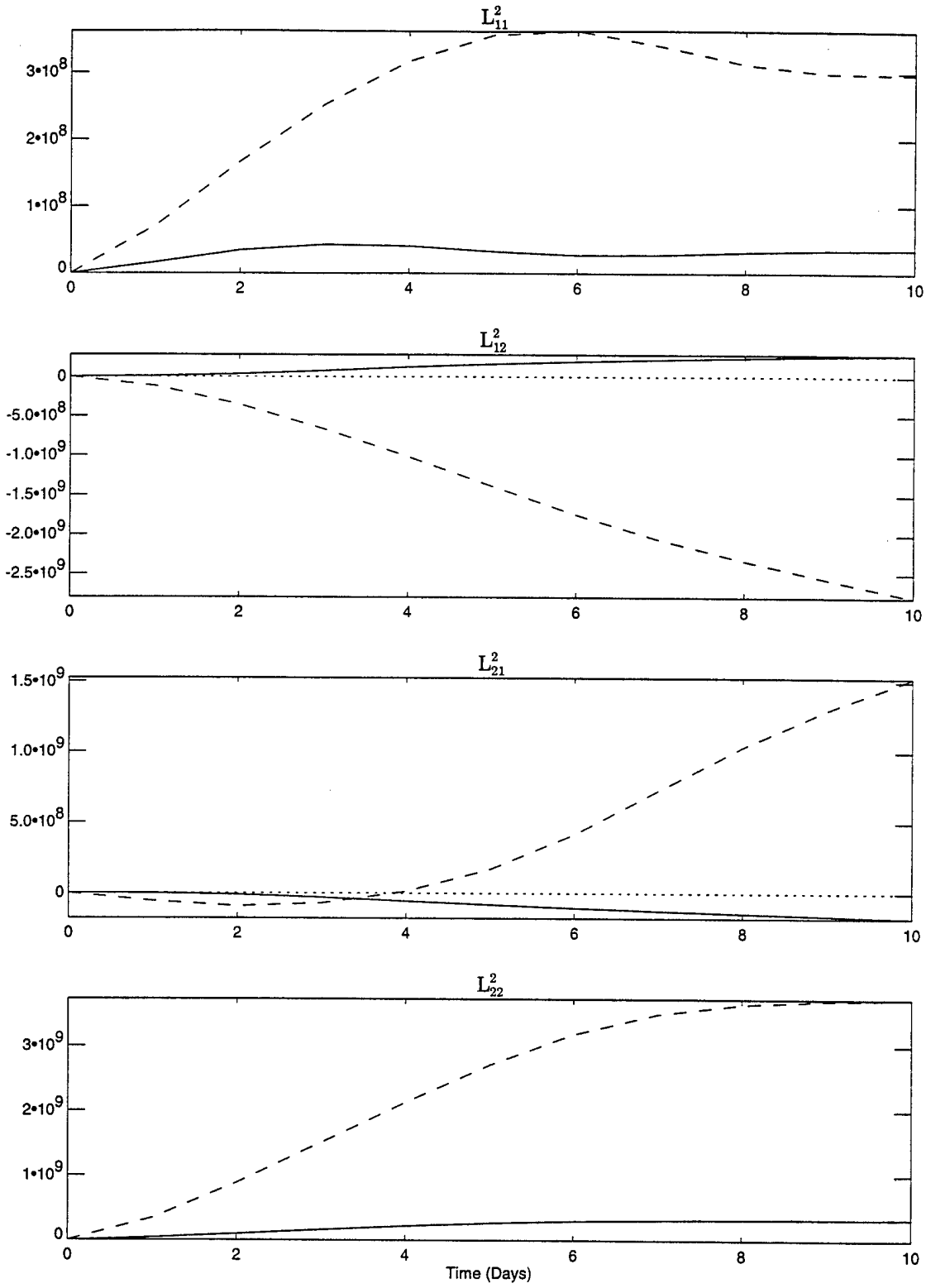

Figure 63: Comparison of L_{ij}^2 (in m^2) for drifter 20519.

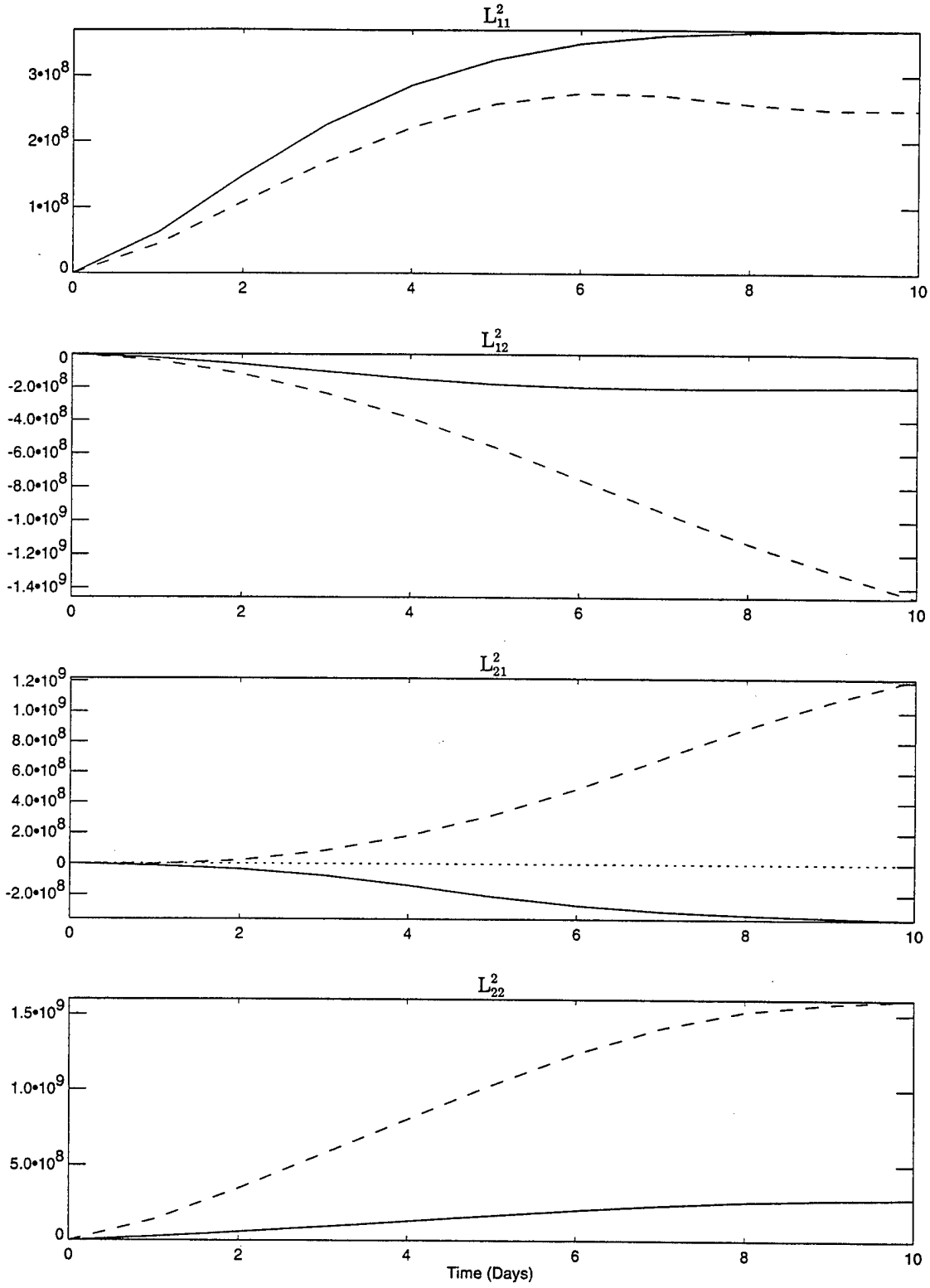

Figure 64: Comparison of L_{ij}^2 (in m^2) for drifter 20528.

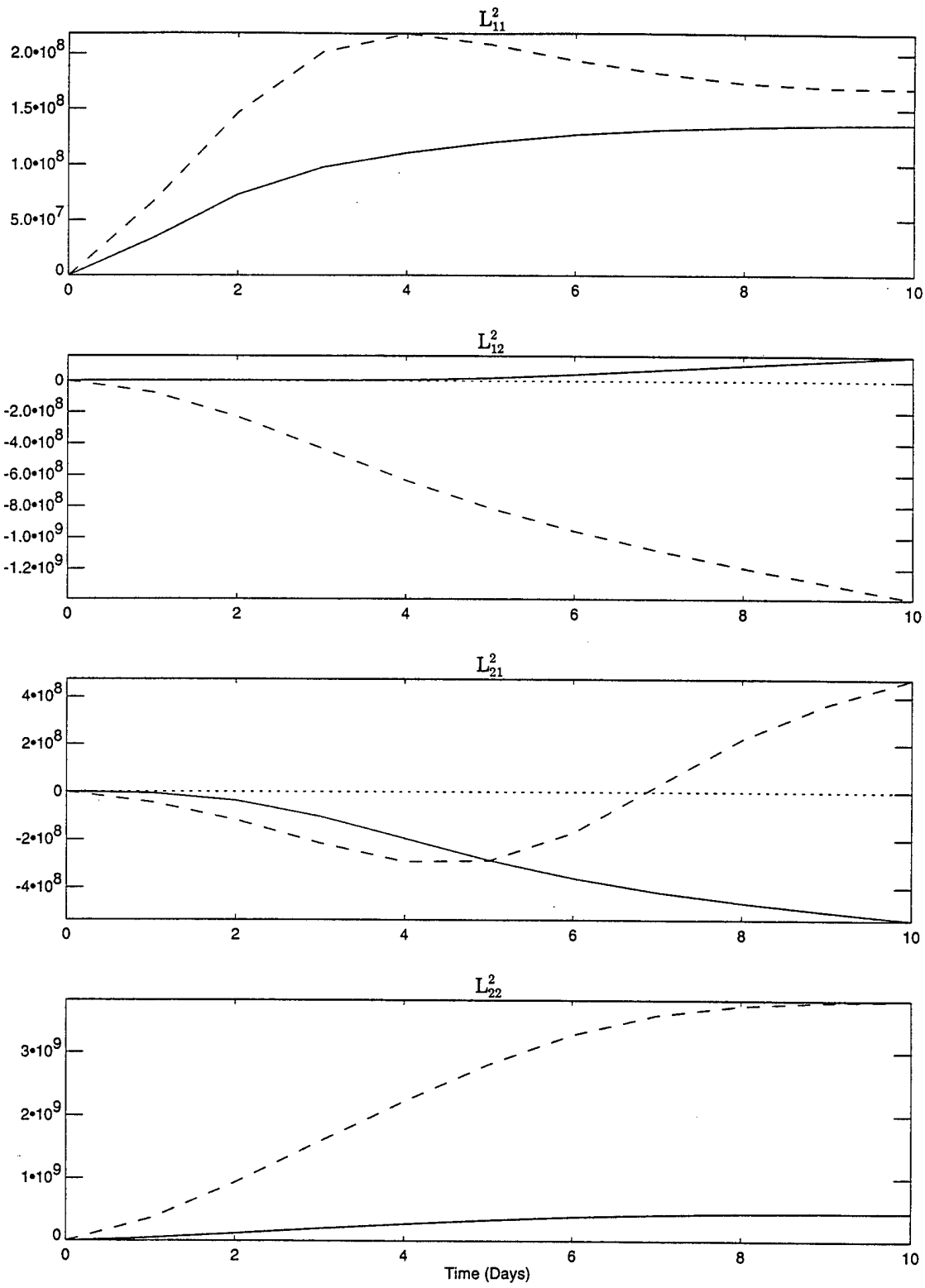

Figure 65: Comparison of L_{ij}^2 (in m^2) for drifter 20531.

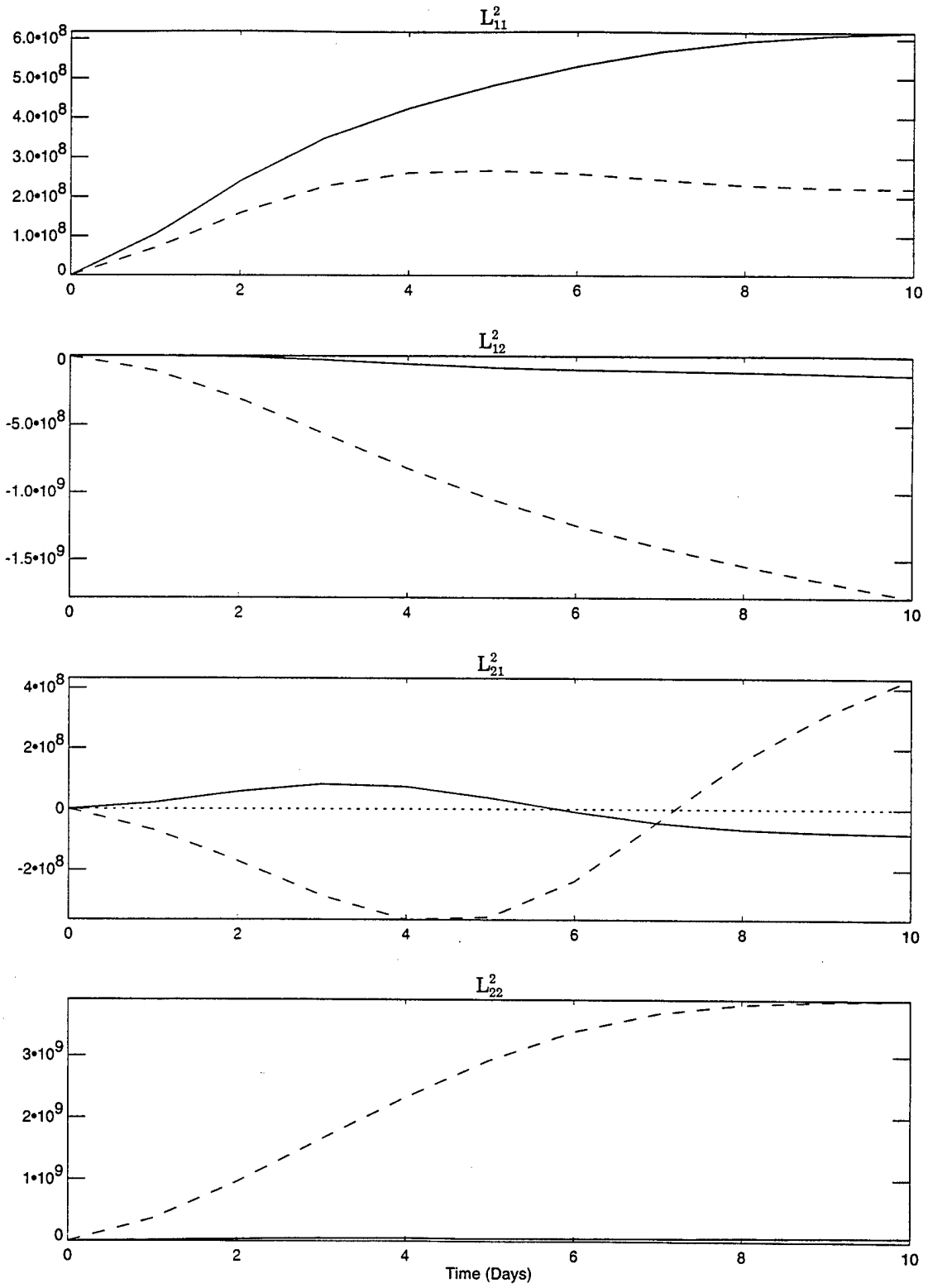

Figure 66: Comparison of L_{ij}^2 (in m^2) for drifter 20533.

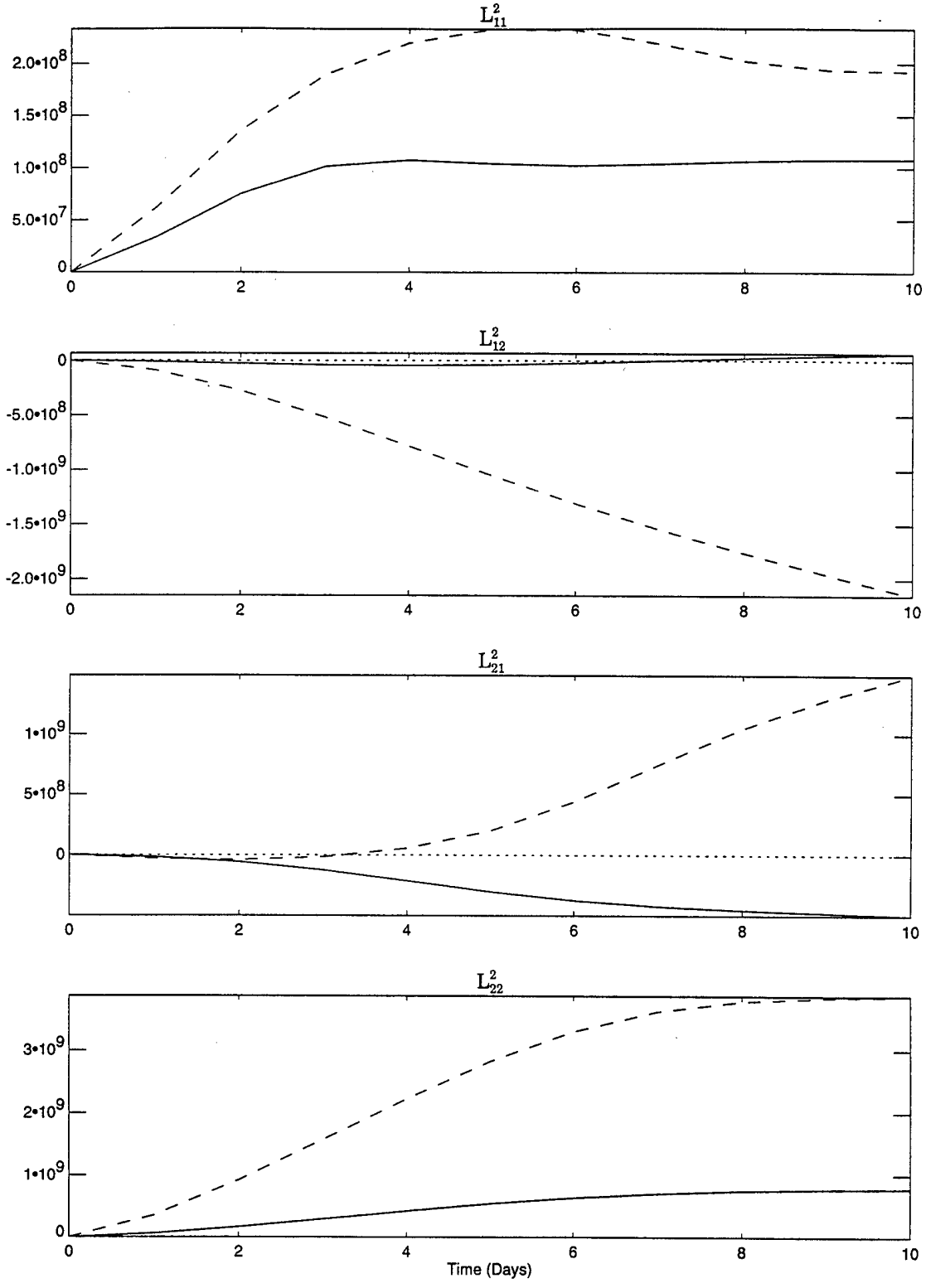

Figure 67: Comparison of L_{ij}^2 (in m^2) for drifter 20536.

A.5 Lagrangian diffusion coefficients

The four Lagrangian diffusion coefficients are expressed as:

$$D_{ij}(t) = \frac{d}{dt} L_{ij}^2(t).$$

Table 5 shows representative values of D_{ij} for the first ten days of each observed and modeled drifter record. The values of D_{ij} shown in the table are the slopes of linear least squares fits through each curve shown in figures 42 –67.

Figure 68 shows scatter plots for each D_{ij} with one data point for each of the 26 modeled drifters. The X axis represents *observed* D_{ij} and the Y axis shows *modeled* D_{ij}. The dashed line in each panel represents the line of correlation between the observed and modeled data.

Table 5: Representative D_{ij} over the first 10 days for observed and modeled drifters (in $10^3\ m^2 s^{-1}$)

Drifter	D_{11}^{obs}	D_{11}^{mod}	D_{12}^{obs}	D_{12}^{mod}	D_{21}^{obs}	D_{21}^{mod}	D_{22}^{obs}	D_{22}^{mod}
20383	0.65	3.60	2.51	-1.62	-0.62	3.02	2.79	1.15
20386	2.68	3.44	0.21	2.58	0.98	3.32	0.17	2.69
20396	7.57	2.31	0.12	0.04	1.72	-0.89	0.17	0.93
20402	0.73	1.72	0.10	-2.20	-0.18	3.51	0.29	2.03
20407	0.65	0.35	-0.00	-1.98	-1.38	-0.07	1.13	4.62
20412	1.90	4.75	1.72	4.65	0.88	3.71	0.94	3.93
20422	0.34	4.01	-0.79	-1.82	0.91	1.60	0.58	1.35
20436	2.96	4.07	0.92	-0.91	-0.74	1.02	0.28	1.10
20440	1.55	3.89	1.27	-1.33	0.37	1.33	0.61	1.04
20446	0.70	3.28	1.39	5.74	-0.85	2.31	0.30	5.75
20449	4.35	0.85	-0.74	-0.47	0.00	0.01	0.07	0.21
20455	1.32	3.87	0.74	-1.33	0.08	1.63	0.43	1.01
20456	0.44	3.81	-0.75	-1.76	0.41	1.59	0.33	1.09
20457	10.30	0.84	4.01	-1.39	-2.85	0.62	0.61	0.28
20461	3.50	2.36	1.17	-0.35	-1.32	-0.98	0.11	1.62
20463	4.28	2.31	6.16	5.50	1.37	0.54	3.73	4.78
20465	2.47	0.87	-0.77	-1.22	-0.04	-0.04	0.11	0.82
20468	0.63	3.52	-0.32	-1.56	0.48	1.01	0.24	1.33
20469	0.48	5.42	-1.19	-2.15	0.57	0.28	1.18	1.40
20498	0.51	2.28	0.54	-1.15	0.07	2.50	0.30	1.28
20513	0.28	0.45	-0.49	-2.38	-0.21	-0.04	0.64	4.95
20519	0.05	0.51	0.34	-3.26	-0.20	1.30	0.47	5.17
20528	0.55	0.40	-0.30	-1.56	-0.45	1.18	0.36	2.12
20531	0.21	0.30	0.13	-1.71	-0.64	0.16	0.63	5.33
20533	0.88	0.38	-0.16	-2.21	-0.05	0.07	0.09	5.48
20536	0.17	0.33	0.02	-2.48	-0.63	1.32	1.05	5.37

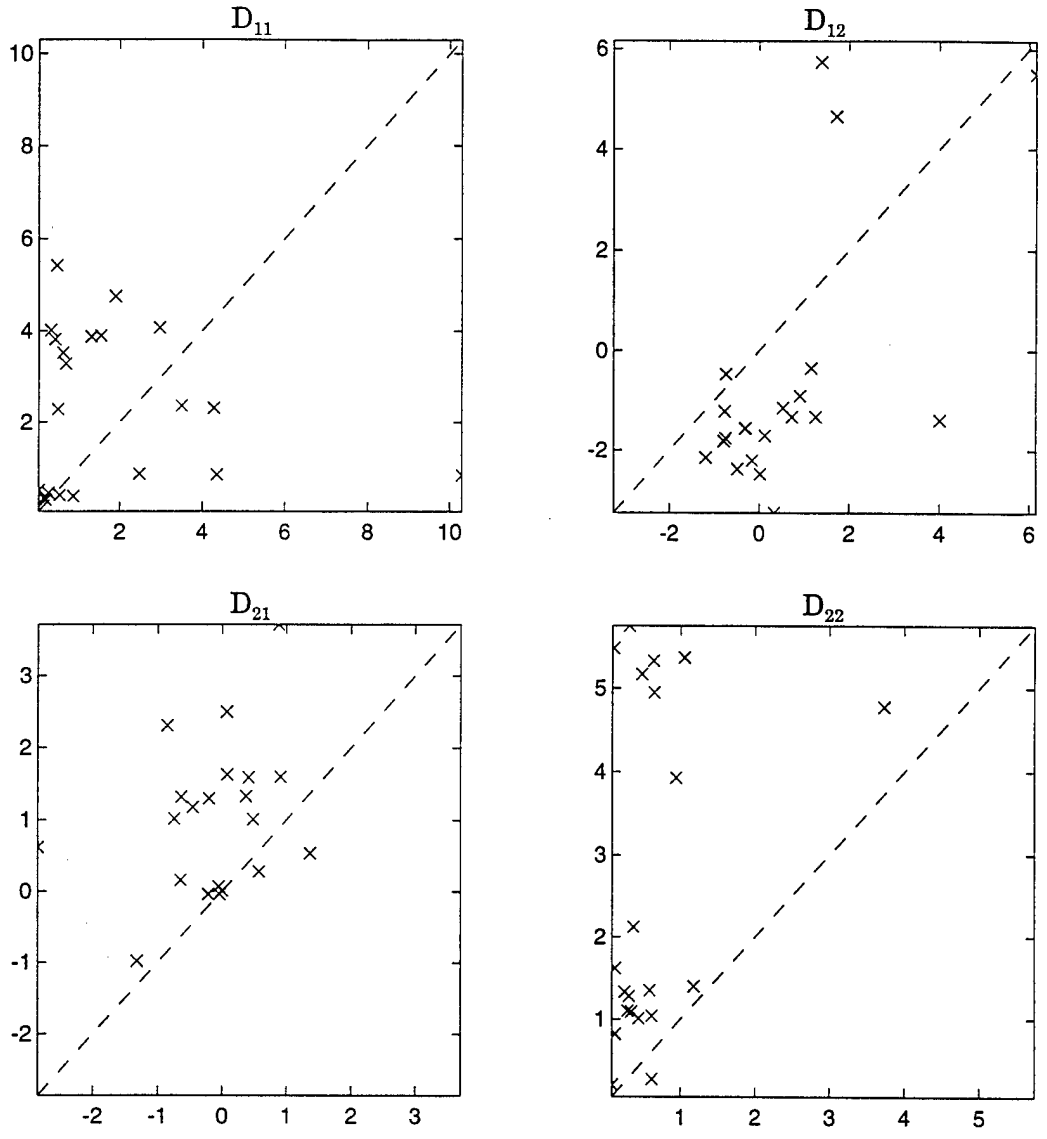

Figure 68: Modeled D_{ij} vs. observed D_{ij} (in $10^3\ m^2 s^{-1}$) for each drifter. The dashed line in each panel represents the line of correlation between the observed and modeled data. The data are tabulated in Table 5.

A.6 Weekly mean surface velocities

Enough drifter observations exist to allow comparison of observed weekly mean surface velocities with weekly mean model surface velocities for the last eight weeks of 1993.

In order to compare the statistics of the observed drifter surface velocities with those of the model surface velocity field, a simple grid of 23 boxes was constructed. Each box spans 1° in latitude and 1° in longitude. To obtain the *observed* mean weekly surface velocity for each box, all drifter observations from anywhere within the box at any time during the week were averaged together. The resulting velocity was taken as the observed weekly mean velocity at the box center.

To obtain the mean weekly *model* surface velocity in each box, the seven daily mean surface velocity fields for the week were averaged to obtain the weekly mean surface velocity on the model grid. Then, all model velocities within a given 1° by 1° box were averaged together, and this mean velocity was taken to represent the model mean velocity at the center of the box.

Figures 69 – 72 show weekly mean surface velocity vectors at the center of each box from the drifter observations (bold arrows) and from the model (thin arrows) for the last eight weeks of 1993. No drifter based velocity vectors are shown for boxes with fewer than five drifter observations during the week. In each figure, the center of each box is shown as a small square.

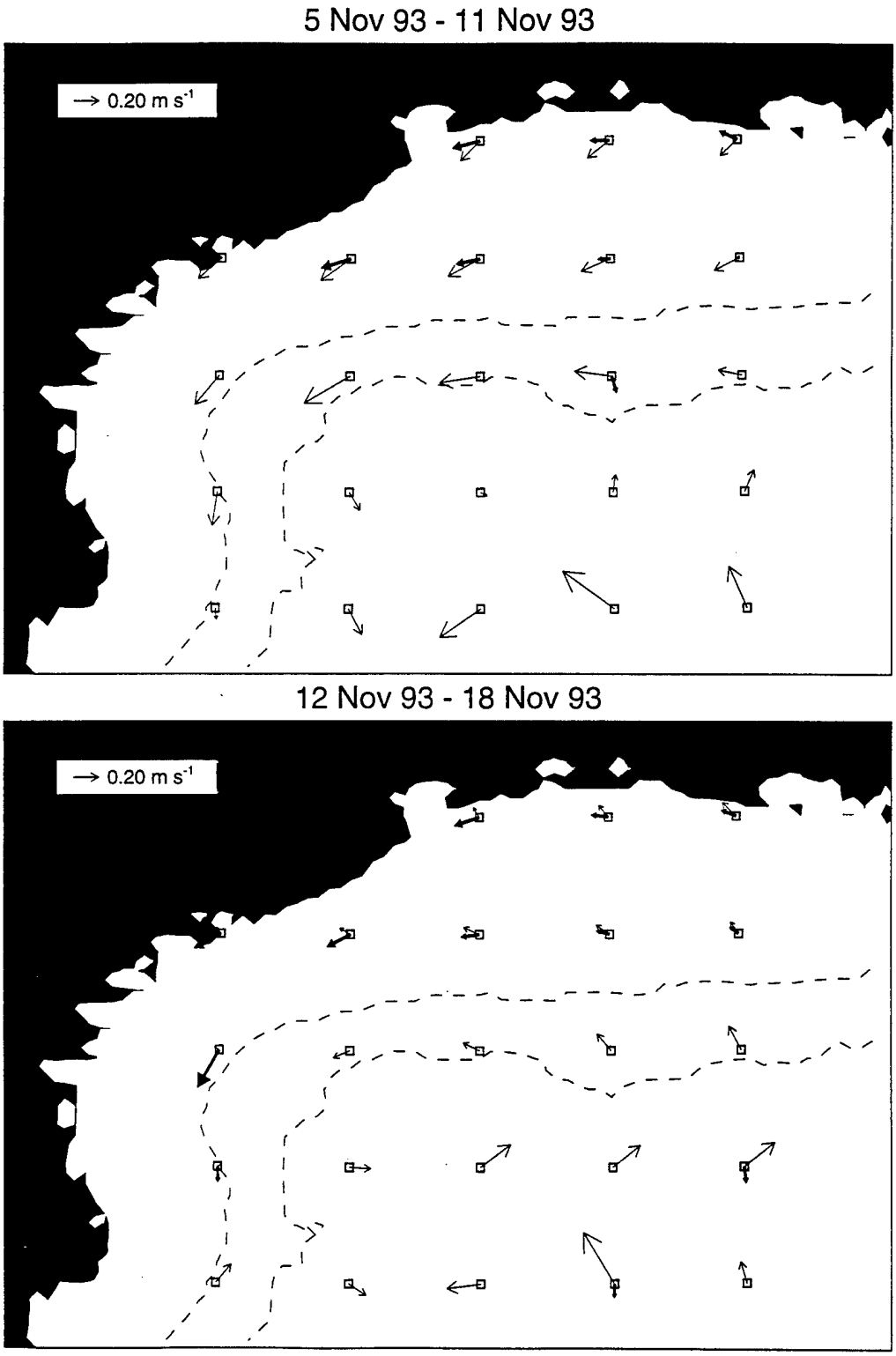

Figure 69: Weekly averaged surface velocities for the SCULP drifters (bold arrows with solid arrow heads) and the model (thinner arrows) for the two weeks shown above each panel.

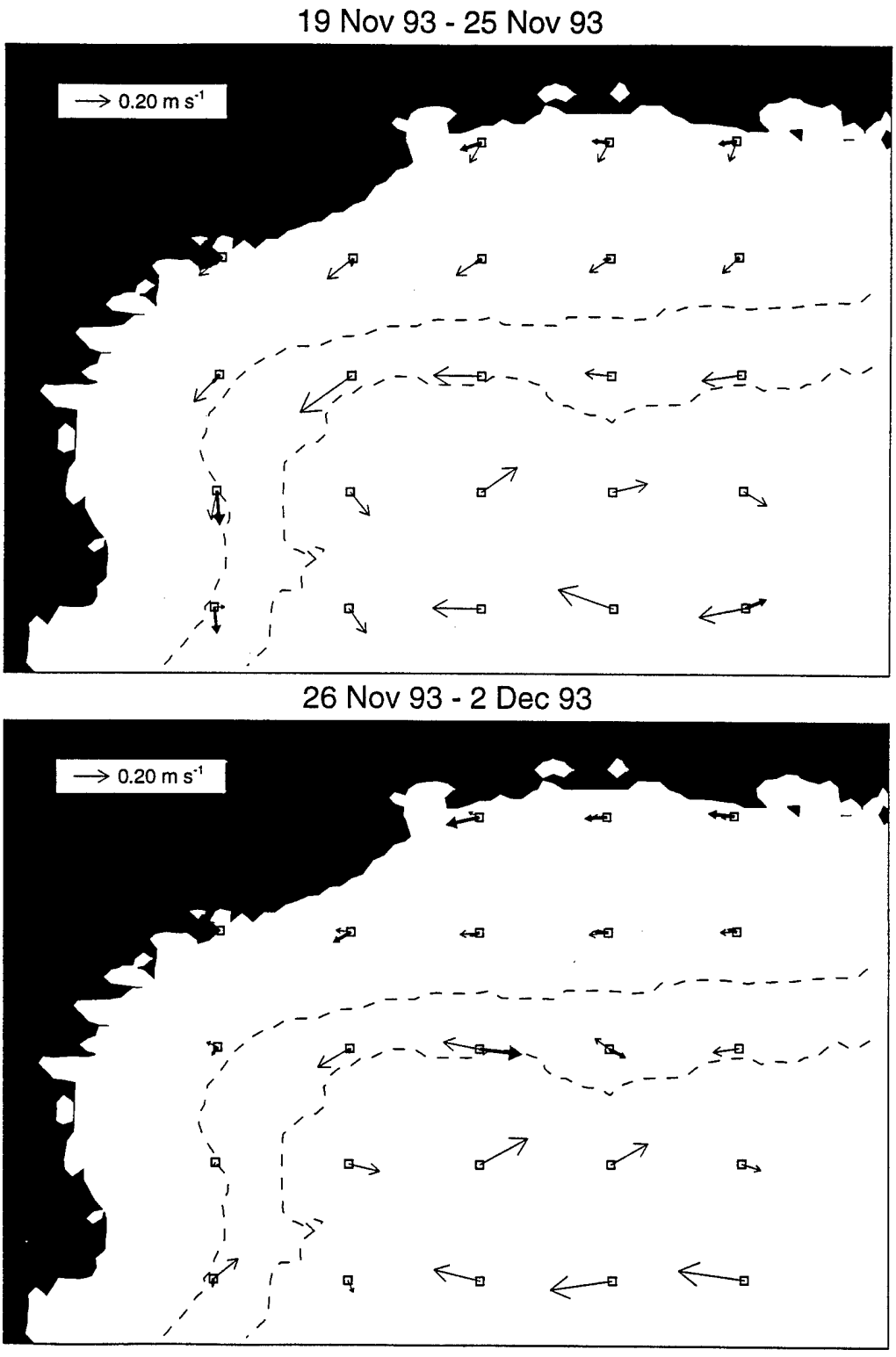

Figure 70: Weekly mean surface velocities for the SCULP drifters (bold arrows with solid arrow heads) and the model (thinner arrows) for the two weeks shown above each panel.

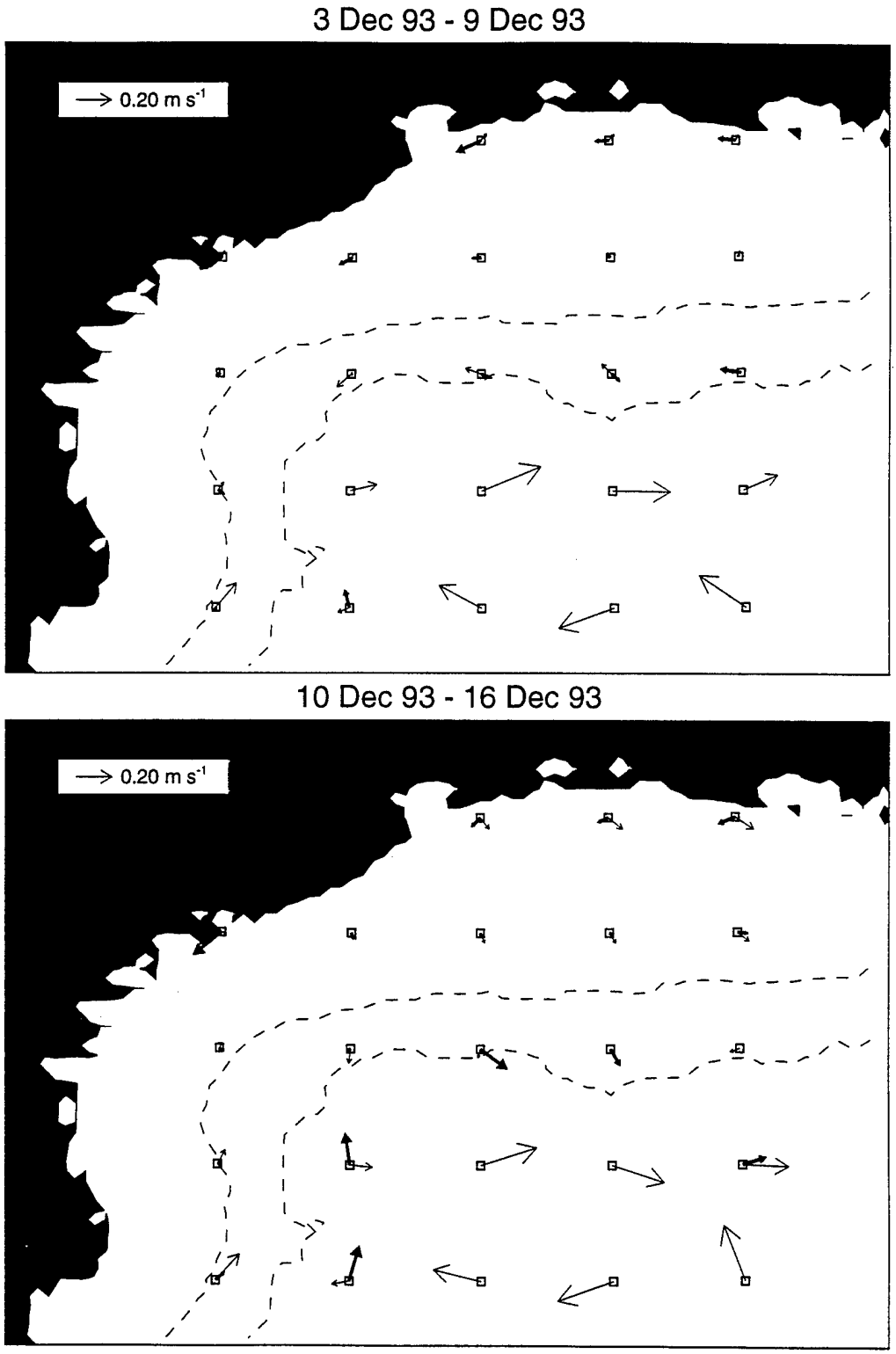

Figure 71: Weekly mean surface velocities for the SCULP drifters (bold arrows with solid arrow heads) and the model (thinner arrows) for the two weeks shown above each panel.

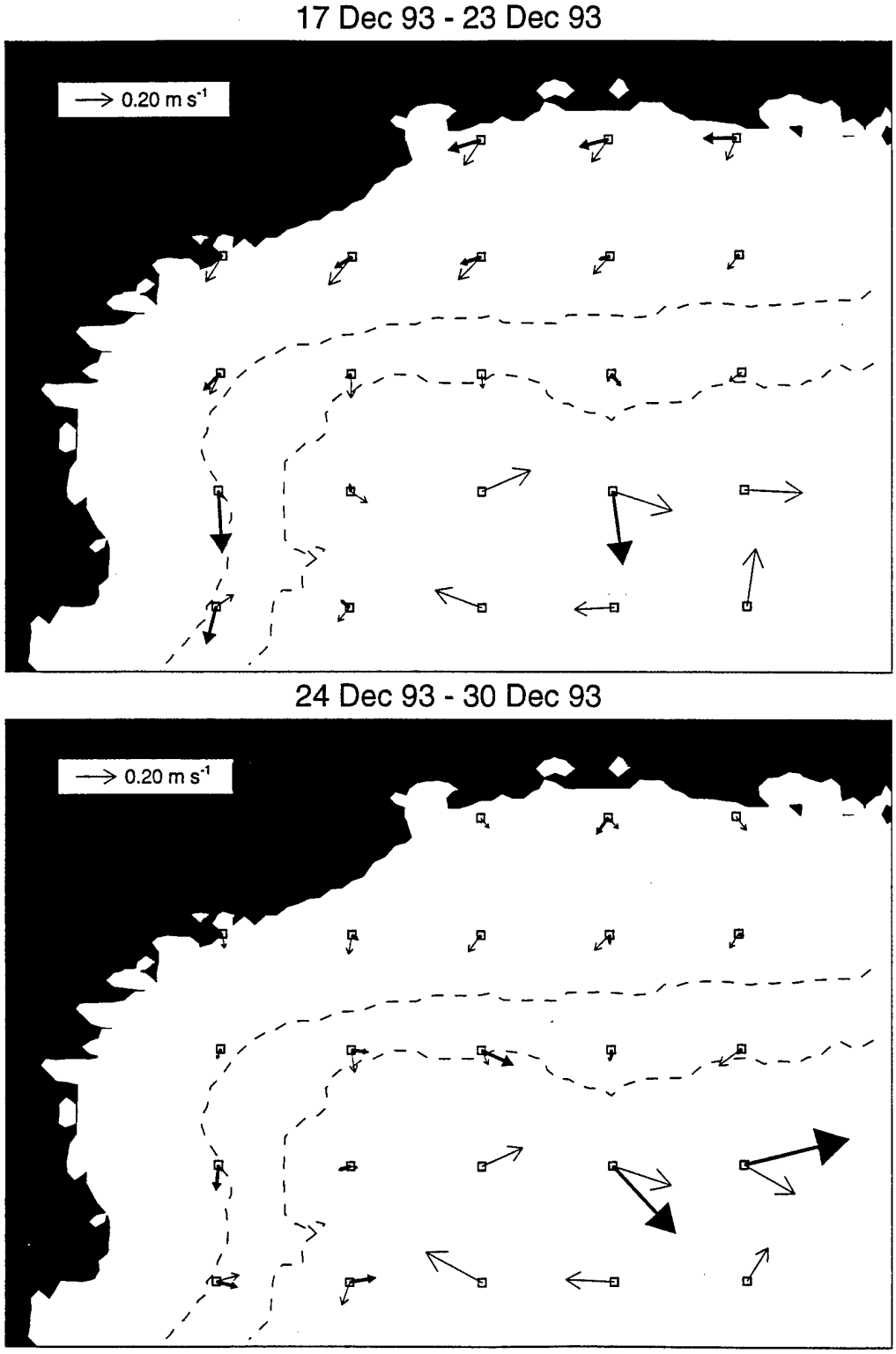

Figure 72: Weekly mean surface velocities for the SCULP drifters (bold arrows with solid arrow heads) and the model (thinner arrows) for the two weeks shown above each panel.

On the inner LATEX shelf, the model mean weekly velocities are usually directed to the southwest, in agreement with the drifter derived velocities, but there are a few cases where the inner shelf velocities show significant direction errors (for example, Figure 71, lower panel, and Figure 72, lower panel). In general, the model velocities on the inner shelf show significant velocity errors when compared with the drifter velocities.

References

Batchelor, G. K. Diffusion in a field of homogeneous turbulence: I. Eulerian analysis. *Aust. J. Sci. Res.*, 2:437–450, 1949.

Batchelor, G. K. Diffusion in a field of homogeneous turbulence: II. The relative motion of particles. *Proc. Cambridge Phil. Soc.*, 48:345–362, 1952.

Blumberg, A. F. and G. L. Mellor. A description of a three–dimensional coastal ocean circulation model. In N. S. Heaps, editor, *Three–dimensional coastal ocean models*, pages 1–16, Washington, D. C., 1987. American Geophysical Union.

Cochrane, J. D. and F. J. Kelly. Low–frequency circulation on the Texas–Louisiana continental shelf. *J. Geophys. Res.*, 91:10,645–10,658, 1986.